



Pontifical Catholic University of Chile  
Faculty of Physics

# Black Holes in Scale-Dependent Frameworks

by

Ángel Rincón

A dissertation presented by Ángel Rincón  
to The Faculty of Physics  
in partial fulfillment of the requirements  
for the degree of Ph.D. in Physics.

Thesis advisor : Dr. Benjamin Koch (PUC)  
Informant Committee : Dr. Máximo Bañados (PUC)  
Dr. Frank Saueressig (Radboud University)

April 2019, Santiago, Chile

©2019, Ángel Rincón



# Declaration of authorship

I, Ángel Rincón, declare that this thesis titled, ‘Black Holes in Scale–Dependent Frameworks’ and the work presented in it are my own. I confirm that:

- This work was done wholly or mainly while in candidature for a research degree at this University.
- Where any part of this thesis has previously been submitted for a degree or any other qualification at this University or any other institution, this has been clearly stated.
- Where I have consulted the published work of others, this is always clearly attributed.
- Where I have quoted from the work of others, the source is always given. With the exception of such quotations, this thesis is entirely my own work.
- I have acknowledged all main sources of help.
- Where the thesis is based on work done by myself jointly with others, I have made clear exactly what was done by others and what I have contributed myself.

Signed:

---

Date:

---



*“ Si del cielo me caen limones, los convierto en papel y escribo un par de ecuaciones.”*

McKlopedia ft Ángel Rincón.



Pontifical Catholic University of Chile

# *Abstract*

Ph.D. in Physics

by *Ángel Rincón*

In the present thesis, we investigate the scale-dependence of some well known black hole solutions in 2+1 dimensions at the level of the effective action in the presence of a cosmological constant or an electrical source. We promote the classical parameters of the theory,  $\{G_0, (\dots)_0\}$ , to scale-dependent couplings,  $\{G_k, (\dots)_k\}$  and then we solve the corresponding effective Einstein field equations. To close the system of equations we impose the null energy condition. This last condition (valid in arbitrary dimension) provides a differential equation which, after solving it, allows to obtain in a simple way the specific form of the gravitational coupling. Furthermore, perfect-fluid like parameters are induced via the scale-dependent gravitational coupling. Finally, to exemplify the effect of the running of the couplings on the properties of the scale-dependent black hole solutions, we show a few concrete examples.



# *Acknowledgements*

It is a great pleasure to thank my advisor, Dr. Benjamin Koch, for an excellent collaboration as well as letting me carry out my own ideas. He inspired me to learn about more complicated problems. In addition, his experience, his ability and his view of how physics works helped me to improve my own point of view about physics.

Thanks in advise to the members of my informant committee Dr. Máximo Bañado and Dr. Frank Saueressing, for the constructive criticism, useful comments and suggestions.

I would like to thank the Physics Department of the Pontifical Catholic University of Chile for its warmest hospitality all these years. Thanks to the Chilean government who supported me by the scholarship CONICYT-PCHA/Doctorado Nacional/2015-21151658.

I would like to thank Javier, Gabriel, Marrón, Jorge, Iván, Julián–Esteban, Eli, Alejandro, Dani, Daniel Thuberg, Niño pequeño, Ivania, Edwin, Rene, Cris, Ernesto, Grig among others, for their collaboration and useful discussions.

Thanks to my collaborators: Dr. Ernesto Contreras, Dr. Pedro Bargeño, Dr. Grigoris Panotopoulos, Dr. J. R. Villanueva, Dr. Ignacio Reyes, Luciano Gabanelli, Carlos Rubio, Felipe Canales and Cristobal Laporte for their help and support in different projects.

I appreciate in advance the patience of my fiancé, Nayker Evies (♡). She has supported and helped in all the phases of my PhD program, which implies paying a high price.

Thanks to my family for all their support and love.



# Contents

<b>Declaration of authorship</b>	<b>iii</b>
<b>Abstract</b>	<b>vii</b>
<b>Acknowledgements</b>	<b>ix</b>
<b>1 Preliminar</b>	<b>1</b>
1.1 Einstein's gravity . . . . .	1
1.1.1 Quantum features: temperature and entropy . . . . .	6
1.2 Beyond Einstein's gravity . . . . .	7
1.3 Structure of the thesis . . . . .	14
<b>2 Scale-dependent black hole in 2+1 dimensions</b>	<b>17</b>
2.1 Introduction . . . . .	17
2.1.1 The classical BTZ solution without scale dependence . . . . .	18
2.1.2 Scale dependent couplings . . . . .	19
2.2 Scale dependent solution without angular momentum . . . . .	20
2.2.1 The null energy condition (NEC) . . . . .	21
2.2.2 A non-trivial solution for scale dependent couplings . . . . .	23
2.2.3 Asymptotic space-times . . . . .	25
2.2.4 Horizon structure . . . . .	27
2.2.5 Black hole thermodynamics . . . . .	28
2.2.6 Comparison to the four dimensional solution . . . . .	33
2.3 Summary and Conclusion . . . . .	34
<b>3 Scale-dependent rotating black hole in 2+1 dimensions</b>	<b>35</b>
3.1 Introduction . . . . .	35
3.2 Classical BTZ solution with $J_0 \neq 0$ . . . . .	38
3.3 Scale dependent couplings and scale setting . . . . .	40
3.4 Scale-dependent BTZ solution with $J_0 \neq 0$ . . . . .	41

3.4.1	Solution . . . . .	42
3.4.2	Horizon structure . . . . .	45
3.5	Invariants and asymptotic space-times . . . . .	46
3.5.1	Asymptotic line element . . . . .	47
3.5.1.1	Behaviuor when $r \rightarrow 0$ . . . . .	47
3.5.1.2	Behaviuor when $r \rightarrow \infty$ . . . . .	47
3.5.2	Asymptotic Invariants . . . . .	48
3.5.2.1	Behaviuor when $r \rightarrow 0$ . . . . .	48
3.5.2.2	Behaviuor when $r \rightarrow \infty$ . . . . .	49
3.6	Thermodynamic properties . . . . .	49
3.6.1	Hawking temperature . . . . .	50
3.6.2	Bekenstein-Hawking entropy . . . . .	51
3.7	Discussion . . . . .	53
3.8	Conclusion . . . . .	54
<b>4</b>	<b>Scale-dependent charged solutions</b>	<b>57</b>
4.1	Introduction . . . . .	57
4.2	Classical linear and non-linear electrodynamics in (2+1) dimensions . . . . .	59
4.2.1	Einstein-Maxwell case . . . . .	61
4.2.2	Einstein-power-Maxwell case . . . . .	62
4.3	Scale-dependent couplings and scale setting . . . . .	63
4.4	The null energy condition . . . . .	64
4.5	Scale dependence in Einstein-Maxwell theory . . . . .	65
4.5.1	Solution . . . . .	66
4.5.2	Asymptotic behaviour . . . . .	68
4.5.3	Horizons . . . . .	70
4.5.4	Thermodynamic properties . . . . .	70
4.5.5	Total charge . . . . .	74
4.6	Einstein-power-Maxwell scale dependence . . . . .	74
4.6.1	Solution . . . . .	75
4.6.2	Asymptotic behaviour . . . . .	75
4.6.3	Horizons . . . . .	77
4.6.4	Thermodynamic properties . . . . .	79
4.6.5	Total charge . . . . .	82
4.7	Discussion . . . . .	83
4.8	Conclusion . . . . .	83
4.9	Appendix . . . . .	84
<b>5</b>	<b>Generalized scale-dependent charged solutions</b>	<b>87</b>
5.1	Introduction . . . . .	87
5.2	Classical Einstein-power-Maxwell theory . . . . .	89
5.3	Black hole solution for Einstein-Maxwell model of arbitrary power . . . . .	90

5.4	Scale-dependent coupling and scale setting . . . . .	92
5.5	The null energy condition . . . . .	93
5.6	Scale dependent Einstein-power-Maxwell theory . . . . .	94
5.6.1	Solution . . . . .	94
5.6.2	Asymptotic behaviour . . . . .	98
5.6.2.1	Asymptotics for $r \rightarrow 0$ . . . . .	100
5.6.2.2	Asymptotics for $r \rightarrow \infty$ . . . . .	100
5.6.3	Horizons . . . . .	101
5.6.4	Thermodynamic properties . . . . .	102
5.7	Conclusions . . . . .	105
<b>6</b>	<b>Discussion and final remarks</b>	<b>107</b>
6.1	Discussion . . . . .	107
6.1.1	Quantum gravity inspired classical theory . . . . .	107
6.1.2	Wetterich equation as tool in scale-dependent gravity? . . . . .	108
6.1.3	Comparison: Scale-Dependence vs Brans-Dicke theory . . . . .	108
6.1.4	Comparison: Scale-Dependence vs RG improving solutions . . . . .	108
6.1.4.1	Technical points . . . . .	109
6.1.4.2	Scale setting and its importance . . . . .	111
6.1.5	Comparison: with and without NEC . . . . .	114
6.1.6	About Thermodynamics . . . . .	116
6.1.7	Charged solutions . . . . .	117
6.1.8	Possible reconciliation . . . . .	118
6.2	Final remarks . . . . .	119
<b>A</b>	<b>On the null energy condition</b>	<b>121</b>
A.1	Introduction . . . . .	121
A.2	Main idea . . . . .	122
A.3	Technique and results . . . . .	123
A.4	Conclusion . . . . .	124
	<b>Bibliography</b>	<b>127</b>



*Dedicated to my Family: My mom Irma-Elena, to my grandmother Mamá Rosa, to my fiancé Nayker and to The Profesor.*



# Chapter 1

## Preliminar

### 1.1 Einstein's gravity

The theory of General Relativity (GR hereafter) developed by Einstein is the fundamental tool to understand how the gravitational field influences the behavior of matter and vice-versa [1]. Roughly speaking, the Einstein field equations can be obtained by “covariantizing” the local form of Newton’s gravitational law. As GR is a tensorial theory, the formalism is still valid for different dimensions. In particular, gravity in 2+1 dimensions can help us to understand interesting effects that appear in the corresponding 3+1 counterpart. The Einstein field equations connect the geometric sector with the matter content. Analogously to the Einstein field equations, one can compare them with the Maxwell field equations, which give us how the charges and currents determine the movement of the electromagnetic fields. Einstein noticed that it is possible to add a constant in order to reproduce a static Universe. This additional value still maintains the validity of the field equations. Although those above constant (the so-called cosmological constant  $\Lambda_0$ ) was originally introduced to explain a static Universe, currently  $\Lambda_0$  is responsible for the expansion of the Universe [2]. General Relativity can be systematically modified when the basic suppositions used to obtain the Einstein field equations are relaxed. We have more than one way to derive the corresponding equations for GR. We only need to satisfy two conditions: i) the theory must be generally co-variant, and ii) the theory must reduce to Special Relativity in the appropriate limit. One can use as the starting point to obtain the Einstein field equations the “classical” action  $S_G$ , where we maintain all the assumptions of Einstein gravity as valid.

Thus, the field equations are obtained via the “principle of least action”, which means

$$\delta S_G = 0, \quad (1.1)$$

where  $S_G$  is the action integral for gravitation.  $S_G[g_{\mu\nu}]$  is of geometrical nature, and it is of the form

$$S_G[g_{\mu\nu}] \equiv \frac{1}{2\kappa_0} \int d^4x \sqrt{-g} \mathcal{L}[g_{\mu\nu}]. \quad (1.2)$$

Here  $G_0$  is Newton’s gravitational constant,  $g = \det(g_{\mu\nu})$  is the determinant of the metric tensor and  $\kappa_0 \equiv 8\pi G_0$  is the Einstein coupling constant. The function  $\mathcal{L}[g_{\mu\nu}]$  has to be a scalar for the integral to transform in an invariant manner. As we know, the simplest scalar involving curvature is the Ricci curvature scalar. Therefore we will use

$$\mathcal{L}[g_{\mu\nu}] = R - 2\Lambda_0, \quad (1.3)$$

being  $R$  the scalar curvature and  $g_{\mu\nu}$  the metric tensor. The action is then written as

$$S_G[g_{\mu\nu}] = \frac{1}{2\kappa_0} \int d^4x \sqrt{-g} [R - 2\Lambda_0]. \quad (1.4)$$

The variation of the action concerning the metric is

$$\delta S_G[g_{\mu\nu}] = \frac{1}{2\kappa_0} \int d^4x \left[ g^{\mu\nu} \sqrt{-g} \delta R_{\mu\nu} + R_{\mu\nu} \delta [g^{\mu\nu} \sqrt{-g}] - 2\Lambda_0 \delta(\sqrt{-g}) \right]. \quad (1.5)$$

The first term is in general different to zero. However in the particular case where the variation of the metric  $\delta g^{\mu\nu}$  vanishes in a neighborhood of the boundary, and this term does not contribute. The last two terms can be computed using the results:

$$\delta(\sqrt{-g}) = \frac{1}{2} \sqrt{-g} g^{\alpha\beta} \left[ -g_{\alpha\mu} g_{\beta\nu} \delta g^{\mu\nu} \right], \quad (1.6)$$

$$\delta [g^{\mu\nu} \sqrt{-g}] = \sqrt{-g} \left[ \delta g^{\mu\nu} - \frac{1}{2} g^{\mu\nu} g_{\alpha\beta} \delta g^{\alpha\beta} \right]. \quad (1.7)$$

Thus, using Eqs. (1.6) and (1.7) we finally get:

$$\delta S_G[g_{\mu\nu}] = \frac{1}{2\kappa_0} \int d^4x \sqrt{-g} \delta g^{\alpha\beta} \left[ R_{\alpha\beta} - \frac{1}{2} R g_{\alpha\beta} + \Lambda_0 g_{\alpha\beta} \right], \quad (1.8)$$

which gives the vacuum field equations demanding  $\delta S_G = 0$  to obtain

$$R_{\mu\nu} - \frac{1}{2}Rg_{\mu\nu} + \Lambda_0g_{\mu\nu} = 0. \quad (1.9)$$

Also,  $R_{\mu\nu}$  is the Ricci curvature tensor, and the other symbols have the usual meaning. The same procedure can be carried out when space is filled with any matter content. Of course, the variational principle is now adapted to be

$$\delta\left(S_G[g_{\mu\nu}] + S_M[g_{\mu\nu}]\right) = 0. \quad (1.10)$$

where the additional action is taken to be

$$S_M[g_{\mu\nu}] \equiv \int d^4x \sqrt{-g} \mathcal{L}_M. \quad (1.11)$$

The variation gives

$$\delta S_M = \int \left[ \frac{\partial[\sqrt{-g}\mathcal{L}_M]}{\partial g^{\mu\nu}} - \left[ \frac{\partial[\sqrt{-g}\mathcal{L}_M]}{\partial g^{\mu\nu},\lambda} \right]_{,\lambda} \right] \delta g^{\mu\nu} d^4x, \quad (1.12)$$

and the term  $\mathcal{L}_M$  describing any matter fields appearing in the theory. On the other hand, the energy–momentum tensor  $T_{\mu\nu}$  associated with  $\mathcal{L}_M$  is computed to be

$$T_{\mu\nu} = -\frac{2}{\sqrt{-g}} \left[ \frac{\partial[\sqrt{-g}\mathcal{L}_M]}{\partial g^{\mu\nu}} - \left[ \frac{\partial[\sqrt{-g}\mathcal{L}_M]}{\partial g^{\mu\nu},\lambda} \right]_{,\lambda} \right]. \quad (1.13)$$

Combining the last two equations we finally get

$$\delta S_M = -\frac{1}{2} \int T_{\mu\nu} \sqrt{-g} \delta g^{\mu\nu} d^4x, \quad (1.14)$$

which lets us obtain full Einstein field equations

$$R_{\mu\nu} - \frac{1}{2}Rg_{\mu\nu} + \Lambda_0g_{\mu\nu} = \kappa_0 T_{\mu\nu}. \quad (1.15)$$

For a more detailed description see [1, 3] where the properties of the Einstein equations are exhaustively studied.

The Einstein field equations have interesting solutions/applications.

One of the most relevant of them is the Schwarzschild solution [4]. It is an exact solution to the Einstein field equations which describes the outer region of a spherical mass considering that the electric charge  $Q$ , the angular momentum  $J$ , and the cosmological constant  $\Lambda$  are equal to zero. Also, the Birkhoff's theorem states that the Schwarzschild solution is the unique spherically symmetric solution to Einstein's equations in vacuum. The metric for this solution is given by

$$ds^2 = - \left(1 - \frac{2GM}{r}\right) dt^2 + \left(1 - \frac{2GM}{r}\right)^{-1} dr^2 + r^2 \left[ d\theta^2 + \sin^2(\theta) d\phi^2 \right], \quad (1.16)$$

where  $M$  is the mass of the central object and  $G$  is the Newton constant. The Schwarzschild metric is a particular case of the Kerr solution [5]. It represents another solution to the Einstein field equations including rotation.

Most experimental tests of GR are related to the motion of test particles in the solar system, and hence geodesics of the Schwarzschild solution. Two of the most popular tests suggested by Einstein are: i) deflection of light by the sun [6, 7], and ii) the perihelion precession of Mercury's orbit [8–11]. The first test states that photons suffer a correction respect the classical orbits, i.e., they are deflected by a factor two respect the Newtonian gravity. The main idea behind the second test can be summarized as follows: given that the shape of the gravitational potential in GR is different than in Newtonian mechanics, the perihelia of bound orbits precess. It is necessary to mention the so-called post-Newtonian formalism, which is, roughly speaking, an expansion of the Einstein field equations in terms of the lowest-order deviations from Newton's law. The aforementioned formalism is considered as a useful tool to test GR, being the parameters  $\{\gamma, \beta\}$  the most important in the expansion. For a detailed discussion see [8] and references therein.

Now, moving us towards the cosmological context, the Friedmann–Lemaître–Robertson–Walker (FLRW hereafter) solutions [12] are known as the Standard Model of modern cosmology. The solutions take as assumption homogeneity and isotropy of space. The line element is

$$ds^2 = -dt^2 + a(t)^2 \left[ \frac{1}{1 + \kappa r^2} dr^2 + r^2 \left( d\theta^2 + \sin^2(\theta) d\phi^2 \right) \right], \quad (1.17)$$

where  $a(t)$  is the scale factor, and  $\kappa$  is a dimensionful quantity which can be either positive, negative, or zero. There is good evidence that the Universe is homogeneous (i.e., all

places look the same) and isotropic (i.e., all directions look the same) at sufficiently large scales (i.e., ignoring smaller scale features), larger than 100 Mpc [13, 14]. Taking these two statements into account, we obtain the so-called Friedmann equations which describe how the Hubble parameter evolves [15, 16]. What is more, for a given equation of state, we get the corresponding evolution of density of matter in different regimes: i) matter dominated epoch, ii) radiation dominated epoch and iii) vacuum energy epoch. These and other aspects of FLRW solutions are briefly reviewed in [17]. For a pedagogical review see [18, 19].

In a more astrophysical scenario, relativistic stars are crucial because they are an ideal laboratory for theoretical physics [20–24]. The first studies considered isotropic spheres, however, given that physics beyond these compact objects is highly non-linear, a more appropriated description is obtained assuming anisotropic models (see for example [25, 26] and references therein). In particular, the Tolman–Oppenheimer–Volkoff (TOV) equation [23] parametrizes the physics of a spherically symmetric body in static gravitational equilibrium, and it is given by

$$\frac{dP}{dr} = -\frac{Gm}{r^2}\rho\left(1 + \frac{P}{\rho}\right)\left(1 + \frac{4\pi r^3}{m}P\right)\left(1 - \frac{2Gm}{r}\right)^{-1}, \quad (1.18)$$

where  $P$  and  $\rho$  are the pressure and density of the object, respectively, and  $m \equiv m(r_{\text{in}})$  is the mass contained in the radius  $r_{\text{in}}$ . We have observational evidence of relativistic stars [27]. In particular, the rotating relativistic stars have been studied during years, both theoretically and observationally. The reason of such studies are: i) they might help us to get some insights about the equation of state of matter at extremely high densities and ii) they are considered to be promising sources of gravitational waves [28].

Gravitational waves are another prediction of the Einstein field equations and, after LIGO direct detection [29], the interest in them has reborn. Currently, we have more detected events, see for instance [30–32]. They can be defined as “ripples” in the fabric of space-time produced by energetic and violent processes in the Universe.

A particular class of solutions of the Einstein field equations are the so-called black holes which are particularly relevant for this thesis. They are defined as a region of spacetime where the gravitational effects are so strong that particles and electromagnetic radiation (such as light) can not escape from inside it [33]. The black holes have event horizon (i.e. the boundary where nothing can escape) and they are parametrized by just three independent values: i) the mass, ii) the charge, and finally iii) the angular momentum. In addition,

the black holes comprise an excellent laboratory to study and understand several aspects of gravitational theories. We will briefly mention how the quantum nature of black holes manifests itself via the Hawking temperature or the Bekenstein–Hawking entropy [34–37].

### 1.1.1 Quantum features: temperature and entropy

It is very well known that gravity and quantum mechanics are not “compatible theories”. However, in the context of black holes physics, there are well-justified approximations that allow the incorporation of quantum features. When we are far enough from the black hole, the gravitational influence of the BH on its surrounding is weak, such that some quantum field theory (QFT) computations (e.g., temperature and entropy) can be applied. Black holes emit electromagnetic radiation, mimicking an almost perfect black body spectrum. However, the emitted particles feel an effective potential barrier in the exterior region. This barrier backscatters a part of the outgoing radiation into the black hole producing deviations from the black body spectrum [38–40].

Two of the most characteristic quantities which incorporate quantum effects are: i) Hawking temperature and ii) Bekenstein–Hawking entropy. We should note that one is the consequence of the other. In the simplest situation, i.e. the four-dimensional case with spherical symmetry, without angular momentum and charged, the black hole temperature is reciprocal to the mass. Taking the Schwarzschild black hole solution, the Hawking temperature is given by the simple relation

$$T_H = \frac{1}{4\pi} \left| \lim_{r \rightarrow r_H} \frac{\partial_r g_{tt}}{\sqrt{-g_{tt}g_{rr}}} \right|, \quad (1.19)$$

which produces  $\kappa_0 T_H = 1/M_0$ . The Hawking temperature is a quantum manifestation near the event horizon, however the temperature in Eq. (1.19) is the temperature measured by an observer at spatial infinity. The Hawking radiation associated with  $T_H$  is expected to reduce the mass and energy of black holes. Thus, the emission of radiation inevitably implies that black holes lose mass!

The Bekenstein-Hawking entropy is another quantity which combines the gravitational effects with quantum mechanics via the well-known relation:

$$S_{BH} = \frac{A}{4L_P^2} = \frac{c^3 A}{4G\hbar}, \quad (1.20)$$

where the parameters of the formula are: the Planck length  $L_P = G_0\hbar/c^3$ , the Planck-Dirac constant  $\hbar$  and finally the speed of light  $c$ . The analysis of the aforementioned quantities (Hawking temperature and Bekenstein-Hawking entropy) plays a crucial role in black hole physics. Thus, both functions should be investigated and compared for each model studied, to get an improved comprehension of the underlying theory.

## 1.2 Beyond Einstein's gravity

General Relativity accounts for most observations in the Solar System and over cosmological distances but, in a laboratory when the characteristic lengths decrease, it becomes harder to test gravity. Thus, below certain distances, physics is described by the standard model of particle physics which is beyond the interest of this thesis. Neither GR nor the standard model can be the ultimate theory of nature. The above theories describe two separate sectors in which the underlying physics is very different. However, each of them has certain problems. One of them is that GR is not able to explain the rotation curves of the galaxies [41] without the inclusion of non-standard matter (the so-called Dark-Matter). We will focus on the problems related to GR which is a non-renormalizable theory. General Relativity loses its predictive power above the Planck energy scale (that is  $10^{19}$  GeV). Currently, physicists attempt to find a quantum theory of the gravitational interaction, that would be predictive at all energy scales. In order to do that, usual GR is expected to be modified in order to incorporate the corresponding quantum effects.

Up to now, we have several well-known theories which extend GR. One of the most famous approaches is the so-called Brans-Dicke (BD) theory in which the Newton gravitational coupling  $G_0$  is replaced by a scalar field  $\phi$  [42]. The scalar field has dynamics and provides the simplest extension of the canonical Einstein field equations of motion. It is remarkable that BD theory is a classical approach in the sense that it is not quantum-inspired theory. Also, the BD theory is less restrictive than Einstein GR and provides a richer family of solutions. We summarize the main points of this approach. The usual Einstein-Hilbert

action should be modified in order to account for the “running” of the gravitational coupling as follows:

$$\Gamma[g_{\mu\nu}, \phi] = \int d^4x \sqrt{-g} \left[ \frac{1}{2\kappa_\phi} \left( R - \omega \frac{\partial_\mu \phi \partial^\mu \phi}{\phi^2} \right) + \mathcal{L}_M \right], \quad (1.21)$$

where the corresponding Einstein coupling is defined in the usual way, namely:  $\kappa_\phi \equiv 8\pi\phi^{-1}$ . In addition, the Brans–Dicke theory includes a kinetic term proportional to  $\omega$ , being this last parameter the Brans–Dicke constant. GR is recovered for large values of  $\omega$  (typically values larger than 40.000) [43]. Despite the fact that BD theory is a generalization of Einstein’s General Relativity, this theory does not consider any quantum correction. However, the BD theory is the first and best-known example which considers a variable gravitational coupling, an idea which will be investigated along with this thesis.

In order to incorporate quantum effects into gravity, different approaches have been considered. One of them is the so-called String Theory which, basically, changes the concept of point-like particles to one-dimensional objects (strings) [44]. Another approach is Loop Quantum Gravity which, roughly speaking, considers the spacetime as granular (interpreted as a consequence of the quantization) and, therefore, it can be considered as a network of “loops” [45]. The usual perturbative approach in QFT needs to be improved in order to be applied to gravity.

One of the most famous approaches to obtain a self-consistent theory of quantum gravity is the so-called Asymptotic Safety (AS hereafter) scenario. Despite gravity is not perturbatively renormalizable beyond two dimensions, Weinberg [46] suggested that it could be non-perturbatively renormalizable if UV completion of Einstein gravity might hits a non trivial (but still well-defined) UV fixed point. In order to test this hypothesis, the so-called Functional Renormalization Group technique is used [47]. First, one defines the effective action  $\Gamma_k$ , which is the generalization to the classical action, and it is parametrized by an infinite set of couplings  $\tilde{u}_\alpha(k)$ . Thus,  $\Gamma_k[\{\tilde{u}_\alpha(k)\}]$  describes a curve into the corresponding “theory space”. To obtain the effective (average) action, one first notes that it contains integrals in two regions: i) momenta  $p$  larger than  $k$  and ii) momenta  $p$  lower than  $k$ . Note that the  $k$  scale is used to separate both sectors. To split the regions, one adds an extra term to the action, containing an IR cutoff function  $\mathcal{R}_k(p^2)$  defined as:

$$\Delta_k S[\phi] \equiv \frac{1}{2} \int \frac{d^d p}{(2\pi)^d} \mathcal{R}_k(p^2) |\hat{\phi}(p)|^2, \quad (1.22)$$

using the symbol  $\phi$  to refer to a generic field. It is remarkable that  $\mathcal{R}_k(p^2)$  is arbitrary, however it should satisfy certain minimum requirements which can be summarized below:

$$\mathcal{R}_k(p^2) \approx \begin{cases} k^2 & \text{if } p^2 \ll k^2, \\ 0 & \text{if } p^2 \gg k^2. \end{cases} \quad (1.23)$$

The first condition leads to a suppression of the small momentum modes by the inclusion of a “soft” mass-like IR cutoff whereas the second condition ensures that the large momentum modes are integrated out, this means that it leaves the momentum above  $k$  untouched. The scale-dependent generator of connected diagrams  $W_k[J]$  is given by:

$$\exp\{W_k[J]\} = \int \mathcal{D}\phi \exp \left\{ -S[\phi] - \Delta_k S[\phi] + \int d^d x \phi(x) J(x) \right\}, \quad (1.24)$$

where  $S$  is the bare action, and  $J$  is a source for the generic field  $\phi$ . By definition, the effective average action  $\Gamma[\phi]$  is the Legendre transformation of  $W[J]$ , i.e.,

$$\Gamma_k[\phi_c] = -W_k[J] - \Delta S_k[\phi_c] + \int_x J \phi_c, \quad (1.25)$$

defining  $\phi_c$  as the classical field  $\phi_c = \delta W_k[J] / \delta J$ . A detailed analysis of this and other issues can be found in Ref. [48] whereas a pedagogical introduction is found in Ref [49]. Using the above definitions, one is able to obtain the Wetterich equation, best known as the Functional Renormalization Field Equation (FRGE hereafter), which describes how the exact functional flow evolves, and it is given by:

$$\partial_t \Gamma_k = \frac{1}{2} \text{Tr} \left( \frac{\partial_t \mathcal{R}_k}{\Gamma_k^{(2)}[\phi] + \mathcal{R}_k} \right), \quad (1.26)$$

where  $\mathcal{R}_k$  is an adequate cut-off function,  $\Gamma_k^{(2)}[\phi]$  is the free propagator, and  $\partial_k$  denotes a derivative with respect to the RG scale  $k$  at fixed values of the fields involved. The Wetterich equation provides, for a given action, how the fundamental couplings change respect to certain energy scale  $k$ . Unfortunately, in practice, it is not easy to solve, reason why one uses a truncation method on the couplings. Assume that one can expand the effective action in certain complete set of “basis functionals”  $\{P_\alpha[\cdot]\}$  in such way that each point of the

theory space has an expansion of the form

$$A[\phi] = \sum_{\alpha=1}^{\infty} \tilde{u}_{\alpha} P_{\alpha}[\phi]. \quad (1.27)$$

The basis  $\{P_{\alpha}[\cdot]\}$ , which are generalized couplings, can be used as coordinates. The functional renormalization group equation defines a vector field  $\vec{\beta}$  on the corresponding theory space. The “RG trajectories” are just the integral curves along this vector field and they are parametrized by  $k$ . Expanding the effective action as (1.27)

$$\Gamma_k[\phi] = \sum_{\alpha=1}^{\infty} \tilde{u}_{\alpha}(k) P_{\alpha}[\phi], \quad (1.28)$$

the trajectory is given by infinite number of running couplings  $\tilde{u}_{\alpha}(k)$ . Inserting (1.28) into (1.26) one obtains a system on coupled differential equations for  $\tilde{u}_{\alpha}$ 's:

$$k\partial_k \tilde{u}_{\alpha}(k) = \tilde{\beta}_{\alpha}(\tilde{u}_1, \tilde{u}_2, \tilde{u}_3, \dots; k), \quad \forall \alpha = 1, 2, \dots. \quad (1.29)$$

Note that usually the flow equation is written in terms of the dimensionless couplings  $u_{\alpha} \equiv k^{-d_{\alpha}} \tilde{u}_{\alpha}$ , where  $d_{\alpha}$  is the canonical mass dimension of  $\tilde{u}_{\alpha}$ . One finally obtains the RG equations

$$k\partial_k u_{\alpha}(k) = \beta_{\alpha}(u_1, u_2, u_3, \dots), \quad \forall \alpha = 1, 2, \dots. \quad (1.30)$$

Thus, for given initial conditions, the above equations determine the evolution of the couplings  $u_{\alpha}$ , which fixes a curve in the theory space and determine the UV behavior (whether there is a fixed point or not). As one has an infinite number of differential equations, one needs to truncate the series (i.e., take a finite number of couplings equal to zero) and solve them numerically. In particular, Reuter and Saueressig [50] analyzed the Einstein truncation where only the gravitational and cosmological coupling can vary. Thus, the Einstein–Hilbert action is taken as a suitable ansatz for  $\Gamma_k$ . What is more, as it was previously pointed out in [50], “the most prominent feature of the RG flow resulting from the Einstein–Hilbert truncation is a non–Gaussian fixed point which acts as an UV-attractor” taking the initial data as positive. The paper above provides further evidence supporting the hypothesis of the non–Gaussian fixed point. It is remarkable that truncations beyond the Einstein–Hilbert (e.g.  $R^2$ ) admit more than two fixed points. Precisely,  $R^2$ -truncation has three non–gaussian fixed points  $(g^*, \lambda^*, \beta^*)$ . Similar to the Einstein–Hilbert truncation,  $R^2$ -truncation proves to be UV attractive in any of the three directions of the  $(g, \lambda, \beta)$  space [50]. Recently, different

authors have considered more complicated  $F(R)$  models, for instance, Falls et al. [51] found evidence for an interacting UV fixed point for polynomial actions up to the 34th power in the Ricci scalar.

It is important to note that the corresponding beta functions are not unique. This effect appears because the solutions depend on the technique used to obtain them. The aforementioned problem introduces uncertainties which suggest using alternative approaches. In the seminal work of Reuter and Weyer [52], a new angle was provided. To be more precise, in that work “the Einstein-Hilbert action is RG-improved by replacing Newtons constant and the cosmological constant by scalar functions in the corresponding Lagrangian density. The position dependence of  $G$  and  $\Lambda$  is governed by a RG equation together with an appropriate identification of RG scales with points in spacetime”. This idea has been subsequently used in several contexts to test whether some quantum features are present in observables as black holes and cosmological models [53–68]. Thus, given a concrete action, the incorporation of quantum corrections can be made allowing that the classical couplings evolve to scale-dependent couplings. The implementation of this idea is usually applied in, at least, two cases: i) at the level of the action, or ii) at the level of the solutions of the equation of motion. We are interested in the use of the above idea for black holes, reason why we restrict our discussion to this particular case. In general, quantum fluctuations will modify the gravitational force law by turning Newtons coupling  $G_0$  into a distance-dependent “running coupling  $G(r)$ ”. Renormalization group improvement should provide a good description of the leading quantum corrections [69, 70]. Along with this thesis, we will use an alternative way to include the quantum corrections to certain black hole solutions. As other approaches, we allow that the gravitational coupling evolves with the energy scale. The corresponding action when  $G_0$  evolves to  $G_k$  and  $\Lambda_0$  evolves to  $\Lambda_k$  is

$$\Gamma[g_{\mu\nu}, k] = \int d^d x \sqrt{-g} \left[ \frac{1}{2\kappa_k} \left( R - 2\Lambda_k \right) + \mathcal{L}_M + \text{Other terms} \right], \quad (1.31)$$

where the functions involved have the usual meaning. When we take the variation respect the metric field, we obtain the Einstein field equations plus an additional term which is labeled  $\Delta t_{\mu\nu}$  and defined to be:

$$\Delta t_{\mu\nu} = G_k \left( g_{\mu\nu} \square - \nabla_\mu \nabla_\nu \right) G_k^{-1}. \quad (1.32)$$

The new tensor encodes any deviation respect the classical solution and tends to zero when

$G_k \rightarrow G_0$ . An extensive discussion (and computation) is made in the seminal paper of [52] by Reuter and Weyer, where this new term emerges from the effective action. We now only motivate this inclusion. We will focus on the Einstein Hilbert action with cosmological constant excluding any additional source. The simplified action, when the couplings vary and for the four-dimensional case, is

$$\Gamma[g_{\mu\nu}, k] = \int d^4x \sqrt{-g} \left[ \frac{1}{2\kappa_k} \left( R - 2\Lambda_k \right) \right]. \quad (1.33)$$

To obtain the EoM we compute  $\delta\Gamma[g_{\mu\nu}, k]/\delta g^{\mu\nu} = 0$ . Doing that we have

$$\delta\Gamma[g_{\mu\nu}, k] = \frac{1}{16\pi} \int d^4x \delta(\sqrt{-g}) \left( \frac{R - 2\Lambda_k}{G_k} \right) + \frac{1}{16\pi} \int d^4x \sqrt{-g} \left( \frac{\delta(R)}{G_k} \right), \quad (1.34)$$

where we use

$$\delta(\sqrt{-g}) = -\frac{1}{2}\sqrt{-g}g_{\mu\nu}\delta g^{\mu\nu}, \quad (1.35)$$

$$\delta(R) = R_{\mu\nu}\delta g^{\mu\nu} + D_\beta (D_\alpha \delta g^{\alpha\beta} - D^\beta \delta g^\alpha{}_\alpha), \quad (1.36)$$

and collecting we have

$$\begin{aligned} \delta\Gamma[g_{\mu\nu}, k] &= \frac{1}{16\pi} \int d^4x (\sqrt{-g}) \delta g^{\mu\nu} \left( \frac{R_{\mu\nu}}{G_k} + \left( -\frac{1}{2}g_{\mu\nu} \right) \frac{R - 2\Lambda_k}{G_k} \right) + \\ &\frac{1}{16\pi} \int d^4x (\sqrt{-g}) \left( \frac{1}{G_k} D_\beta (D_\alpha \delta g^{\alpha\beta} - D^\beta \delta g^\alpha{}_\alpha) \right), \end{aligned} \quad (1.37)$$

and redefining by convenience:

$$\delta\Gamma[g_{\mu\nu}, k] = \delta\Gamma[g_{\mu\nu}, k]_1 + \delta\Gamma[g_{\mu\nu}, k]_2, \quad (1.38)$$

where  $\delta\Gamma[g_{\mu\nu}, k]_1$  corresponds to the first contribution and  $\delta\Gamma[g_{\mu\nu}, k]_2$  to the second. Taking this last term and doing integration by parts we get:

$$\delta\Gamma[g_{\mu\nu}, k]_2 = \frac{1}{16\pi} \int d^4x (\sqrt{-g}) \delta g^{\mu\nu} (g_{\mu\nu} \square - D_\mu D_\nu) G_k^{-1}, \quad (1.39)$$

and finally, we can take  $\delta\Gamma[g_{\mu\nu}, k]/\delta g^{\mu\nu} = 0$  to obtain

$$G_{\mu\nu} + \Lambda_k g_{\mu\nu} = -G_k \left( g_{\mu\nu} \square - \nabla_\mu \nabla_\nu \right) G_k^{-1} \equiv -\Delta t_{\mu\nu}. \quad (1.40)$$

As we do not use the Renormalization group formalism, we just take advantage of the spherical/circumferential symmetry to assume  $\{G_k, (\dots)_k\} \rightarrow \{G(r), (\dots)(r)\}$ . In order to supplement the Einstein field equations, we can obtain a consistency equation after varying the effective action respect the scalar field  $k$ . This algebraic equation  $\delta\Gamma_k/\delta k = 0$  is however not unique, and the resulting field equations are very complicated to solve. Instead, we introduce a new condition on the system which allows to make progress. This is the case of the Null Energy Condition which is the less restrictive of the usual four energy conditions. For certain null vector  $\ell^\mu$ , the energy condition is

$$T_{\mu\nu} \ell^\mu \ell^\nu \geq 0. \quad (1.41)$$

The specific details of the implementation of this idea will be discussed in the next chapter, but the simplest case is  $T_{\mu\nu} \ell^\mu \ell^\nu = 0$ . This condition can serve as an auxiliary equation to obtain the specific form of  $G(r)$  (see appendix for details). It is relevant to note that the NEC was chosen firstly, because it is the less restrictive of the four energy conditions, and secondly because it reproduces a suitable property in black hole physics at the level of the metric functions. We recognize that, in general for complex black hole solutions, the connection between the metric functions is not clear and we consider  $g_{rr}$  and  $g_{tt}$  as independent functions. However, for some black hole solutions, the Schwarzschild ansatz ( $g_{tt}g_{rr} = -1$ ) is maintained at the classical level. We assume as valid the same condition in the case of scale-dependent couplings, the reason why we take as auxiliary condition the NEC. Finally, the effective Einstein field equations supplemented by the Null Energy Condition provides sufficient information to get insights in the black hole physics. Schematically Fig. (1.1) shows how we extend the classical solutions to scale-dependent solutions (which are different than improved solutions [71, 72]) via the running of the gravitational coupling  $G(r)$ . Our solutions are a natural generalization of classical black hole solutions allowing for scale-dependent couplings.

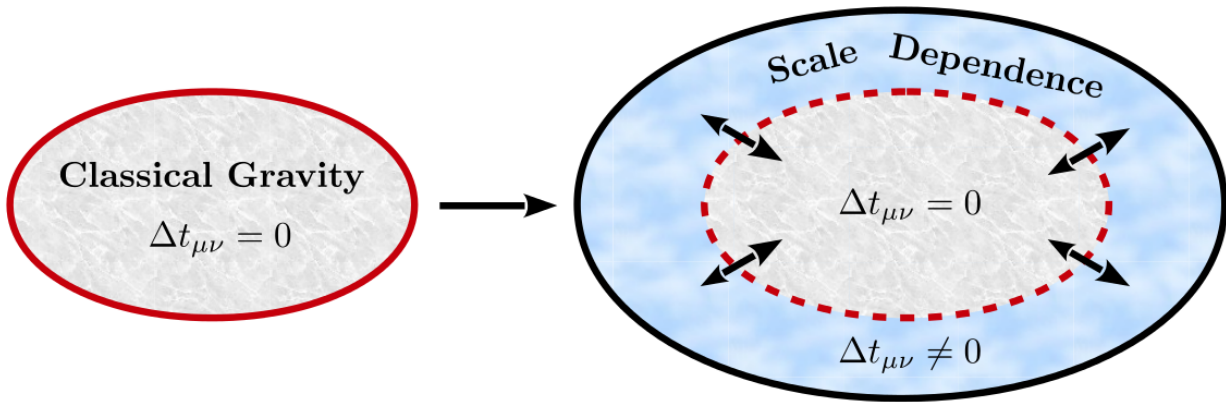


**Figure 1.1:** The picture shows how the inclusion of scale-dependent couplings extend the classical solution.

### 1.3 Structure of the thesis

This thesis summarizes the knowledge and some results obtained during the journey of my Ph.D. The manuscript is divided into four additional chapters, each of them is self-consistent in the sense that can be read separately without the need of having read the preceding chapters. Also, we add a concluding “take-home message” chapter to sum up the main features obtained during this work. The aim of the present thesis is to investigate the effect of scale-dependent couplings on some well known black hole solutions.

The second chapter is based on [56] and it is devoted to analyzing the so-called BTZ black hole, which is a solution in 2+1 dimensions with a negative cosmological constant. We first start reviewing the classical BTZ black hole solution without angular momentum as well as the standard thermodynamics. Then we introduce the framework and the relevant equations to finally obtain the corresponding scale-dependent solutions. After that, we analyze and compare it with the classical counterpart. The thermodynamics of this new black hole is analyzed too.

In the third chapter, which is based on [64], we continue the study of the BTZ black hole, but now taking into account the angular momentum contribution. We follow the same structure of the previous chapter in the sense that the classical solution is shown, and the corresponding thermodynamics and the horizon structure is analyzed and properly compared with the usual case.

Then, the fourth chapter is devoted to the study of charged solutions in 2+1 dimensions and it is based on [57]. We particularly focus on two interesting cases of the so-called Einstein–power–Maxwell action. We also analyze the effect of scale-dependent coupling in the electric field as well as the evolution of the electromagnetic coupling. We compare the two studied cases with the non-running solution.

In chapter 5 we extend the study of charged solutions in 2+1 dimensions, but now we will solve the generalized Einstein–power–Maxwell case, solution which was reported in [61]. It should be noticed that the aforementioned action  $(F_{\mu\nu}F^{\mu\nu})^\beta$  is the natural extension of the standard Maxwell action ( $\beta = 1$ ) and provides a wide range of solutions.

Finally, in chapter 6 we summarize the most relevant features found developing this work.

In the context of gravity in 2+1 dimension, we analyze the effect of scale-dependent couplings on classical black hole solutions. Furthermore, we discuss and compute the thermodynamics in all cases and, at least in the reported cases, the gravitational coupling maintains the same structure. This interesting feature is briefly commented in the first chapter and studied with more detail in the appendix.

Besides, during my Ph.D. I have written more than the papers mentioned here, following similar ideas of scale-dependent couplings. In particular, papers in four-dimensional space-time (and dimension higher than four) are not discussed, but these solutions are consistent with the results reported in this thesis.

This thesis gave rise to the publications listed hereinbelow:

- ▶ B. Koch, I. A. Reyes and Á. Rincón, *Class. Quant. Grav.* **33**, no. 22, 225010 (2016) [arXiv:1606.04123 [hep-th]].
- ▶ Á. Rincón, B. Koch and I. Reyes, *J. Phys. Conf. Ser.* **831**, no. 1, 012007 (2017) [arXiv:1701.04531 [hep-th]].
- ▶ Á. Rincón, E. Contreras, P. Bargeño, B. Koch, G. Panotopoulos and A. Hernández-Arboleda, *Eur. Phys. J. C* **77**, no. 7, 494 (2017) [arXiv:1704.04845 [hep-th]].
- ▶ Á. Rincón and B. Koch, *J. Phys. Conf. Ser.* **1043**, no. 1, 012015 (2018) [arXiv:1705.02729 [hep-th]].

- ▶ E. Contreras, Á. Rincón, B. Koch and P. Bargueño, *Int. J. Mod. Phys. D* **27**, no. 03, 1850032 (2017) [arXiv:1711.08400 [gr-qc]].
- ▶ Á. Rincón and G. Panotopoulos, *Phys. Rev. D* **97**, no. 2, 024027 (2018) [arXiv:1801.03248 [hep-th]].
- ▶ A. Hernández-Arboleda, Á. Rincón, B. Koch, E. Contreras and P. Bargueño, “Preliminary test of cosmological models in the scale-dependent scenario,” arXiv:1802.05288 [gr-qc].
- ▶ E. Contreras, Á. Rincón, B. Koch and P. Bargueño, *Eur. Phys. J. C* **78**, no. 3, 246 (2018) [arXiv:1803.03255 [gr-qc]].
- ▶ Á. Rincón and B. Koch, *Eur. Phys. J. C* **78**, no. 12, 1022 (2018) [arXiv:1806.03024 [hep-th]].
- ▶ Á. Rincón, E. Contreras, P. Bargueño, B. Koch and G. Panotopoulos, *Eur. Phys. J. C* **78**, no. 8, 641 (2018) [arXiv:1807.08047 [hep-th]].
- ▶ E. Contreras, Á. Rincón and J. M. Ramírez-Velasquez, *Eur. Phys. J. C* **79**, no. 1, 53 (2019) [arXiv:1810.07356 [gr-qc]].
- ▶ F. Canales, B. Koch, C. Laporte and Á. Rincón, “Vacuum energy density: deflation during inflation,” arXiv:1812.10526 [gr-qc].
- ▶ Á. Rincón, E. Contreras, P. Bargueño and B. Koch, “Scale-dependent planar Anti-de Sitter black hole,” arXiv:1901.03650 [gr-qc].
- ▶ Á. Rincón and J. R. Villanueva, “The Sagnac effect on a scale-dependent rotating BTZ black hole background,” arXiv:1902.03704 [gr-qc].
- ▶ E. Contreras, Á. Rincón, P. Bargueño “Five-dimensional scale-dependent black holes with constant curvature and Solv horizons” arXiv:1902.05941 [gr-qc].
- ▶ M. Fathi, Á. Rincón and J. R. Villanueva, “Photons trajectories on a first order scale-dependent static BTZ black hole,” arXiv:1903.09037 [gr-qc].

# Chapter 2

## Scale-dependent black hole in 2+1 dimensions

This chapter was published in *Classical and Quantum Gravity* [56]

### 2.1 Introduction

Gravity in  $(2 + 1)$  dimensions is a vibrant field of research. This is in part due to the fact that the absence of propagating degrees of freedom makes things simpler than in  $(3 + 1)$  dimensions, in particular when dealing with the challenge of formulating a quantization of this theory. Another important feature of gravity in  $(2+1)$  dimensions is the deep connection to Chern-Simons theory [73–75]. This by itself makes the black hole solution [76, 77] found by Bañados, Teitelboim, and Zanelli (BTZ) an extremely interesting research object, which has been generalised in many directions. An additional component that motivates the research on black holes in three dimensions is their prominent role in the context of the AdS/CFT correspondence [78–81].

Despite of some progress, the consistent formulation of quantum gravity remains an open task which is attacked in many different ways [82–98] (for a review see [99]). Even though many approaches to quantum gravity are very different, most of them have the common feature that the resulting effective action of gravity acquires a scale dependence. This means that the couplings appearing in the quantum- effective action (such as Newtons coupling  $G_0$ ,

or the cosmological term  $\Lambda_0$ ) become scale dependent quantities ( $G_0 \rightarrow G_k, \Lambda_0 \rightarrow \Lambda_k$ ). There is quite some evidence that this scaling behavior is in agreement with Weinberg’s Asymptotic Safety program [46, 50, 100–105]. In particular, the effective action and running couplings in three dimensions have been studied in [106, 107]. In any case, scale dependent couplings can be expected to produce differences to classical general relativity, such as modifications of classical black hole backgrounds [53–55, 69, 71, 72, 108–122].

In this chapter the possible effects of scale dependence on the black hole in three dimensional gravity will be investigated in the light of the effective action approach. We will use the scale-field method applied to the Einstein-Hilbert truncation, which allows to derive generalized Einstein equations for the case of scale dependent couplings [52, 123–125]. The theoretical uncertainty concerning the functional form of the scale dependence of  $G_k$  and  $\Lambda_k$  will be avoided. Instead, the most general stationary spherically symmetric solution without angular momentum, which is in agreement with the common “null energy condition” for the effective stress energy tensor, will be derived. It is further shown that this solution corresponds also to the most general case which is in agreement with the “Schwarzschild relation”  $g_{tt} = -1/g_{rr}$ .

The chapter is organized as follows: In subsection 2.1.1 a small collection of basic properties of the classical BTZ solution is presented. In subsection 2.1.2 the concept of effective action with scale dependent couplings is reviewed. In section 2.2 those techniques will be used to derive and discuss a new black hole solution in three dimensions with scale dependent couplings. In subsection 2.2.1 the “null energy condition” for the effective stress energy tensor is formulated and its connection to the “Schwarzschild relation” is reviewed. The solution is presented in subsection 2.2.2, in subsection 2.2.3 the asymptotic behavior of the solution is discussed, the horizon structure is analyzed in subsection 2.2.4, and the thermodynamic properties are discussed in subsection 2.2.5. Results are summarized in section 2.3.

### 2.1.1 The classical BTZ solution without scale dependence

In this subsection the key features such as line element and thermodynamics of the classical BTZ black hole solution [76, 77] will be listed. This summary will be limited to the case of zero angular momentum.

In the metric formulation the gravitational action in three dimensions

$$\mathcal{S}(g_{\mu\nu}) = \int d^3x \sqrt{-g} \frac{(R - 2\Lambda_0)}{16\pi G_0}, \quad (2.1)$$

gives the equations of motion

$$G_{\mu\nu} = -g_{\mu\nu}\Lambda_0, \quad (2.2)$$

where  $\Lambda_0$  is the cosmological constant and  $G_0$  is Newton's constant. For the non rotating BTZ solution, the line element takes the form

$$ds^2 = -f_0(r) dt^2 + f_0(r)^{-1} dr^2 + r^2 d\phi^2, \quad (2.3)$$

with

$$f_0(r) = -G_0 M_0 + \frac{r^2}{\ell_0^2}, \quad (2.4)$$

where  $\Lambda_0 = -1/\ell_0^2$  and  $M_0$  is the mass of the black hole. For this solution the black hole entropy and temperature read

$$S_{BTZ} = 4\pi\ell_0 \sqrt{\frac{M_0}{G_0}}, \quad T_{BTZ} = \frac{\sqrt{M_0 G_0}}{2\pi\ell_0}. \quad (2.5)$$

### 2.1.2 Scale dependent couplings

This subsection summarizes the equations of motion for the scale dependent space-times in three dimensions. The notation and scale setting procedure is according to [52, 123–126].

The scale dependent effective action is

$$\Gamma(g_{\mu\nu}, k) = \int d^3x \sqrt{-g} \frac{(R - 2\Lambda_k)}{16\pi G_k}. \quad (2.6)$$

By varying (2.6) with respect to the metric field one obtains

$$G_{\mu\nu} = -g_{\mu\nu}\Lambda_k + 8\pi G_k T_{\mu\nu}. \quad (2.7)$$

The effective stress energy tensor  $T_{\mu\nu}$  contains the actual matter contribution  $T_{\mu\nu}^m$  and a contribution  $\Delta t_{\mu\nu}$  induced by the possible coordinate dependence of  $G_k$  [52]

$$T_{\mu\nu} = T_{\mu\nu}^m - \frac{1}{8\pi G_k} \Delta t_{\mu\nu}, \quad (2.8)$$

where

$$\Delta t_{\mu\nu} = G_k (g_{\mu\nu} \square - \nabla_\mu \nabla_\nu) \frac{1}{G_k}. \quad (2.9)$$

By varying (2.6) with respect to the scale-field  $k(x)$  one obtains the algebraic equations

$$\left[ R \frac{\partial}{\partial k} \left( \frac{1}{G_k} \right) - 2 \frac{\partial}{\partial k} \left( \frac{\Lambda_k}{G_k} \right) \right] = 0. \quad (2.10)$$

The above equations of motion are consistently complemented by the Bianchi identity, reflecting invariance under coordinate transformations

$$\nabla^\mu G_{\mu\nu} = 0. \quad (2.11)$$

## 2.2 Scale dependent solution without angular momentum

Let us now turn to solving the system of equations (2.7-2.11) assuming a stationary space-time with rotational symmetry and no angular momentum. The most general line element in agreement with this symmetry is

$$ds^2 = -f(r) dt^2 + g(r) dr^2 + r^2 d\phi^2. \quad (2.12)$$

Apart from the two functions  $f(r)$  and  $g(r)$ , the system has to be solved for the scale field  $k(r)$ . In principle this is possible, as soon as the functional form of the scale dependent couplings  $G_k$  and  $\Lambda_k$  is known, for example from some Functional Renormalisation Group (FRG) equation. Those functions have been calculated by using various methods and approximations. However, it has up to now not been possible to obtain an exact and scheme independent expression of the effective average action. Therefore, the functional form of  $\Lambda_k$  and  $G_k$  is subject to very large theoretical uncertainties. This problem is aggravated by the fact that most functional forms of  $\Lambda_k$  and  $G_k$  are either only valid in the UV or in the IR.

Given those drawbacks we will proceed with a method that has been previously applied in four dimensions [52, 123–125]: The first step is to realize that the only appearance of the scale field  $k(r)$  is within the couplings and that for any solution of the system the functions  $\Lambda_k$  and  $G_k$  will inherit a radial dependence from  $k(r)$ . Thus, one might try to solve the system for  $\{f(r), g(r), \Lambda(r), G(r)\}$  (instead of solving for  $\{f(r), g(r), k(r)\}$ ). However, since one dealt one unknown function  $k(r)$  for two unknown functions  $\Lambda(r)$  and  $G(r)$ , the system is underdetermined. In order to obtain a determined system again one has to impose an additional condition.

We therefore stress that in this approach, we shall make no attempt to fix the renormalization scale  $k = k(r)$ . Our strategy is converse: regardless of the specific form of  $k(r)$ , any running-coupling solution will inherit a spatial coupling dependence. Any solution to Einstein's equations that is static, spherically symmetric and fulfills the null-energy condition (see below) must belong to the family of configurations described below. They are determined by four integration constants.

### 2.2.1 The null energy condition (NEC)

The most common type of conditions in classical general relativity are energy conditions [33, 127, 128], where one typically distinguishes between the dominant, weak, strong, and null condition. The less restrictive of those conditions is the null condition, which states that for a null vector field  $l^\nu$  the matter stress energy tensor satisfies

$$T_{\mu\nu}^m l^\mu l^\nu \geq 0. \quad (2.13)$$

Since we are interested in black hole solutions it is crucial to note that the energy condition (2.13) is actually necessary for the proof of fundamental black hole theorems such as the no hair theorem [129] or the second law of black hole thermodynamics [36]. Therefore, if one is looking for black hole solutions that are in agreement with those two fundamental theorems, it is natural to impose that appearance of scale dependence does not spoil or alter this property for the effective stress energy tensor

$$T_{\mu\nu} l^\mu l^\nu \stackrel{!}{=} T_{\mu\nu}^m l^\mu l^\nu \geq 0. \quad (2.14)$$

A physical interpretation of this condition is that one imposes that not even a light-like observer can observe a difference between the energy density due to the presence of matter and the effective energy density due to the combined matter and scale dependence effects. The relation (2.14) holds if one maintains the standard matter condition (2.13) and one further imposes that the extra contribution to the stress tensor (2.9) induced by the variation of the couplings satisfies

$$\Delta t_{\mu\nu} l^\mu l^\nu = 0. \quad (2.15)$$

In a spherically symmetric setting one can solve this condition for the scale dependent coupling (2.12) without the use of the equations of motion (2.7) giving

$$G(r) = a \left[ \int_{r_0}^r \sqrt{f(r') \cdot g(r')} dr' \right]^{-1}, \quad (2.16)$$

where  $a$  and  $r_0$  are constants. The next step consists in finding the metric functions  $f(r)$  and  $g(r)$  which appear in this integral. This can be achieved by a straight forward argument following Jacobson [130]: one can choose the null vector field to be  $l^\mu = \{\sqrt{g}, \sqrt{f}, 0\}$ . Combining the equations of motion (2.7) for this vector field with the condition (2.14) gives in regions without external matter ( $T_{\mu\nu}^m = 0$ )

$$R_{\mu\nu} l^\mu l^\nu = (f \cdot g)' \frac{1}{2rg} = 0 \quad (2.17)$$

and thus  $f \sim 1/g$ . By making use of time reparametrization invariance, this allows to write  $f(r) = 1/g(r)$ , which corresponds to the so called Schwarzschild relation. It is interesting to note that this common relation further ensures that the radius coordinate is an affine parameter on the radial null geodesics [130]. With this relation the line element is

$$ds^2 = -f(r) dt^2 + f(r)^{-1} dr^2 + r^2 d\phi^2 \quad (2.18)$$

and the equations of motion can be completely solved for the three functions  $\{f(r), \Lambda(r), G(r)\}$ .

The necessity of imposing an additional condition arises due to the fact that we avoid using an ansatz for  $G_k$  and  $\Lambda_k$ , (with an additional field variable  $k(r)$ ). Instead we are dealing directly with  $G(r)$  and  $\Lambda(r)$  and thus need an additional constraint. In [53], for the case of a spherically symmetric solutions, this additional constraint was chosen to be the usual Schwarzschild relation  $f \cdot g \equiv 1$ , which can be derived from the null energy condition (2.15).

However, as discussed above, the null energy condition has a stronger physical motivation and a broader applicability, allowing to go beyond spherically symmetric black holes.

### 2.2.2 A non-trivial solution for scale dependent couplings

Based on (2.14) one finds that the equations (2.7) are solved by

$$G(r) = \frac{G_0^2}{G_0 + \epsilon r(1 + G_0 M_0)}, \quad (2.19)$$

$$f(r) = f_0(r) + 2M_0 G_0 \left( \frac{G_0}{G(r)} - 1 \right) \left[ 1 + \left( \frac{G_0}{G(r)} - 1 \right) \ln \left( 1 - \frac{G(r)}{G_0} \right) \right], \quad (2.20)$$

$$\begin{aligned} \Lambda(r) = & \frac{-G(r)^2}{\ell_0^2 G_0^2} \left[ 1 + 4 \left( \frac{G_0}{G(r)} - 1 \right) + \left( 5M_0 G_0 \frac{\ell_0^2}{r^2} + 3 \right) \left( \frac{G_0}{G(r)} - 1 \right)^2 + \right. \\ & 6M_0 G_0 \frac{\ell_0^2}{r^2} \left( \frac{G_0}{G(r)} - 1 \right)^3 + 2M_0 G_0 \frac{\ell_0^2}{r^2} \frac{G_0}{G(r)} \times \\ & \left. \left( 3 \left( \frac{G_0}{G(r)} - 1 \right) + 1 \right) \left( \frac{G_0}{G(r)} - 1 \right)^2 \ln \left( 1 - \frac{G(r)}{G_0} \right) \right], \end{aligned} \quad (2.21)$$

where  $G_0, M_0, \ell_0, \epsilon$  are four integration constants. This represents a family of solutions that includes the classical BTZ black hole: the choice of the integration constants was made by demanding that the classical BTZ solution is recovered when one dimensionless constant (labeled  $\epsilon$ ) vanishes. Indeed, one easily verifies that

$$\lim_{\epsilon \rightarrow 0} G(r) = G_0, \quad (2.22)$$

$$\lim_{\epsilon \rightarrow 0} f(r) = -G_0 M_0 + \frac{r^2}{\ell_0^2}, \quad (2.23)$$

$$\lim_{\epsilon \rightarrow 0} \Lambda(r) = -\frac{1}{\ell_0^2} \quad (2.24)$$

which justifies the naming of the constants ( $G_0, M_0, \Lambda_0 = -1/\ell_0^2$ ) in terms of their meaning in the absence of scale dependence. The connection between the new solution and the BTZ solution is given in terms of the difference between the “running”  $G(r)$  and the fixed  $G_0$ . One further verifies the transition to empty  $AdS_3$  space for the classical “mass gap” relation

$$M_0 \rightarrow -\frac{1}{G_0}$$

$$\lim_{\substack{\epsilon \rightarrow 0 \\ M_0 \rightarrow -1/G_0}} G(r) = G_0, \quad (2.25)$$

$$\lim_{\substack{\epsilon \rightarrow 0 \\ M_0 \rightarrow -1/G_0}} f(r) = 1 + \frac{r^2}{\ell_0^2}, \quad (2.26)$$

$$\lim_{\substack{\epsilon \rightarrow 0 \\ M_0 \rightarrow -1/G_0}} \Lambda(r) = -\frac{1}{\ell_0^2} \quad (2.27)$$

Note that in this limit, all dependence on  $\epsilon$  vanishes. Thus,  $AdS_3$  constitutes the appropriate vacuum of the theory, which is invariant under perturbations due to the running of the couplings controlled by  $\epsilon$ . Note further that  $M_0$  is the mass of the black hole only if  $\epsilon \rightarrow 0$ , while for  $\epsilon \neq 0$  it is much harder to determine the mass. We will come back to this point at the end of section 2.2.

Since the constant  $\epsilon$  controls the strength of the new scale dependence effects, in some cases it is useful to treat it as small expansion parameter

$$\begin{aligned} G(r) &= G_0 - \epsilon \cdot (1 + G_0 M_0)r + \mathcal{O}(\epsilon^2), \\ f(r) &= -G_0 M_0 + \frac{r^2}{\ell_0^2} + 2\epsilon \cdot M_0(1 + G_0 M_0)r + \mathcal{O}(\epsilon^2), \\ \Lambda(r) &= -\frac{1}{\ell_0^2} - \epsilon \cdot \frac{2r}{\ell_0^2 G_0}(1 + G_0 M_0) + \mathcal{O}(\epsilon^2). \end{aligned} \quad (2.28)$$

In figure 2.1 the lapse function  $f(r)$  is shown for different values of  $\epsilon$  in comparison to the classical BTZ solution.

As can be seen in the solution (2.19)-(2.21), one observes that  $f(r)$  is monotonically growing for all chosen values of  $\epsilon$ , that  $\lim_{r \rightarrow 0} f(r) = -G_0 M_0$  independent of  $\epsilon$ , and that all functions grow as  $\sim r^2$  for large values of  $r$ . One further notes that, even though  $\lim_{\epsilon \rightarrow 0} f(r) = -G_0 M_0 + r^2/\ell_0^2$ , the first derivative of  $f(r)$  at the origin is strongly dependent on  $\epsilon$ . As discussed below, the non vanishing of this derivative induced by  $\epsilon$  produces a curvature singularity at the origin proportional to  $\epsilon$ .

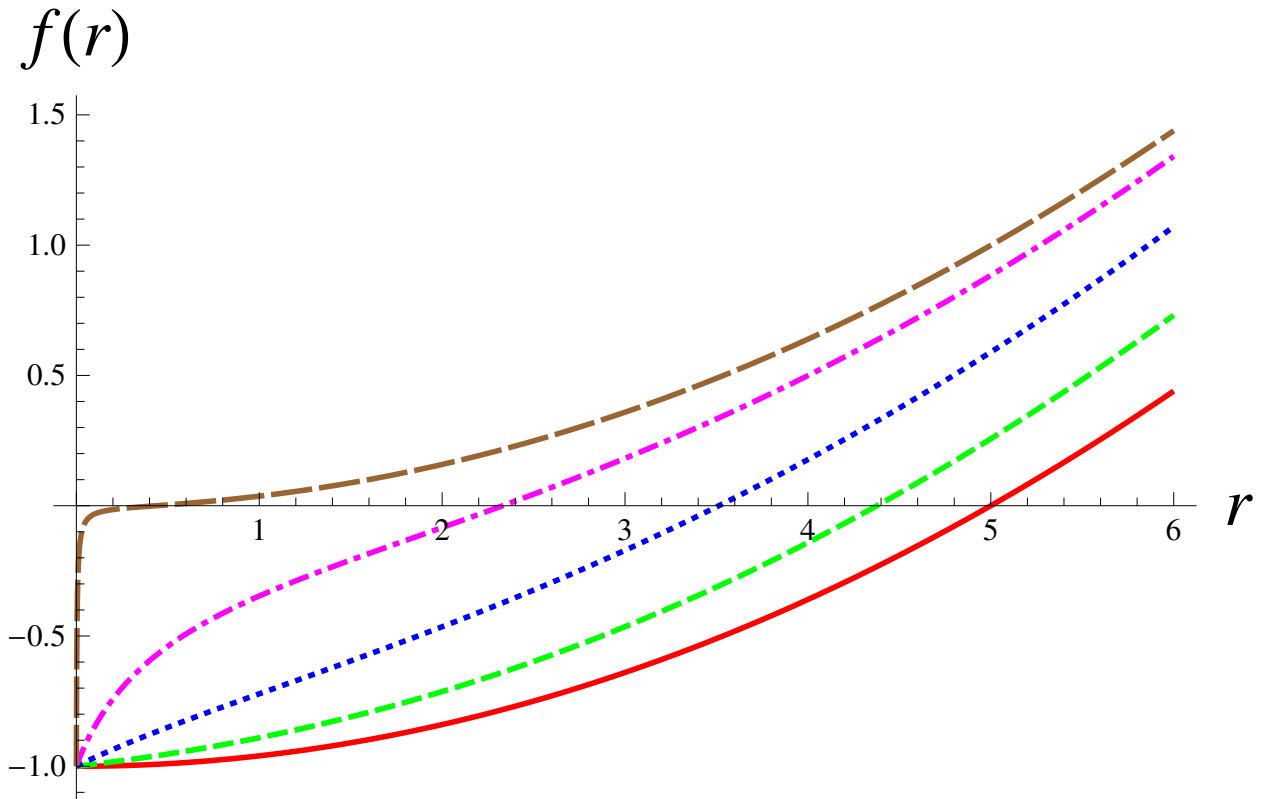


**Figure 2.1:** Radial dependence of the lapse function  $f(r)$  for  $\ell_0 = 5$ ,  $G_0 = 1$  and  $M_0 = 1$ . The different curves correspond to the classical case  $\epsilon = 0$  solid red line,  $\epsilon = 0.02$  short dashed green line,  $\epsilon = 0.09$  dotted blue line,  $\epsilon = 0.5$  dot-dashed magenta line, and  $\epsilon = 100$  long dashed brown line.

### 2.2.3 Asymptotic space-times

For small radial coordinate a new singularity appears, which is absent in the classical BTZ solution. This can be verified by evaluating for example the invariant Ricci scalar for the metric ansatz (2.18)

$$R = -f''(r) - 2\frac{f'(r)}{r}, \quad (2.29)$$

in the limit of  $r \rightarrow 0$ . One finds that the leading terms are

$$R = -4M_0\epsilon(1 + G_0M_0) \cdot \frac{1}{r} - \left( \frac{6}{\ell_0^2} + 10\frac{M_0}{G_0}(1 + G_0M_0)^2\epsilon^2 \right) + \mathcal{O}(r^1). \quad (2.30)$$

This quantity is divergent for  $\epsilon \neq 0$  and it is finite for  $\epsilon = 0$ . In particular, when  $\epsilon = 0$  one recovers the classical Ricci scalar for BTZ solution  $R_0 = -6/\ell_0^2$ .

It is surprising that allowing for scale dependent couplings results in the appearance of a singularity, which was absent in the classical solution. This effect was also observed in [53–55, 72, 120, 121]. The reason is that only a very particular class of lapse functions renders the Ricci scalar finite at the origin. This can be seen by solving the relation (2.29) for finite and constant  $R = b$  at  $r \rightarrow 0$ . The solution to this is

$$f(r) \approx c_1 + \frac{c_2}{r} - \frac{br^2}{6}. \quad (2.31)$$

This shows that any lapse function which has a linear term in  $r$  (or any other power  $r^n$  with  $n \leq 2$  and  $n \neq \{-1, 0\}$ ) necessarily produces a divergence in the Ricci scalar at  $r \rightarrow 0$ . For the solution (2.20), the problematic linear term can be seen in the expansion (2.28).

Concerning the limit  $r \rightarrow \infty$ , the exact solution (2.20) is asymptotically  $AdS_3$ :  $f(r) \sim \frac{r^2}{\ell_0^2}$  at leading order in  $r$ . But although asymptotically the metric behaves as BTZ, neither  $\Lambda(r)$  nor  $G(r)$  mimic their BTZ analogs. Indeed,  $\Lambda(r) = -3/\ell_0^2 = 3\Lambda_0$  at  $r \rightarrow \infty$ . This 'effective' cosmological constant at infinity arises from the extra term in Einstein's equation. Evaluating this term for the solution in the large  $r$  regime, one has

$$\Delta t_{\mu\nu}|_{r \rightarrow \infty} = \frac{2}{\ell_0^2} g_{\mu\nu}. \quad (2.32)$$

When analyzing such asymptotics one has to be careful since even though  $\epsilon$  is a small dimensionless parameter, other quantities like  $\epsilon r/G_0$  might actually become large at large radial coordinates. On the other hand, it is clear from (2.19) that the behavior of  $G(r)$  possesses two very different regimes: for  $\epsilon r(1 + M_0 G_0) \ll G_0$ , it behaves effectively as a constant  $G_0$ , while for  $\epsilon r(1 + M_0 G_0) \gg G_0$  it falls to zero. To consider this latter non-standard regime, one performs an expansion of the lapse function (2.20), where the smallness parameter is  $\frac{G(r)}{G_0} \ll 1$ . This yields, at first order,

$$\begin{aligned} f|_{G \ll G_0}(r) &\approx \left(\frac{r}{\ell_0}\right)^2 - \frac{2}{3} M_0 G(r) \\ &= \left(\frac{r}{\ell_0}\right)^2 - \frac{2}{3} M_0 G_0 \frac{G_0}{(1 + M_0 G_0) \epsilon r}. \end{aligned} \quad (2.33)$$

where  $\ell_0$  remains arbitrary. We shall use this approximation for the analysis of the next sections.

## 2.2.4 Horizon structure

Horizons are crucial for understanding the structure of a black hole. Unfortunately, the zero of the lapse function (2.20) implies a transcendental equation for  $r$ , which can not be solved analytically. We approach this problem in three different ways: First, we study the leading corrections with respect to the classical regime ( $\epsilon$  small). Second, we focus on a specific region of parameter space that exhibits a particularly interesting strong scale dependence effects, namely  $G(r)/G_0 \ll 1$ , that display some novel features. Third, those two approaches are compared with a numerical analysis.

- Expansion in  $\epsilon \ll 1$ : For weak scale dependence one can use the expansion (2.28), for which one finds the horizon

$$r_h|_{\epsilon \ll 1} = \sqrt{G_0 M_0} \ell_0 - \epsilon \ell_0^2 M_0 (1 + G_0 M_0) + \mathcal{O}(\epsilon^2). \quad (2.34)$$

Unfortunately, an analytic result is again limited to order  $\epsilon$ . One sees that the scale dependence tends to decrease the apparent horizon radius.

- Expansion in  $G(r_h)/G_0 \ll 1$ : from (2.19), Newton's coupling evaluated at the horizon will be much smaller than its classical value provided that

$$\epsilon r_h (1 + M_0 G_0) \gg G_0 \quad (2.35)$$

In this limit the horizon can be obtained from (2.33). It is the real root of

$$r_h^3|_{G(r)/G_0 \ll 1} \approx \frac{2}{3} \frac{M_0 G_0^2 \ell_0^2}{(1 + M_0 G_0) \epsilon}. \quad (2.36)$$

For consistency, this must satisfy (2.35). Therefore, (2.35) and (2.36) will hold valid if the parameters satisfy the condition:

$$\frac{M_0 (1 + M_0 G_0)^2 \epsilon^2 \ell_0^2}{G_0} \gg 1 \quad (2.37)$$

A particularly interesting region of the parameter space is  $M_0 G_0 \gg 1$ . Indeed, provided that (2.37) is satisfied in this limit, namely, if

$$M_0 G_0 \gg 1 \quad \text{and} \quad (\epsilon \ell_0)^2 \gg \frac{1}{M_0^3 G_0} \quad (2.38)$$

then, the radius of the horizon converges to a finite value,

$$r_h^3 \Big|_{G(r)/G_0 \ll 1 \ \& \ M_0 G_0 \gg 1} \approx \frac{2}{3} \frac{G_0 \ell_0^2}{\epsilon} \quad (2.39)$$

We thus see the crucial difference with its constant-coupling counterpart: for a fixed cosmological constant, the radius of the horizon remains finite as  $M_0 \rightarrow \infty$ . In the light of this result one should keep in mind that  $M_0$  is only the mass parameter for the classical solution and it is not the actual mass of the black hole. However, in the next section we show that for the particular case when (2.38) is valid, the physical mass indeed diverges as  $M_0 \rightarrow \infty$ , and nevertheless the horizon remains at finite constant distance from the origin (note however that, as  $\epsilon \rightarrow 0$ , the horizon radius becomes unbounded). We shall come back to this case below.

- Numerical analysis: For given values, the above analytical estimates can be compared with a numerical solution of  $f(r) \stackrel{!}{=} 0$ . In figure 2.2 the horizon  $r_h$  is shown as a function of the classical mass parameter  $M_0$ .

One observes that for small  $M_0$ , the horizon is in agreement with the classical result. Finally, one notes that for very large values of  $M_0$  the numerical value of the horizon saturates at constant  $r_h$  which is given by the horizontal line in accordance with the  $G \ll G_0$  approximation (2.36).

## 2.2.5 Black hole thermodynamics

After having gained knowledge on the horizon structure one can now turn towards the thermodynamic properties of the solution (2.19-2.21). The temperature of a black hole with the metric structure (2.18) is given by

$$T = \frac{1}{4\pi} \frac{\partial f(r)}{\partial r} \Big|_{r=r_h}. \quad (2.40)$$

Leaving the horizon radius implicit one finds

$$T = \frac{1}{2\pi r} \frac{G_0^2 M_0}{G_0 + r\epsilon(1 + G_0 M_0)} \Big|_{r=r_h}. \quad (2.41)$$

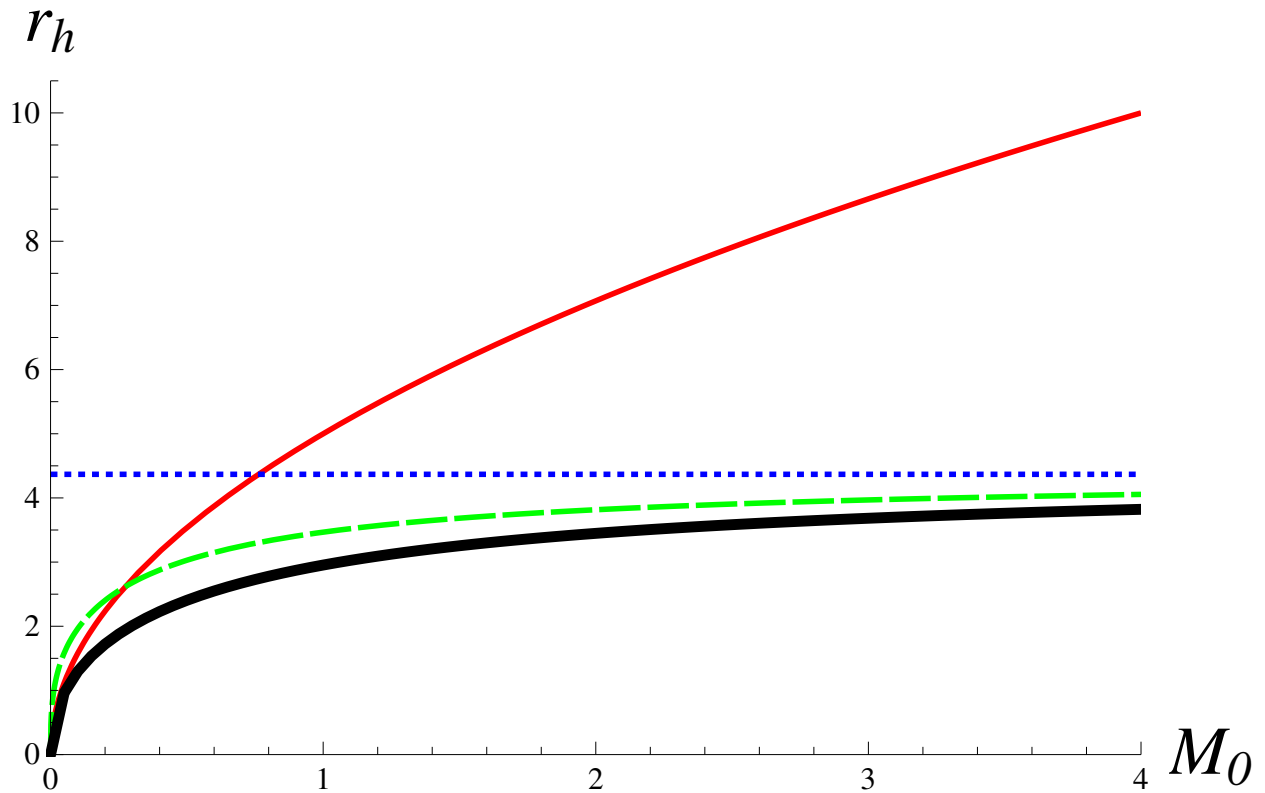


**Figure 2.2:** Apparent black hole horizon  $r_h$  as a function of  $M_0$  for  $\ell_0 = 5$ ,  $G_0 = 1$  and  $\epsilon = 0.2$ . The different curves correspond to the classical case (solid red line) the expansion (2.36) for small  $G/G_0$  (long dashed green line) the expansion (2.39) for small  $G/G_0$  and large  $G_0 M_0$  (dotted blue line), and the numerical solution (thick solid black line). The expansion (2.34) for small  $\epsilon$  is not shown since for the given numerical values it would only be reliable for very small  $M_0 < 0.2$ .

Inserting the perturbative value for the horizon radius (2.34) one finds that the  $\mathcal{O}(\epsilon)$  corrections to the temperature cancel out and that the leading correction to the classical temperature enters at order  $\epsilon^2$

$$T|_{\epsilon \ll 1} = \frac{\sqrt{G_0 M_0}}{2\pi \ell_0} + \mathcal{O}(\epsilon^2). \quad (2.42)$$

The transcendent structure of the solution does not allow to go straight forwardly beyond this  $\mathcal{O}(\epsilon)$  approximation. However, in the opposite limit the lapse function becomes polynomial again, and one can again explore the non-classical case considered above, (2.37), namely  $G \ll G_0$  and one finds from (2.33) that

$$T|_{G \ll G_0} \approx \frac{1}{4\pi} \left( 18 \frac{M_0 G_0^2}{\ell_0^4 (1 + G_0 M_0) \epsilon} \right)^{1/3}, \quad (2.43)$$

And again, within this scenario, for the particular regime of interest (2.38), the temperature converges to a constant,

$$T|_{G \ll G_0 \text{ \& } G_0 M_0 \gg 1} \approx \frac{1}{4\pi} \left( 18 \frac{G_0}{\ell_0^4 \epsilon} \right)^{1/3}. \quad (2.44)$$

for any finite  $\epsilon, \ell_0$ . Those analytical results can again be compared to a numerical solution of (2.41). In figure 2.3 the numerical temperature is shown as a function the parameter  $M_0$  in comparison to the analytical and classical results. One finds that the temperature behavior as a function of  $M_0$  is actually a rescaled version of the horizon radius in figure 2.2. This is a particularity of the three dimensional case. One further sees that for small  $M_0$ , the numerical curve of the new solution approaches the behavior of the classical BTZ case. However, in the opposite limit of large  $M_0$  the temperature of the new solution saturates at the values given by the approximations (2.43 and 2.44).

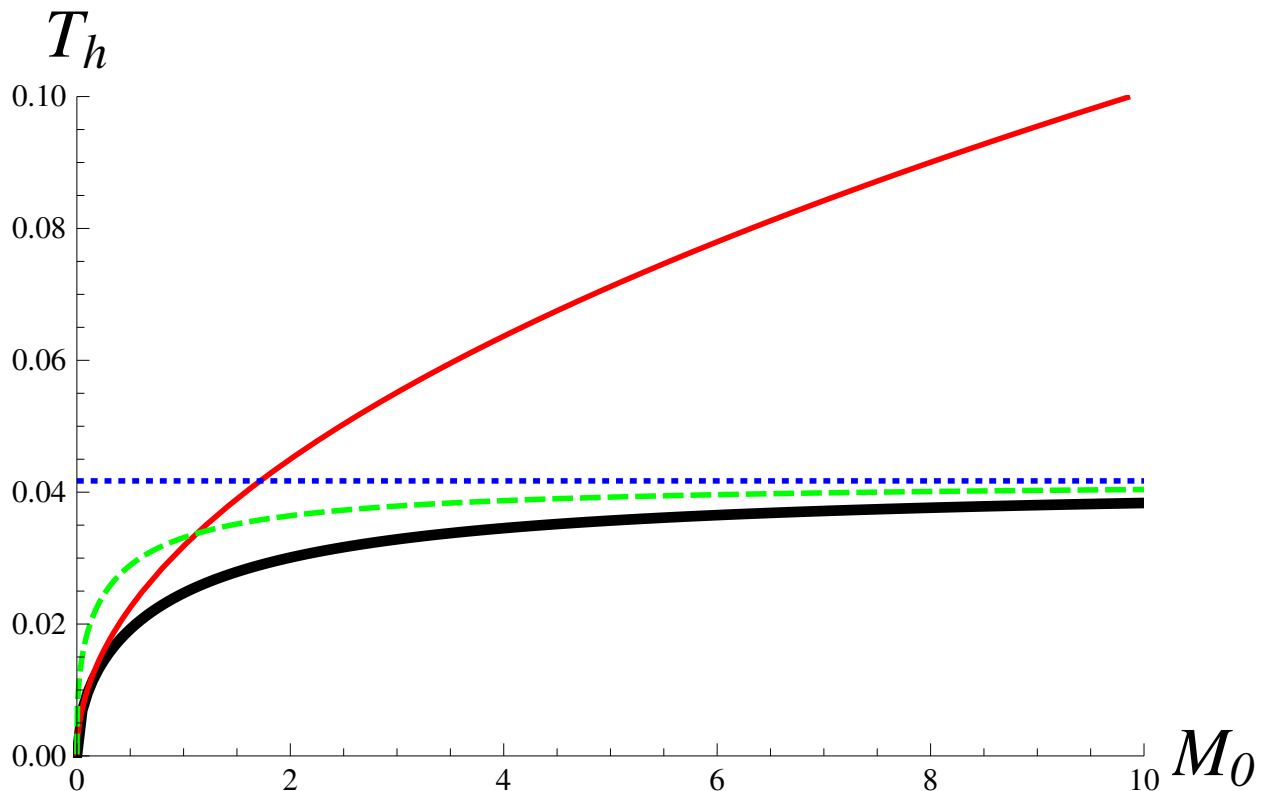


**Figure 2.3:** Temperature  $T_h$  as a function of  $M_0$  for  $\ell_0 = 5$ ,  $G_0 = 1$ , and  $\epsilon = 0.2$ . The different curves correspond to the classical case (thin solid red line), the expansion (2.43) for small  $G/G_0$  (dashed green line), the expansion (2.44) for small  $G/G_0$  and large  $G_0 M_0$  (dotted blue line), and the numerical solution (thick solid black line).

Another window for the understanding the thermodynamic properties of a black hole is its entropy. As it is well known from Brans-Dicke theory [131–135], the entropy of black hole

solutions in  $D + 1$  spacetime dimensions with varying Newton's constant is given by

$$S = \frac{1}{4} \oint_{r=r_h} d^{D-1}x \frac{\sqrt{h}}{G(x)}, \quad (2.45)$$

where  $h_{ij}$  is the induced metric at the horizon  $r_h$ . For the present spherically symmetric solution this integral is trivial. The induced metric for constant  $t$  and  $r$  slices is simply  $ds = rd\phi$  and moreover  $G(x) = G(r_h)$  is constant along the horizon due to spherical symmetry. Therefore, the entropy for this solution is

$$S = \frac{A}{4G(r_h)} = \frac{A}{4G_0} \left[ 1 + \frac{(1 + G_0 M_0) \epsilon r_h}{G_0} \right]. \quad (2.46)$$

where  $A = \oint_{r_h} d^2x \sqrt{h} = 2\pi r_h$ . We notice that the correction to the entropy is not of the form expected from many other quantum gravity programs, namely proportional to  $\ln(A)$ .

As expected, the entropy behaves differently in the two regimes highlighted above. Those two regimes can be addressed by the corresponding approximations  $\epsilon \ll 1$  or  $G \ll G_0$ . For very small scale dependence effects ( $\epsilon \ll 1$ ) one finds that the  $\mathcal{O}(\epsilon)$  contribution cancels out, leaving the classical BTZ entropy up to subleading corrections

$$S|_{\epsilon \ll 1} = \frac{\pi}{2} \sqrt{\frac{M_0}{G_0}} \ell_0 + \mathcal{O}(\epsilon^2). \quad (2.47)$$

and the entropy obeys the holographic principle according to the Bekenstein-Hawking law. This result can also be read directly from (2.46) in the limit of  $(1 + G_0 M_0) \epsilon r_h \ll G_0$ .

The opposite limit is however much more interesting. If the condition (2.37) is satisfied, namely if the parameters satisfy (2.38), the holographic principle is not fulfilled in its usual form. The black hole entropy is not any more proportional to the area, but rather the area times the horizon radius, which is of course due to the variation of  $G(r)$ . Indeed, by inserting (2.35) into (2.46), the leading contribution to the entropy is

$$\begin{aligned} S|_{G \ll G_0} &\approx \frac{A}{4G_0} \left( \frac{1 + M_0 G_0}{G_0} \right) \epsilon r_h \\ &\approx \pi \left[ \frac{\ell_0^4 M_0^2 (1 + M_0 G_0) \epsilon}{18 G_0^2} \right]^{1/3}. \end{aligned} \quad (2.48)$$

Moreover, in the regime  $M_0 G_0 \gg 1$ , this further reduces to

$$S|_{G \ll G_0 \text{ \& } G_0 M_0 \gg 1} \approx \frac{A}{4G_0} M_0 \epsilon r_h = \pi M_0 \left( \frac{\ell_0^4 \epsilon}{18G_0} \right)^{1/3} \quad (2.49)$$

This transition from an “area law” to an “area  $\times$  radius law” is a very striking consequence of the simple assumption of allowing for scale dependent couplings. Actually, it can be shown that this feature occurs for all spacetime dimension  $d \geq 3$ . Indeed, if the parameters of the scale-dependent Schwarzschild-AdS $_d$  solution satisfy a condition analogous to (2.37), the leading term in the entropy of the black hole scales not as  $r_h^{d-1}$  but as  $r_h^d$ .

Since the entropy (2.46) is directly given from the knowledge of the horizon radius  $r_h$  it is straight forward to implement the graphical analysis of the approximations (2.36, 2.39) in comparison to the numerical result. This is done in figure 2.4. One notes again that the classical behavior is dominant for small  $M_0$ , while for large  $M_0$  a different scaling behavior appears, which is given by the approximations (2.48) and (2.49) respectively.

Lets now come back to the physical mass of the black hole  $M$ . As the discussion above showed, the classical mass parameter  $M_0$  is actually only the mass of the black hole if  $G \rightarrow G_0$

$$M|_{G \rightarrow G_0} = M_0. \quad (2.50)$$

In general the physical mass differs from the mass parameter,  $M \neq M_0$ , but it is a very difficult task to express it in a closed form. However, for the non-classical regime  $G \ll G_0$  considered above, we posses analytic expressions. What is the actual mass in this regime? This question can be answered by integrating the thermodynamic relation

$$dM = TdS, \quad (2.51)$$

which yields

$$M - m = \frac{1}{4} \left( M_0 + \frac{1}{G_0} - \frac{1}{3G_0} \ln(1 + M_0 G_0) \right) \quad (2.52)$$

where  $m$  is a constant of integration independent of  $M_0$ , irrelevant for these purposes. This proves the statement claimed earlier, that for fixed values of  $\epsilon$ ,  $G_0$ ,  $\ell_0$  the limit of  $M_0 \rightarrow \infty$  implies, according to (2.52), that the physical mass grows without bound as  $M \sim M_0 \rightarrow \infty$ , and nevertheless the horizon converges to the finite distance given in (2.39).

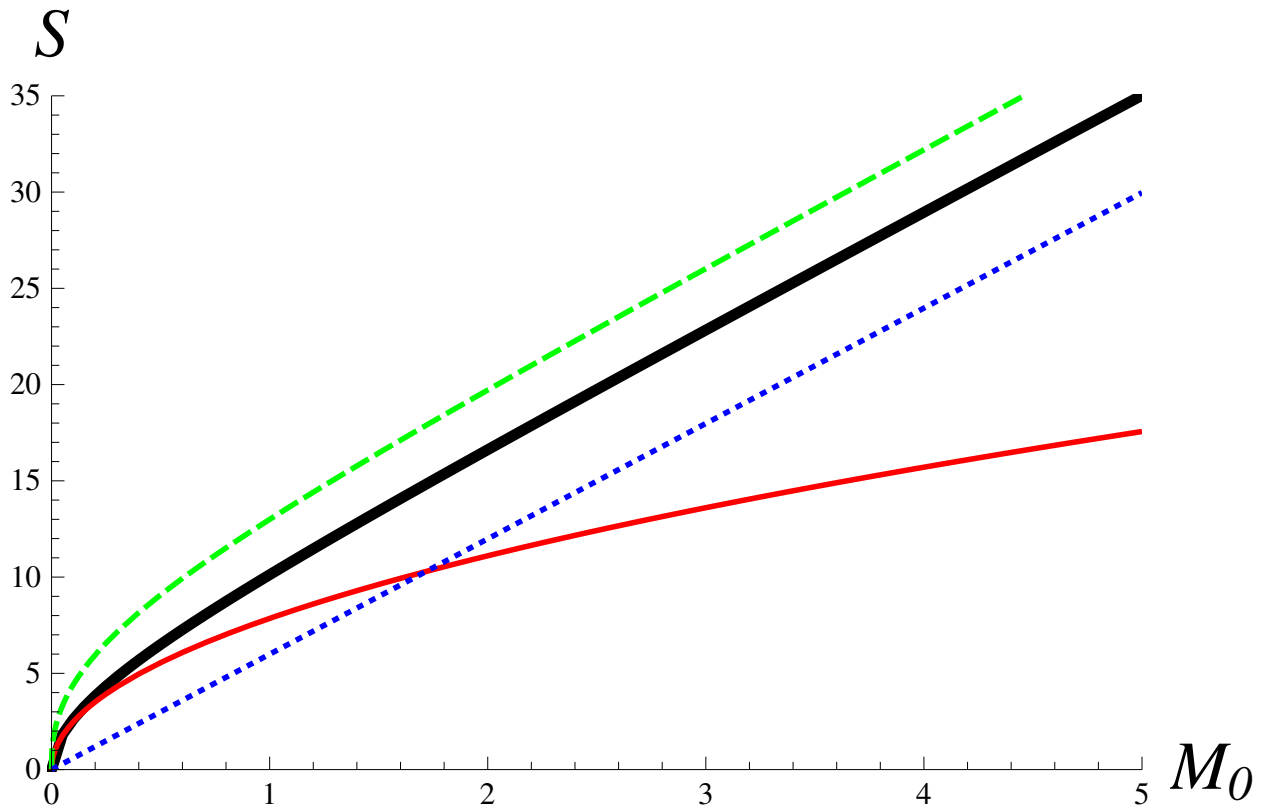


**Figure 2.4:** Entropy as a function of  $M_0$  for  $\ell_0 = 5$ ,  $G_0 = 1$ , and  $\epsilon = 0.2$ . The different curves correspond to the classical case (thin solid red line), the expansion for small  $G/G_0$  (dashed green line), the expansion for small  $G/G_0$  and large  $G_0 M_0$  (dotted blue line), and the numerical solution (thick solid black line).

Since our initial input was the condition (2.14), it would be very interesting to analyse this result in future studies in the context of the “Quantum Null Energy Conjecture” [136–140].

## 2.2.6 Comparison to the four dimensional solution

In [53] the scale-dependent 3 + 1 black hole was considered. In both cases, the solution for Newton’s coupling was of the form  $G(r) = G_0/(1 + \alpha r)$  with  $\alpha$  an integration constant. This is not a coincidence: it can be readily shown that in any dimension the gravitational coupling takes this form [56]. Also, as shown above, both the three and four dimensional solutions develop a singularity of the curvature scalar at the origin. However, the effect mentioned after (2.52) was only discussed for the three dimensional solution. It might actually not be the case in four dimensions, because the mass plays a very different role in the three dimensional problem as it does in higher dimensions.

## 2.3 Summary and Conclusion

A possible scale dependence of the gravitational coupling introduces an additional contribution to the stress energy tensor of the generalized field equations (2.7). By imposing that the usual “null energy condition” is not modified by this contribution it is shown that in those cases any stationary solution with spherical symmetry necessarily follows the “Schwarzschild relation”  $g_{tt} = -1/g_{rr} \equiv f(r)$ . Based on this observation an exact spherically symmetric black hole solution for three dimensionally gravity with scale dependent couplings is derived. It is shown that the functional form of  $f(r)$ , of Newtons coupling  $G(r)$ , and of the cosmological coupling  $\ell(r)$  is completely determined by the field equations. The properties of the solution are analyzed from various perspectives. Particular attention is dedicated to a meaningful interpretation of the integration constants which is given in terms of the classical parameters  $G_0$ ,  $\ell_0$ ,  $M_0$  and one additional constant  $\epsilon$ , that parametrizes the strength of scale dependence. Asymptotic spacetimes, horizon structure, and black hole thermodynamics are discussed in detail. It is found that the large  $r$  asymptotic is  $AdS_3$  and that the  $r \rightarrow 0$  asymptotic has a singular behavior. It is found that for fixed values of  $\epsilon$ ,  $G_0$ ,  $\ell_0$  the horizon radius saturates for  $M_0 \rightarrow \infty$  to a finite value given by (2.39). Although  $M_0$  is not equal to the physical mass of the black hole in general, in the limit of  $G \ll G_0$  &  $G_0 M_0 \gg 1$  the physical mass  $M$  grows without bound as  $M_0 \rightarrow \infty$ , while the radius of the horizon still converges to (2.39). The analysis of the thermodynamics showed another novel result. Whereas for small black holes, the usual “area law” holds up to order  $\mathcal{O}(\epsilon)$ , the opposite limit (which occurs when  $G(r)$  deviates strongly from  $G_0$ ) follows an “area  $\times$  radius law”. This apparent deviation from the holographic principle is probably the most interesting feature of this new black hole solution with scale dependent couplings.

# Chapter 3

## Scale–dependent rotating black hole in $2+1$ dimensions

This chapter was published in *The European Physical Journal C* [64]

### 3.1 Introduction

To formulate a consistent and predictive quantum theory of gravity (QG) is one of the mayor challenges for the community seeking a unified description of the known fundamental interactions. Currently, at least 16 major approaches to quantum gravity have been proposed in the literature (see [141] and references therein), but none of these approaches have reached the goal in a completely satisfactory way.

In this chapter we contribute to the topic of quantum gravity by studying black hole solutions of effective scale–dependent gravity in  $2 + 1$  dimensions. We thus, combine three different aspects, namely, scale dependence, gravity in  $2+1$  dimensions and black holes. Each of those aspects hast a motivation of its own, but all of those aspects have an important motivation from the perspective of quantum gravity:

- Black holes (**BHs**):

Black Holes are objects of paramount importance in gravitational theories [142]. They allow to study gravitational systems at the transition between a quantum and a classical

regime as for example through the the famously predicted Hawking radiation [34, 35]. BHs are thus excellent laboratories to investigate and understand several aspects of general relativity at the transition between a classical and quantum regime [143].

- 2 + 1 dimensions:

It can be expected that the features of a successful solution of the problem of quantum gravity are universal for gravitational theories of different dimensionality. Since gravity in 2 + 1 dimensions is mathematically less involved than in 3 + 1 dimensions, this lower dimensional theory is a good toy model if one aims to understand the underlying mechanisms of full quantum gravity in 3 + 1 dimensions. Apart from this motivation by quantum gravity, the study of gravity in 2 + 1 dimensions is of interest because of its deep connection to Chern-Simons theory [73, 75] and because of its applications in the context of the AdS/CFT correspondence [78–81]. Within this lower dimensional gravitation theory the black hole solution found by Bañados, Teitelboim, and Zanelli (BTZ) [76, 77] plays a crucial role.

- Scale dependence (**SD**):

Before actually attacking the whole problem of QG with all its different, and up to now limited, realizations, one can begin with a more modest approach and concentrate on generic common features, which are expected from such a theory. One feature which is shared by most of the candidate theories for quantum gravity (actually by most quantum field theories) is that they predict a scale dependence of the coupling constants in the corresponding effective action. Luckily there is a well defined formalism which allows to deduce background solutions from a given effective action. We will follow those techniques which have been previously probed with a variety of problems [53, 55–60, 65, 67, 123, 125, 126, 144, 145]. In this chapter we aim to study the dominant effects such a scale dependence could have on the BTZ black hole in the Einstein Hilbert truncation of the effective action of gravity in 2+1 dimensions. By using a well defined method which is based on the variational principle one can explore leading local effects of quantum gravity on a rotationally symmetric space-time in a source free region (like BTZ), even without the knowledge of the exact underlying theory.

The important connection of those three ingredients with the underlying topic of QG is shown in figure 3.1, showing clearly that the study of corrections to the classical BTZ solution, as those derived in this chapter, are a key test for any theory of QG.

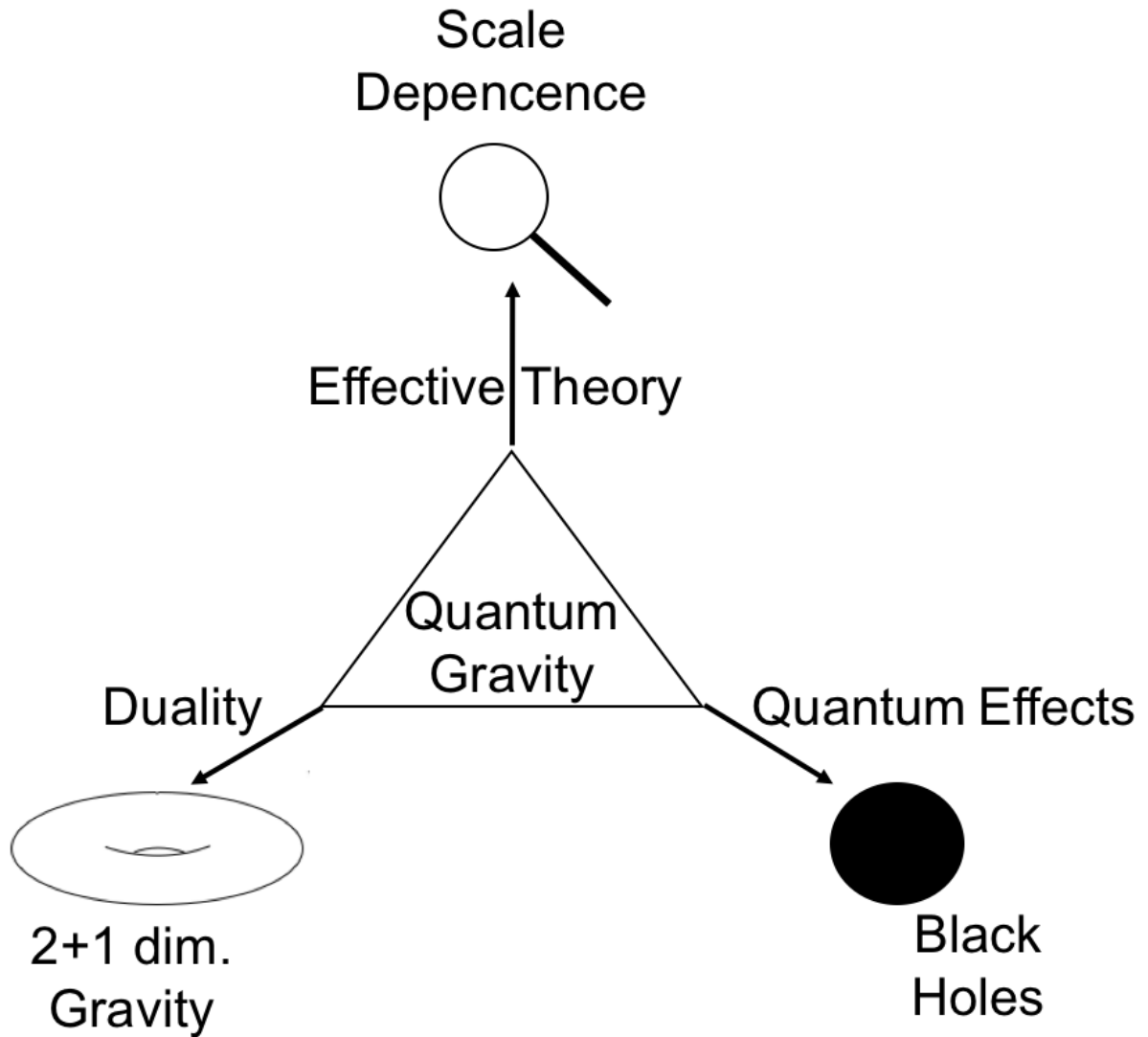


**Figure 3.1:** Conceptual flow chart for the interplay of SD, BHs, and 2 + 1 dimensions with QG.

What is more, the idea of the inclusion of quantum effects via scale-dependent coupling is the main lesson learned from renormalization group. Certainly, different approaches try to deal with deviations from classical gravity and many of them including scale dependent couplings (e.g., Brans–Dicke theory,  $f(R)$  gravity, RG improvement, and many others). We can then allow a more complicated action assuming constant coupling constants or take a standard action and allow the couplings to evolve. We prefer this second option inspired by the renormalization group.

This chapter is organized as follows: after this introduction, we present the action and the classical BTZ solution in the next section. Then, the general framework of this work is

introduced in section 3.3. The scale dependence for a rotating BTZ black hole is presented in section 3.4. The behaviour of the Ricci scalar, the asymptotic space-time as well as the thermodynamics is investigated in Sect. 3.5 and 3.6 respectively. The discussion of this result and remarks are shown in section 3.7. The main ideas and results are summarized in the conclusion section 3.8. Note that throughout the chapter we will use natural units with ( $c = \hbar = k_B = 1$ ).

## 3.2 Classical BTZ solution with $J_0 \neq 0$

This section reminds of some key features of the classical BTZ black hole solution [76, 77], such as line element, event horizons, and thermodynamics. Besides, the contribution of angular momentum will be considered focussing on the extremal black hole case. The minimal coupling between gravity and matter is described by the the Einstein Hilbert action

$$I_0[g_{\mu\nu}] = \int d^3x \sqrt{-g} \left[ \frac{1}{2\kappa_0} (R - 2\Lambda_0) + \mathcal{L}_M \right], \quad (3.1)$$

where  $g_{\mu\nu}$  is the metric field,  $R$  is the Ricci scalar,  $\kappa_0 \equiv 8\pi G_0$  is the gravitational coupling,  $\Lambda_0$  is the cosmological constant,  $\mathcal{L}_M$  is the matter Lagrangian, and  $g$  is the determinant of the metric field. The classical Einstein field equations are obtained from (3.1) by varying the action with respect to the metric field

$$G_{\mu\nu} + \Lambda_0 g_{\mu\nu} = \kappa_0 T_{\mu\nu}, \quad (3.2)$$

where  $T_{\mu\nu}$  is the energy momentum tensor associated to a matter source

$$T_{\mu\nu} \equiv T_{\mu\nu}^M = -2 \frac{\delta \mathcal{L}_M}{\delta g^{\mu\nu}} + \mathcal{L}_M g_{\mu\nu}. \quad (3.3)$$

For the case of rotational symmetry without any matter contribution, the metric solution of (3.2) takes the form

$$ds^2 = -f_0(r) dt^2 + f_0(r)^{-1} dr^2 + r^2 \left[ N_0(r) dt + d\phi \right]^2. \quad (3.4)$$

Here,  $f_0(r)$  and  $N_0(r)$  are the lapse function and the shift function respectively, which are given by

$$f_0(r) = -8M_0G_0 + \frac{r^2}{\ell_0^2} + \frac{16G_0^2J_0^2}{r^2}, \quad (3.5)$$

$$N_0(r) = -\frac{4G_0J_0}{r^2}, \quad (3.6)$$

where  $\ell_0$  is defined by  $\Lambda_0 \equiv -1/\ell_0^2$ . The two constants of integration  $M_0$  and  $J_0$  are the conserved charges associated to asymptotic invariance under time shifts (mass) and rotations (angular momentum) respectively. The horizons

$$(r_0^\pm)^2 = 4G_0M_0\ell_0^2[1 \pm \Delta], \quad (3.7)$$

are defined through the condition  $f(r_0^\pm) = 0$ . Here, the parameter  $\Delta$  encodes the impact of the rotational contribution on the event horizon

$$\Delta = \sqrt{1 - \left(\frac{J_0}{M_0\ell_0}\right)^2}. \quad (3.8)$$

The positive root  $r_0^+$  is the black hole's outer horizon. One can express the lapse function in terms of the event horizons

$$f_0(r) = \frac{1}{\ell_0^2 r^2} \left[ (r^2 - (r_0^+)^2)(r^2 - (r_0^-)^2) \right]. \quad (3.9)$$

It is important to note that, the parameters must satisfy

$$M_0 > 0, \quad \wedge \quad |J_0| \leq M_0\ell_0, \quad (3.10)$$

in order to get physical solutions. When the classical angular momentum takes a maximum value given by

$$J_0^{\max} = M_0\ell_0, \quad (3.11)$$

the solution is called an extremal black hole. Regarding black hole thermodynamics, the Bekenstein-Hawking entropy is given by

$$S_0(r_0^+) = \frac{\mathcal{A}_H(r_0^+)}{4G_0}. \quad (3.12)$$

The corresponding Hawking temperature is

$$T_0(r_0^+) = \frac{1}{4\pi} \left| \frac{16G_0 M_0}{r_0^+} \Delta \right|, \quad (3.13)$$

where  $\mathcal{A}_H(r_0)$  is the horizon area which is given by

$$\mathcal{A}_H(r_0^+) = \oint dx \sqrt{h} = 2\pi r_0^+. \quad (3.14)$$

### 3.3 Scale dependent couplings and scale setting

This section resumes the implementation of scale dependence that was used for the present work. The notation and procedures follow [52, 53, 55–60, 65, 67, 123–126, 144, 145]. In this framework the scale dependence is implemented at the level of an effective action as a generalization of the classical action. For the case of (3.1), the truncated effective action takes the form

$$\Gamma[g_{\mu\nu}, k] = \int d^3x \sqrt{-g} \left[ \frac{1}{2\kappa_k} (R - 2\Lambda_k) + \mathcal{L}_M \right]. \quad (3.15)$$

As shown in [56], this action is consistent at the classical level if one sets the arbitrary scale based on a variational principle, which means that the scale  $k$  considered as a non-dynamical field instead of a global constant. A variation of (3.15) with respect to the metric field  $g_{\mu\nu}$  gives the modified Einstein equations

$$G_{\mu\nu} + g_{\mu\nu} \Lambda_k = \kappa_k T_{\mu\nu}^{\text{effec}}. \quad (3.16)$$

Here, the effective stress energy tensor is defined as

$$\kappa_k T_{\mu\nu}^{\text{effec}} = \kappa_k T_{\mu\nu}^M - \Delta t_{\mu\nu}, \quad (3.17)$$

which consists of the usual stress energy of the matter Lagrangian  $T_{\mu\nu}^M$  and an additional contribution due to the scale dependence of the gravitational coupling

$$\Delta t_{\mu\nu} = G_k \left( g_{\mu\nu} \square - \nabla_\mu \nabla_\nu \right) G_k^{-1}. \quad (3.18)$$

For the vacuum solution presented in this chapter, the pure matter contribution is absent  $T_{\mu\nu}^M = 0$ .

Varying the action (3.15) with respect to the scale-field  $k(x)$  gives

$$\left[ R \frac{\partial}{\partial k} \left( \frac{1}{G_k} \right) - 2 \frac{\partial}{\partial k} \left( \frac{\Lambda_k}{G_k} \right) \right] \cdot \partial k = 0. \quad (3.19)$$

The above equations of motion are consistently complemented by the Bianchi identity, reflecting invariance under coordinate transformations

$$\nabla^\mu G_{\mu\nu} = 0. \quad (3.20)$$

### 3.4 Scale-dependent BTZ solution with $J_0 \neq 0$

The line element consistent with a static space-time, with rotational symmetry is given by

$$ds^2 = -f(r)dt^2 + g(r)dr^2 + r^2 \left[ N(r)dt + d\phi \right]^2, \quad (3.21)$$

where  $f(r)$ ,  $g(r)$ ,  $N(r)$ , and  $k(r)$  are functions that must be determined from the equations of motion (3.16-3.20). When the functional scale dependence of the couplings  $G_k$  and  $\Lambda_k$  is known, the system closes into itself and the equations (3.16-3.20) allow, at least numerically to determine the functions  $f(r)$ ,  $g(r)$ ,  $N(r)$ , and  $k(r)$  [125]. In certain truncations and functional approaches such as the functional renormalization group approach it is indeed possible to study scale dependence and approximate improvement of classical black hole solutions [54, 69, 71, 109–112, 114, 117–121, 146, 147]. However, those approximation scenarios are subject to theoretical uncertainties related to the truncations used to calculate the beta functions. Further, due to the implicit assumption of improvement of classical solutions, they typically do not solve the whole selfconsistent system of equations (3.16-3.20) anymore.

The idea is to avoid the theoretical uncertainties inflicted with the usage of given functions  $G_k$  and  $\Lambda_k$ , and instead to learn about the radial dependence of the functions  $G(r)$  and  $\Lambda(r)$  directly from the selfconsistent system of equations (3.16-3.20). Thus, instead of trying to solve for the four functions  $\{f(r), g(r), N(r), k(r)\}$  for given, but uncertain,  $G_k$  and  $\Lambda_k$  one can try to solve the equations (3.16-3.20) directly for the five functions  $\{f(r), g(r), \Lambda(r), G(r), N(r)\}$ . Here,  $G(r)$  and  $\Lambda(r)$  have inherited their radial dependence from  $k(r)$ . The problem for this elegant workaround is that there are now five unknown functions in a system which only has four independent equations. Thus, one additional condition is needed in order to be able to fully solve this system of equations. Following previous findings [57, 58, 123–126] this additional condition is that we restrict to solutions which fulfill the so-called Schwarzschild relation, namely that  $g(r) \equiv f(r)^{-1}$ . Therefore, the corresponding line element is

$$ds^2 = -f(r)dt^2 + f(r)^{-1}dr^2 + r^2 \left[ N(r)dt + d\phi \right]^2 \quad (3.22)$$

and the equations of motion can be solved for the four functions  $\{f(r), \Lambda(r), G(r), N(r)\}$ .

### 3.4.1 Solution

Based on the ansatz (3.22) one finds that the equations (3.16) are solved by

$$G(r) = \frac{G_0}{1 + r\epsilon}, \quad (3.23)$$

$$N(r) = -\frac{4G_0J_0}{r^2}Y(r), \quad (3.24)$$

$$f(r) = -8M_0G_0Y(r) + \frac{r^2}{\ell_0^2} + \frac{16G_0^2J_0^2}{r^2}Y(r)^2, \quad (3.25)$$

$$\Lambda(r) = -\frac{r + 3r^2\epsilon - 8G_0\ell_0^2M_0\epsilon Y(r)}{\ell_0^2r(1 + r\epsilon)} - \frac{4G_0^2J_0^2}{r^2} \left( \frac{dY(r)}{dr} \right)^2 + \frac{4G_0(M_0r + 2M_0r^2\epsilon - 4G_0J_0^2\epsilon Y(r))}{r^2(1 + r\epsilon)} \left( \frac{dY(r)}{dr} \right), \quad (3.26)$$

where

$$Y(r) \equiv 1 - 2r\epsilon + 2(r\epsilon)^2 \ln \left( 1 + \frac{1}{r\epsilon} \right). \quad (3.27)$$

This solution involves five constants of integration, which are labeled  $\{G_0, J_0, M_0, \Lambda_0 = -1/\ell_0^2, \text{ and } \epsilon\}$ . Their naming and physical meaning is given from their interpretation in two complementary limits. First, the constant  $J_0 \rightarrow 0$  does not appear in the scale dependent but non-rotating case [56]. Thus, one imposes that for  $J_0 \rightarrow 0$  the solution (3.23) reduces to the solution reported in [56], namely

$$\lim_{J_0 \rightarrow 0} G(r) = \frac{G_0}{1 + r\epsilon}, \quad (3.28)$$

$$\lim_{J_0 \rightarrow 0} N(r) = 0, \quad (3.29)$$

$$\lim_{J_0 \rightarrow 0} f(r) = -8M_0G_0Y(r) + \frac{r^2}{\ell_0^2}, \quad (3.30)$$

$$\begin{aligned} \lim_{J_0 \rightarrow 0} \Lambda(r) = & -\frac{r + 3r^2\epsilon + 8G_0\ell_0^2M_0\epsilon Y(r)}{\ell_0^2r(1 + r\epsilon)} \\ & + \frac{4G_0(M_0r + 2M_0r^2\epsilon)}{r^2(1 + r\epsilon)}Y(r)'. \end{aligned} \quad (3.31)$$

The second limit is the rotating classical solution (referring to constant couplings as in (3.5)), which is obtained when the running parameter  $\epsilon$  is taken to be zero,

$$\lim_{\epsilon \rightarrow 0} G(r) = G_0, \quad (3.32)$$

$$\lim_{\epsilon \rightarrow 0} N(r) = N_0(r) \equiv -\frac{4G_0J_0}{r^2}, \quad (3.33)$$

$$\lim_{\epsilon \rightarrow 0} f(r) = f_0(r) \equiv -8M_0G_0 + \frac{r^2}{\ell_0^2} + \frac{16G_0^2J_0^2}{r^2}, \quad (3.34)$$

$$\lim_{\epsilon \rightarrow 0} \Lambda(r) = \Lambda_0. \quad (3.35)$$

Moreover, when  $\{\epsilon, M_0\} \rightarrow \{0, -1/8G_0\}$  the appropriate vacuum of the theory is  $AdS_3$  which is invariant under perturbations due to the running of the couplings controlled by  $\epsilon$ . Further asymptotic corrections can be seen from (3.47). Since corrections due to quantum scale dependence should be small, it is useful to expand the solutions around  $\epsilon \approx 0$

$$G(r) = G_0 \left[ 1 - r\epsilon + \mathcal{O}(\epsilon^2) \right], \quad (3.36)$$

$$N(r) = N_0(r) \left[ 1 - 2r\epsilon + \mathcal{O}(\epsilon^2) \right] \quad (3.37)$$

$$f(r) = f_0(r) + 16 \left[ G_0M_0 - \frac{4G_0^2J_0^2}{r^2} \right] r\epsilon + \mathcal{O}(\epsilon^2), \quad (3.38)$$

$$\Lambda(r) = \Lambda_0 \left[ 1 + 2r\epsilon + \mathcal{O}(\epsilon^2) \right]. \quad (3.39)$$

Making this expansion one assumes that the dimensionfull quantity  $\epsilon$  is much smaller than

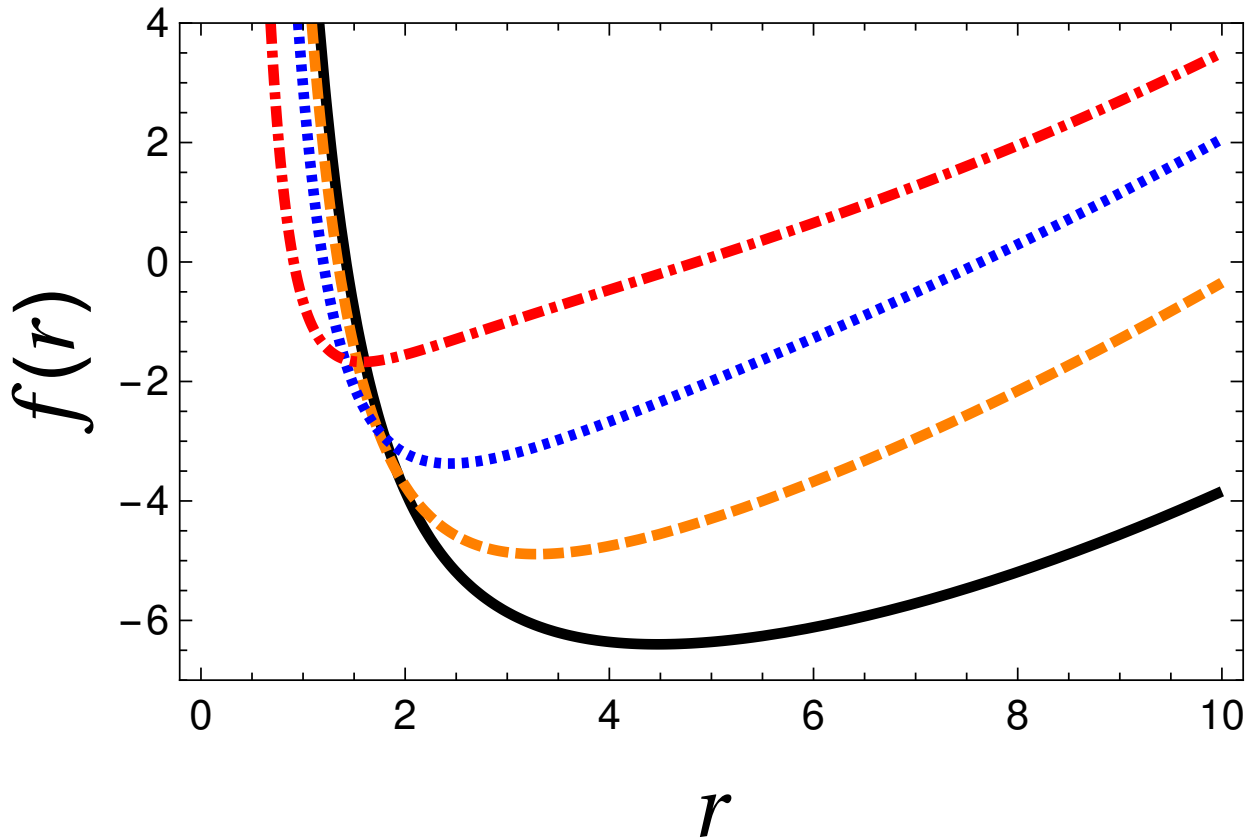


**Figure 3.2:** Radial dependence of the lapse function  $f(r)$  for  $\ell_0 = 5$ ,  $G_0 = 1$ ,  $M_0 = 1$ , and  $J_0 = 1$ . The different curves correspond to the classical case  $\epsilon = 0$  solid black line,  $\epsilon = 0.05$  dashed orange line,  $\epsilon = 0.2$  dotted blue line, and  $\epsilon = 1$  dot-dashed red line.

observes that the lapse function  $f(r)$  presents two real valued horizons after the inclusion of non-zero angular momentum, just like the classical case. However, the location of those two horizons changes due to the inclusion of scale dependence. Thus, for non vanishing  $J_0$ , there are two horizons independent of the presence ( $\epsilon \neq 0$ ) or absence ( $\epsilon = 0$ ) of scale dependence. One remembers that for vanishing angular momentum, there is only a single horizon for the BTZ black hole which also gets shifted to lower values if one allows for scale dependence  $\epsilon > 0$  [56]. In the scale dependent case there does not exist any finite  $\epsilon$  value for which the black hole becomes extremal. This will be discussed in more detail in section 3.6. However, if one considers the limit  $\epsilon \rightarrow \infty$ , the lapse function approaches that of an extremal black hole.

It is important to note that, some relevant quantities, such as the black hole radius  $r_H$ , depend on the scale dependence parameter  $\epsilon$ . However, the asymptotic space-time for  $r \rightarrow \infty$

does not show this dependence. This important fact will be discussed in more detail in section 3.5.

### 3.4.2 Horizon structure

The appearance of horizons is the defining criterium justifying that solution can be called black hole solution. The event horizons are defined by  $f(r_H) = 0$ , which can be written as the solutions of the equation

$$Y(r_H) = \frac{1}{4} \frac{M_0}{G_0 J_0^2} \left[ 1 \pm \Delta \right] r_H^2 \quad (3.40)$$

where  $\Delta$  remains the same definition given in Eq. (3.8). Unfortunately, this condition has no closed analytical solution for the scale-dependent lapse function (3.25). Therefore, one has to restrict to a numerical analysis of the black hole horizons and of the related subjects. Fig. 3.3 shows the dependence of the horizons  $r_H$  on the classical mass parameter  $M_0$ . One observes that for vanishing angular momentum  $J_0 = 0$  there is only one real valued horizon with and without scale dependence  $\epsilon$ . For finite angular momentum  $J_0 \neq 0$  there appears a second inner horizon. In all studied cases, the effect of the scale dependence  $\epsilon > 0$  was to reduce the outer horizon radius with respect to the non-scale dependent case  $\epsilon = 0$ . Even though the analytical solution for the horizon is not obtained, one still can analyze the lapse function in a regime when the  $\epsilon$  correction is small. The event horizon, up to leading order, is

$$r_H \approx r_0 \left[ 1 - \epsilon r_0 + \mathcal{O}(\epsilon^2) \right], \quad (3.41)$$

where one indeed observes the expected deviation of the horizon with respect the classical case. One notes that in the scale-dependent scenario the event horizon decreases when  $\epsilon > 0$  or increases when  $\epsilon < 0$ . This feature reveals that the black hole thermodynamics is directly affected.

For the inner horizon and for large values of  $M_0$ , the lapse function takes an simplified form, which allows to express the horizon as

$$r_H^0 = \sqrt{\frac{2G_0}{M_0}} J_0 \left[ 1 - 2 \left( \sqrt{\frac{2G_0}{M_0}} J_0 \right) \epsilon + \mathcal{O}(\epsilon^2) \right], \quad (3.42)$$

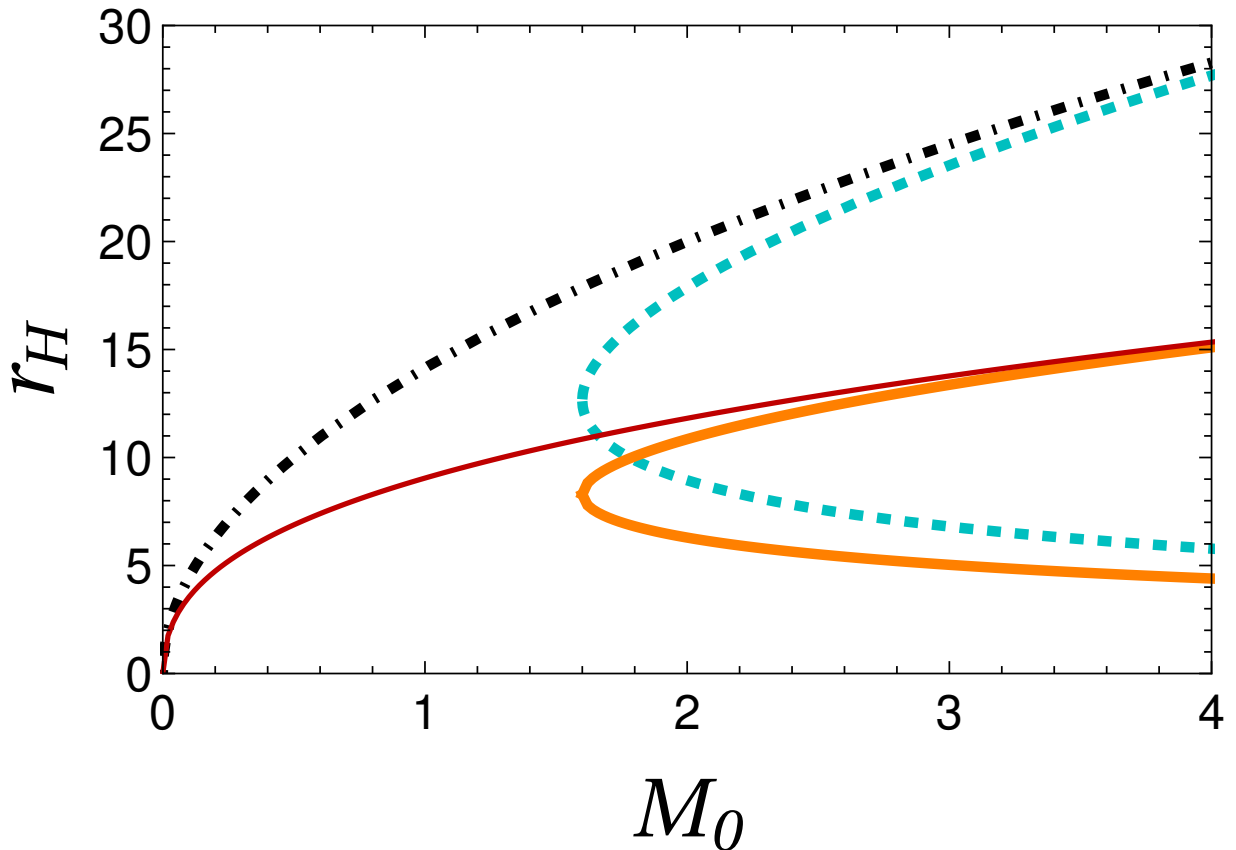


**Figure 3.3:** Black hole horizons  $r_H$  as a function of the mass  $M_0$  for  $\epsilon = 0$  and  $J_0 = 0$  (dotted dashed black line),  $\epsilon = 0$  and  $J_0 = 8$  (blue dashed line),  $\epsilon = 0.1$  and  $J_0 = 0$  (solid thin red line) and  $\epsilon = 0.1$  and  $J_0 = 8$  (solid thick orange line). In addition  $\ell_0 = 5$  and the values of the rest of the parameters have been taken as unity.

where one recovers the classical horizon in the limit  $\epsilon \rightarrow 0$ .

### 3.5 Invariants and asymptotic space-times

This section discusses different asymptotic limits. In particular, we will focus on the asymptotic line element and the behavior of the the Ricci scalar  $R$ .

### 3.5.1 Asymptotic line element

#### 3.5.1.1 Behaviour when $r \rightarrow 0$

When we are close to the horizon, the lapse and shift functions suffer deviations respect the classical solution. In order to emphasize that, we expand our result around  $r$  up to first order to get

$$ds_{0+}^2 = -f_{0+} dt^2 + f_{0+}^{-1} dr^2 + r^2 [N_{0+} dt + d\phi]^2, \quad (3.43)$$

with

$$f_{0+}(r) = -8M_0 G_0 [1 - 2\epsilon r] + \frac{16G_0^2 J_0^2}{r^2} [1 - 4\epsilon r] + \mathcal{O}(r^2), \quad (3.44)$$

$$N_{0+}(r) = N_0(r) [1 - 2\epsilon r + \mathcal{O}(r^2)], \quad (3.45)$$

where we only are considering terms up to linear order in  $\epsilon$ . Given these expressions, it is very obvious that the lapse and shift functions decreases if  $\epsilon > 0$ , respect the usual solution.

#### 3.5.1.2 Behaviour when $r \rightarrow \infty$

The asymptotic line element is expressed in terms of asymptotic lapse and shift function (at large radii respect to the inverse of scale dependent parameter), i.e.

$$ds_{\infty}^2 = -f_{\infty} dt^2 + f_{\infty}^{-1} dr^2 + r^2 [N_{\infty} dt + d\phi]^2. \quad (3.46)$$

where the aforementioned functions are shown below

$$f_{\infty}(r) = \frac{r^2}{\ell_0^2} - 8M_0 G_0 \left( \frac{2}{3} \frac{1}{r\epsilon} \right) + \mathcal{O} \left( \frac{1}{r^2} \right), \quad (3.47)$$

$$N_{\infty}(r) = N_0(r) \left( \frac{2}{3} \frac{1}{r\epsilon} \right) + \mathcal{O} \left( \frac{1}{r^4} \right). \quad (3.48)$$

It is important to note that the asymptotic lapse function mimics at leading order an  $AdS_3$  behavior. Going further, we observe that the lapse function given in Eq. (3.47), at sub-leading order, reflects the effect of the scale-dependent scenario through a factor  $1/(\epsilon r)$ . For the shift function, the scale dependent effect is dominant at leading order in  $r$  (which is given

in Eq. (3.48)), which means that asymptotically the running of the gravitational coupling modifies the classical behavior. In addition, the quantum correction in both functions appear as a term  $\sim 1/(r\epsilon)$ . Regarding the lapse function, if one remains only the dominant term in the large radius limit, the asymptotic structure does not change, therefore, it is equivalent to  $AdS_3$ , which is consistent with our previous work [56].

When studying the sub-leading corrections one has to be careful with the two competing limits  $\epsilon \rightarrow 0$  and  $r \rightarrow \infty$ , which can not be commuted. In this context we note that the naming of the integration constants ( $J_0, M_0, \dots$ ) and thus of their physical interpretation was based on the classical limit  $\epsilon \rightarrow 0$ .

### 3.5.2 Asymptotic Invariants

For the study of coordinate independent properties of a solution it is useful to refer to invariants. For the given metric (3.22) the Ricci scalar is given below

$$R = \frac{1}{2r} (r^3 N'(r)^2 - 4f'(r)) - f''(r), \quad (3.49)$$

which, after explicit insertion, reads as follows

$$R = R_0 + 16G_0 M_0 \frac{Y'(r)}{r} \left[ 1 + \frac{2G_0 J_0^2 Y(r)}{M_0 r^2} - \frac{3G_0 J_0^2 Y'(r)}{2M_0 r} \right] + 8M_0 G_0 Y''(r) \left[ 1 - \frac{4G_0 J_0^2 Y(r)}{M_0 r^2} \right] \quad (3.50)$$

From Eq. (3.50) we get the classical solution after demand that  $\epsilon \rightarrow 0$ , which reads

$$R_0 \equiv 6\Lambda_0, \quad (3.51)$$

#### 3.5.2.1 Behaviour when $r \rightarrow 0$

For small  $r$  the invariant expansion of Eq. (3.50) gives

$$R = -\frac{64G_0^2 J_0^2}{r^3} \epsilon (1 + \mathcal{O}(r)). \quad (3.52)$$

One observes that the presence of scale-dependent couplings ( $\epsilon \neq 0$ ) produces a singularity at  $r = 0$ . This finding is somewhat surprising since one might have hoped that quantum induced scale dependence would help with singularity problems of the classical theory and not make them worse. However, the implementation of scale dependence that was used here is clear and determinating the solution under the given assumptions. Thus, one has to conclude that the solution of the singularity problem shown in (3.52) has to come from a framework that falls outside of our assumptions such as a line element with different structure, or the addition of non-local or higher order terms in the effective action.

### 3.5.2.2 Behaviour when $r \rightarrow \infty$

The other asymptotic regime of interest is the large radius expansion  $r \rightarrow \infty$ . In this regime one can approximate the logarithm contribution according to  $\ln(1+z) \approx z - z^2/2$  (using  $z = 1/\epsilon r$ ). In this limit the Ricci scalar is given by

$$R = R_0 - \frac{32M_0G_0}{\epsilon r^3} + \mathcal{O}\left(\frac{1}{r^4}\right). \quad (3.53)$$

Please note that the Ricci is asymptotically finite independent of the order one takes the competing limits  $r \rightarrow \infty$  and  $\epsilon \rightarrow 0$ . However, due to the expansion of the logarithms, the expression (3.53) is only valid if  $r \gg 1/\epsilon$ . As we know, the Ricci scalar is constant in the classical case (3.51) and therefore for certain values of the parameter  $\epsilon$ , asymptotically the Ricci scalar is well-behaved take the classical value (3.51).

## 3.6 Thermodynamic properties

The (numerical) knowledge of the horizons allows to study the thermodynamic properties of the scale dependent rotating black hole solution (3.25).

### 3.6.1 Hawking temperature

The Hawking temperature of a black hole assuming a circularly symmetric line element (3.22), is defined by

$$T_H(r_H) = \frac{1}{2\pi} \left| \frac{1}{2} \frac{\partial f}{\partial r} \Big|_{r=r_H} \right|, \quad (3.54)$$

which gives for the solution of (3.25)

$$T_H(r_H) = \frac{1}{4\pi} \left| \frac{16M_0G_0}{r_H(1 + \epsilon r_H)} \Delta \right|. \quad (3.55)$$

Please, note that this formula coincides with the classical expression, if one replaces  $G_0$  by  $G(r_H)$  in Eq. (3.13). As it can be seen from (3.55), the Hawking temperature vanishes for  $\Delta = 0$ . The extremal black hole is given when  $M_0\ell_0$ , which is the same extremality condition as in the classical case (3.11). Figure 3.4 shows the temperature which takes into account the running coupling effect in comparison to the “classical” temperature, as a function of the parameter  $M_0$ . We notes that indeed the curves with ( $\epsilon \neq 0$ ) and without scale dependence ( $\epsilon = 0$ ) coincide at the same minimal mass  $M_0 = J_0/\ell_0$ .

Since scale dependence is motivated by quantum corrections and since those corrections are typically small, it can be expected that the integration constant  $\epsilon$ , which parametrizes the scale dependence, is small. Under this assumption one can expand for  $r\epsilon \ll 1$  to get the well-known Hawking temperature (at leading order) i.e.

$$T_H(r_H^0) = T_0(r_{0+}) |1 + 4r_{0+}\epsilon + \mathcal{O}(\epsilon^2)| \quad (3.56)$$

where  $r_{0+}$  is the classical horizon  $r_H$  which is a solution of (3.5) evaluated when  $r$  is close to zero. We wish to remark that this approximation is used because we always assume a weak coupling  $\epsilon$ . Besides, the classical Hawking temperature  $T_0(r_{0+})$  is computed following the usual procedure for the lapse function (3.5) when  $r$  is small.

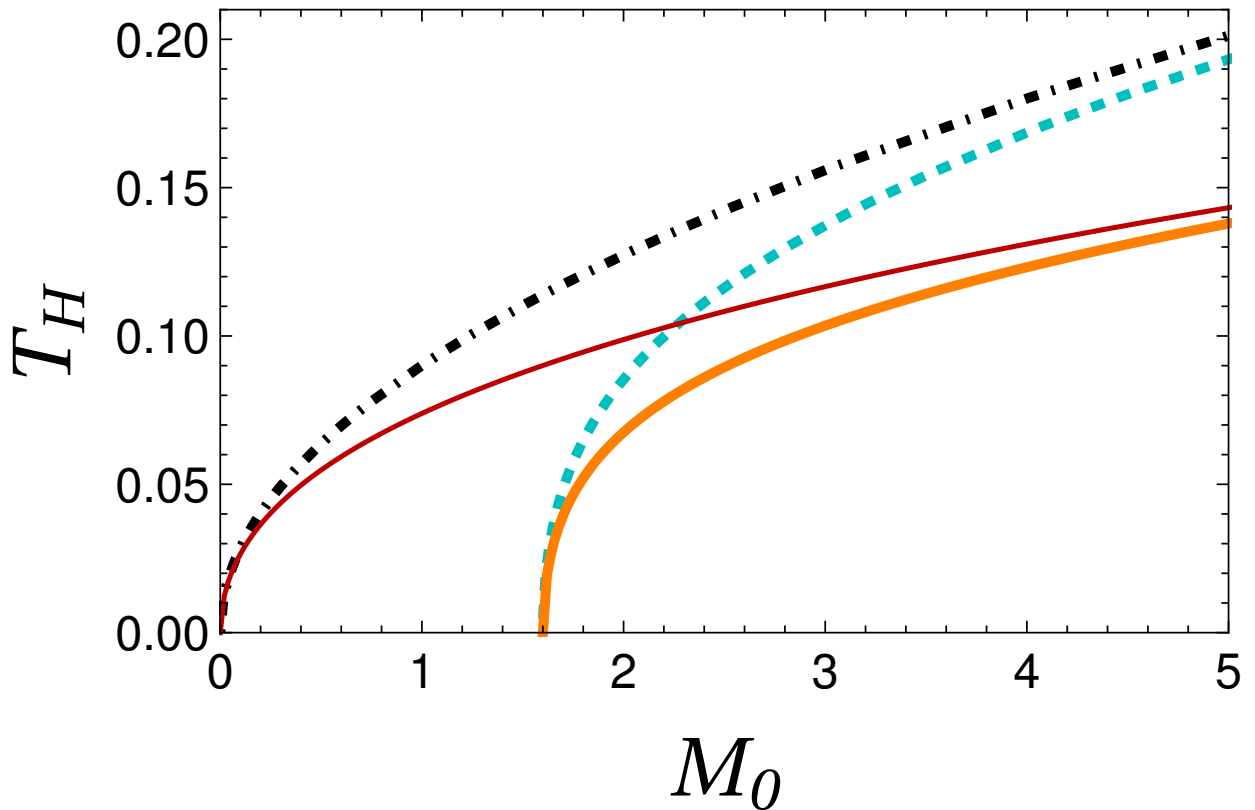


**Figure 3.4:** The Hawking temperature  $T_H$  as function of the classical mass  $M_0$  for four different cases:  $\epsilon = 0$  and  $J_0 = 0$  (dotted dashed black line),  $\epsilon = 0$  and  $J_0 = 8$  (blue dashed line),  $\epsilon = 0.1$  and  $J_0 = 0$  (solid thin red line) and  $\epsilon = 0.1$  and  $J_0 = 8$  (solid thick orange line). In addition  $\ell_0 = 5$  and the values of the rest of the parameters have been taken as unity.

### 3.6.2 Bekenstein-Hawking entropy

The Bekenstein-Hawking entropy is also valid for theories in which the gravitational coupling is variable [131–134]. For black hole solutions in  $D + 1$  dimensions with varying Newton’s coupling the entropy is given by

$$S = \oint d^{D-1}r \frac{\sqrt{h}}{4G(r)}, \quad (3.57)$$

where  $h_{ij}$  is the induced metric at the horizon  $r = r_H$ . For the present circularly symmetric solution the aforementioned integral is straightforward. The induced line element for constant  $t$  and  $r$  slices is simply  $ds = r d\theta$  and moreover  $G_H = G(r_H)$  is constant along the horizon. Therefore, the entropy for the solution (3.25) is

$$S = \frac{\mathcal{A}_H(r_H)}{4G(r_H)} = S_0(r_H)(1 + \epsilon r_H). \quad (3.58)$$

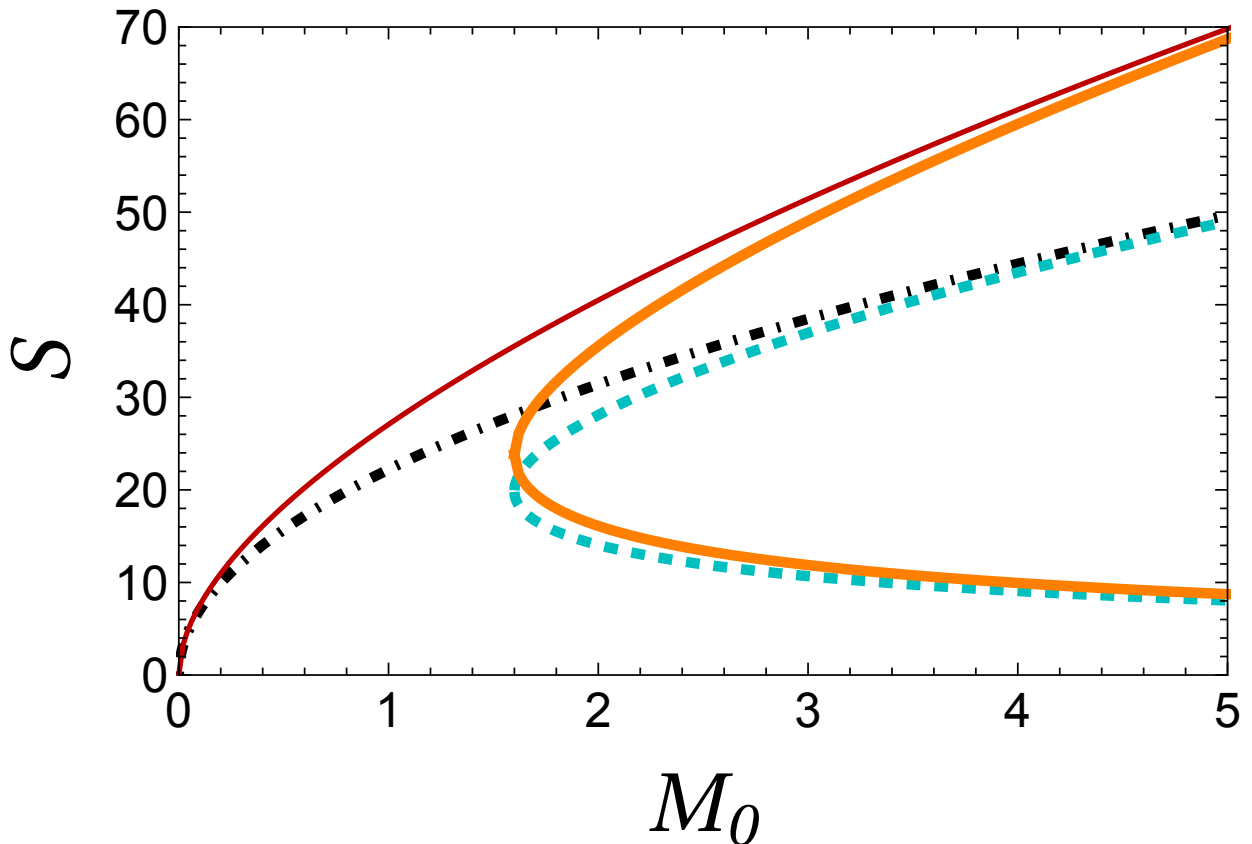


**Figure 3.5:** The Bekenstein-Hawking entropy  $S$  as function of classical mass  $M_0$  for four different cases:  $\epsilon = 0$  and  $J_0 = 0$  (dotted dashed black line),  $\epsilon = 0$  and  $J_0 = 8$  (blue dashed line),  $\epsilon = 0.1$  and  $J_0 = 0$  (solid thin red line) and  $\epsilon = 0.1$  and  $J_0 = 8$  (solid thick orange line). In addition  $\ell_0 = 5$  and the values of the rest of the parameters have been taken as unity.

Figure 3.5 shows the entropy for our BTZ rotating scale-dependent black hole as a function of  $M_0$ . We observe that when  $J_0 = 0$  both, the classical entropy ( $\epsilon = 0$ ) and the scale-dependent entropy ( $\epsilon \neq 0$ ) tend to zero for  $M_0 \rightarrow 0$ , whereas for  $J_0 \neq 0$  both, the classical and the scale-dependent solution, present a cut-off for the critical mass  $M_0 = J_0/\ell_0$ . An analytic expression can be obtained in certain limit. By considering small values of  $\epsilon$  it is possible to expand this expression

$$S(r_H^0) = S_0(r_H^0) [1 + \epsilon r_H^0 + \mathcal{O}(\epsilon^3)]. \quad (3.59)$$

Thus, the quantum effect increases the entropy respect the classical solution.

### 3.7 Discussion

Effective quantum corrections can be systematically introduced to the BTZ black hole by assuming a scale-dependent framework. This implies non-trivial deviations from classical black hole solutions. In this work, one of the integration constants ( $\epsilon$ ) of the generalized field equations is used as a control parameter, which allows to regulate the strength of scale dependence, such that for  $\epsilon \rightarrow 0$ , the well-know classical BTZ background is recovered. This chapter discusses the BTZ black hole taking into account angular momentum in the context of scale dependent couplings. A solution of the corresponding field equations is presented and compared it with three different known cases: the classical case ( $\epsilon = 0$ ) without angular momentum, the classical case ( $\epsilon = 0$ ) with angular momentum, and the scale dependent case ( $\epsilon \neq 0$ ) without angular momentum.

The new scale-dependent solution has some interesting features, for instance the lapse function increases rapidly when  $r \rightarrow \infty$  (which is present in the classical case) but now the effect is deeper, see Fig. 3.2 and compare the black curve ( $\epsilon = 0$ ) with red curve ( $\epsilon = 1$ ). By comparing Eq. (3.5) with Eq. (3.47) and with Eq. 3.44, we observe the deviation given by the scale-dependent framework respect to the classical solution. It is remarkable that when we are close to the origin the lapse function suffers a shift, while when we are far from the origin it shows a decrease by a factor of  $1/\epsilon r$ . In both cases the solution is affected.

Furthermore, according to Fig. 3.3, the outer horizons decrease when  $\epsilon$  increases. The effect of the scale dependent approach is thus that it produces smaller horizons, when compared to the usual case. Interestingly this decrease does not come with a change of the critical mass, where the two outer horizons merge.

An analysis of the Ricci scalar reveals that a singularity appears at  $r \rightarrow 0$  which is absent in the corresponding classical BTZ solution. Indeed, the BTZ black hole has a constant scalar, according to Eq. (3.51), whereas in the scale dependent case ( $\epsilon \neq 0$ ) the singularity at  $r = 0$  is always present according with Eqs. (3.52). This is a consequence of the scale-dependent scenario.

Regarding the Hawking temperature, it is interesting that the scale dependent formula and the corresponding classical counterpart, coincide, under the replacement  $G_0 \rightarrow G(r_H) = G_0/(1 + \epsilon r_H)$  (3.23). It is further remarkable that the extreme black hole condition is also maintained and, therefore, the Hawking temperature is equal to zero when  $M_0^{\min} = J_0/\ell_0$ ,

independent of the strength of scale dependence  $\epsilon$ . Moreover, we note that in presence of scale-dependent couplings the temperature is lowered with respect to the classic BTZ solution for large values of  $M_0$ . Whereas when  $M_0$  is close to zero (for  $J_0 = 0$ ) and when  $M_0$  is close to  $M_0^{\min}$  (for  $J_0 \neq 0$ ), the classical and the scale dependent solution are very similar. One notes that the Bekenstein-Hawking entropy is increased by the scale dependence  $\epsilon \neq 0$  and that for large values of  $M_0$  the solutions with and without angular momentum match for a given value of  $\epsilon$ , but they differ for different values of  $\epsilon$ . Throughout the numeric analysis we also have used a relatively “small” value of  $\epsilon$ , a choice which can be motivated by the assumption of relatively weak quantum effects provoking scale dependence at the level of the effective action (3.15). Lets mention in this context that the integration constant  $\epsilon$  can be made dimensionless for example by defining  $\epsilon = \bar{\epsilon}M_0$ , in which case the graphical and analytical results with respect to  $\bar{\epsilon}$  would have to be rescaled correspondingly.

Finally, lets comment on the ansatz (3.22). This type of ansatz also works for the spherically symmetric case. However, inspired by the ideas presented by Jacobson [130] it was possible to show that, for spherically symmetric static black holes, this type of ansatz is actually a consequence of a simple Null Energy Condition (NEC) [56–58].

This condition allows the avoidance of pathologies such as tachyons, instabilities, and ghosts [33, 127]. Further, the NEC plays a crucial role in the Penrose singularity theorem [148]. However, a straight forward implementation of a generalized NEC to the rotating BH was not achieved, since the appearance of angular momentum reduces the symmetry of the problem. One would first have to generalize the arguments given in [130] to the rotational symmetry, before one can try to build an argument deriving the ansatz (3.22), as a consequence of some kind of NEC. Thus, at this point the use of the ansatz (3.22) is well justified, since it agrees with the NEC for vanishing rotation and since it further implements the structure of the line element for the case of the classical (not scale-dependent) counterpart.

## 3.8 Conclusion

In this chapter we have studied the scale dependence of the rotating BTZ black hole assuming a finite cosmological term in the action. After presenting the models and the classical black hole solutions, we have allowed for a scale dependence of the cosmological “constant” as well as the gravitational coupling, and we have solved the corresponding generalized field equations with static circular symmetry. We have compared the classical solutions distinguishing

---

two different cases, i.e. with and without angular momentum, with the corresponding scale dependent solution for same values of angular momentum. In addition, the horizon structure, the asymptotic spacetime and the thermodynamics were analyzed. In particular, the analysis of the Hawking temperature allowed to find a extremal black hole which coincides with the classical counterpart.



# Chapter 4

## Scale-dependent charged solutions

This chapter was published in *The European Physical Journal C* [57]

### 4.1 Introduction

In recent years gravity in (2+1) dimensions has attracted a lot of interest for several reasons. The absence of propagating degrees of freedom, its mathematical simplicity, the deep connection to Chern-Simons theory [73–75] are just a few of the reasons why to study three-dimensional gravity. In addition (2+1) dimensional black holes are a good testing ground for the four-dimensional theory, because properties of (3+1)-dimensional black holes, such as horizons, Hawking radiation and black hole thermodynamics, are also present in their three-dimensional counterparts.

On the other hand, the main motivation to study non-linear electrodynamics (NLED) was to overcome certain problems of the standard Maxwell theory. In particular, non-linear electromagnetic models are introduced in order to describe situations in which this field is strong enough to invalidate the predictions provided by the linear theory. Originally the Born-Infeld non-linear electrodynamics was introduced in the 30's in order to obtain a finite self-energy of point-like charges [149]. During the last decades this type of action reappears in the open sector of superstring theories [150, 151] as it describes the dynamics of D-branes [152]. Also, these kind of electrodynamics have been coupled to gravity in order to obtain, for example, regular black holes solutions [153–155], semiclassical corrections to the black hole

entropy [156] and novel exact solutions with a cosmological constant acting as an effective Born–Infeld cut–off [157]. A particularly interesting class of NLED theories is the so called power-Maxwell theory described by a Lagrangian density of the form  $\mathcal{L}(F) = F^\beta$ , where  $F = F_{\mu\nu}F^{\mu\nu}/4$  is the Maxwell invariant, and  $\beta$  is an arbitrary rational number. When  $\beta = 1$  one recovers the standard linear electrodynamics, while for  $\beta = D/4$  with  $D$  being the dimensionality of spacetime, the electromagnetic energy momentum tensor is traceless [158, 159]. In 3 dimensions the generic black hole solution without imposing the traceless condition has been found in [160], while black hole solutions in linear Einstein-Maxwell theory are given in [161, 162]. Also, interesting solutions and properties of black holes in the presence of power-Maxwell theory have been found in Refs. [163–166] whereas some topological black hole solutions with power-law Maxwell field have been investigated in [167–169]. Moreover, the relation between Einstein-power-Maxwell theory and  $F(R)$  gravity have been obtained in Refs. [170, 171].

Scale dependence at the level of the effective action is a generic result of quantum field theory. Regarding quantum gravity it is well-known that its consistent formulation is still an open task. Although there are several approaches to quantum gravity (for an incomplete list see e.g. [84, 86, 88–90, 92, 96–98] and references therein), most of them have something in common, namely that the basic parameters that enter into the action, such as the cosmological constant or Newton’s constant, become scale dependent quantities. Therefore, the resulting effective action of most quantum gravity theories acquires a scale dependence. Those scale dependent couplings are expected to modify the properties of classical black hole backgrounds. To be more precise, we use the term classical black hole, when we refer to the corresponding non-scale dependent case. Thus, despite both Einstein- Maxwell and Einstein-power-Maxwell black hole are classical solutions, we split each black hole into two cases: the classical case (if the gravitational coupling is constant) and the scale dependent case (if the gravitational coupling is not constant anymore). Therefore, in the rest of the chapter we shall only use the term “classical” for non–scale dependent black holes.

Please note that this scale dependent theory is similar to Brans-Dicke scalar-tensor theory [42, 172–175] in the sense that the gravitational coupling is not a constant any more. However, the two theories differ by the fact that for the considered pure scale dependence, the underlying action does not have a kinetic term for this coupling.

It is the aim of this chapter to study the scale dependence at the level of the effective action of three-dimensional charged black holes in linear (Einstein - Maxwell) and non-linear

(Einstein-power-Maxwell) electrodynamics. We use the formalism and notation of [56, 58] where the authors applied the same technique to the BTZ black hole [76, 77]. Our work is organized as follows: After this introduction, in the next section we present the action and the classical black hole solution both in Einstein-Maxwell and Einstein-power-Maxwell theories. The framework and the “null” energy condition are introduced in sections 4.3 and 4.4. The scale dependence for linear electrodynamics is presented in the section 4.5, while the corresponding solutions for non-linear theory are given in section 4.6. The discussion of our results and remarks are shown in section 4.7 whereas in section A.4 we summarize the main ideas and conclude. Finally, we present a brief appendix in which we show the effective Einstein field equations for an arbitrary index  $\beta$  in the last section.

## 4.2 Classical linear and non-linear electrodynamics in (2+1) dimensions

In this section we present the classical theories of linear and non-linear electrodynamics. Those theories will then be investigated in the context of scale dependent couplings. The starting point is the so-called Einstein-power-Maxwell action without cosmological constant ( $\Lambda_0 = 0$ ), assuming a generalized electrodynamics i.e.  $\mathcal{L}(F) = C|F|^\beta$  which reads

$$I_0[g_{\mu\nu}, A_\mu] = \int d^3x \sqrt{-g} \left[ \frac{1}{16\pi G_0} R - \frac{1}{e_0^{2\beta}} \mathcal{L}(F) \right], \quad (4.1)$$

where  $G_0$  is Einstein’s constant,  $e_0$  is the electromagnetic coupling constant,  $R$  is the Ricci scalar,  $\mathcal{L}(F)$  is the electromagnetic Lagrangian density where  $C$  is a constant,  $F$  is the Maxwell invariant defined in the usual way i.e.  $F = (1/4)F_{\mu\nu}F^{\mu\nu}$  and  $F_{\mu\nu} = \partial_\mu A_\nu - \partial_\nu A_\mu$  is the electromagnetic field strength tensor. We use the metric signature  $(-, +, +)$ , and natural units ( $c = \hbar = k_B = 1$ ) such that the action is dimensionless. Note that  $\beta$  is an arbitrary rational number, which also appears in the exponent of the electromagnetic coupling in order to maintain the action dimensionless. It is easy to check that the special case  $\beta = 1$  reproduces the classical Einstein-Maxwell action, and thus the standard electrodynamics is recovered. For  $\beta \neq 1$  one can obtain Maxwell-like solutions. In the following we shall consider both cases: first when  $\beta = 3/4$ , since it is this value that allows us to obtain a trace-free electrodynamic tensor, precisely as in the four-dimensional standard Maxwell theory, and second when  $\beta = 1$  because is the usual electrodynamics in 2+1 dimensions. In

both cases one obtains the same classical equations of motion, which are given by Einstein's field equations

$$G_{\mu\nu} = \frac{8\pi G_0}{e_0^{2\beta}} T_{\mu\nu}. \quad (4.2)$$

The energy momentum tensor  $T_{\mu\nu}$  is associated to the electromagnetic field strength  $F_{\mu\nu}$  through

$$T_{\mu\nu} \equiv T_{\mu\nu}^{\text{EM}} = \mathcal{L}(F)g_{\mu\nu} - \mathcal{L}_F F_{\mu\gamma} F_{\nu}{}^{\gamma}, \quad (4.3)$$

remembering that  $\mathcal{L}_F = d\mathcal{L}/dF$ . In addition, for static circularly symmetric solutions the electric field  $E(r)$  is given by

$$F_{\mu\nu} = (\delta_{\mu}^r \delta_{\nu}^t - \delta_{\nu}^r \delta_{\mu}^t) E(r). \quad (4.4)$$

For the metric circular symmetry implies

$$ds^2 = -f(r)dt^2 + g(r)dr^2 + r^2 d\phi^2. \quad (4.5)$$

Note that, in the classical solution, we are able to deduce the Schwarzschild ansatz, namely  $g(r) = f(r)^{-1}$ . Finally, the equation of motion for the Maxwell field  $A_{\mu}(x)$  reads

$$D_{\mu} \left( \frac{\mathcal{L}_F F^{\mu\nu}}{e_0^{2\beta}} \right) = 0. \quad (4.6)$$

With the above in mind, for charged black holes one only needs to determine the set of functions  $\{f(r), E(r)\}$ . Using Einstein's field equations 4.2 and Eq. 4.6 combined with Eq 4.4 and the definition of  $\mathcal{L}_F$ , one obtains the classical electric field as well as the lapse function  $f(r)$ .

It is possible to determine the electric field as well as the lapse function without assuming a particular value for  $\beta$  for classical solutions, however we will focus on two of them. First, the Einstein-Maxwell case is in itself interesting due to its relation with the four-dimensional case. On the other hand, the Einstein-power-Maxwell case with  $\beta = 3/4$  is a desirable one due to a remarkable property: it has a null trace, which is also present in the four-dimensional case. The general treatment for any value of  $\beta$  can be found in the appendix 4.9.

### 4.2.1 Einstein-Maxwell case

The classical (2+1)-dimensional Einstein-Maxwell black hole solution ( $\beta = 1$ ) is given by

$$f_0(r) = -M_0 G_0 - \frac{1}{2} \frac{Q_0^2}{e_0^2} \ln \left( \frac{r}{\tilde{r}_0} \right), \quad (4.7)$$

$$E_0(r) = \frac{Q_0}{r} e_0^2, \quad (4.8)$$

where  $M_0$  is the mass and  $Q_0$  is the electric charge of the black hole and  $\tilde{r}_0$  stands for the radius where the electrostatic potential vanishes. The event horizon  $r_0$  is obtained by demanding that  $f_0(r_0) = 0$ , which reads

$$r_0 = \tilde{r}_0 e^{-\frac{2M_0 G_0 e_0^2}{Q_0^2}}, \quad (4.9)$$

and rewriting the lapse function using the event horizon one gets

$$f_0(r) = -\frac{Q_0^2}{2e_0^2} \ln \left( \frac{r}{r_0} \right). \quad (4.10)$$

Black holes have thermodynamic behaviour. Here, the Hawking temperature  $T_0$ , the Bekenstein-Hawking entropy  $S_0$ , as well as the heat capacity  $C_0$  are found to be

$$T_0(r_0) = \frac{1}{4\pi} \left| \frac{Q_0^2}{2e_0^2 r_0} \right|, \quad (4.11)$$

$$S_0(r_0) = \frac{\mathcal{A}_H(r_0)}{4G_0}, \quad (4.12)$$

$$C_0(r_0) = T \left. \frac{\partial S}{\partial T} \right|_Q = -S_0(r_0). \quad (4.13)$$

Note that  $\mathcal{A}_H(r_0)$  is the horizon area which is given by

$$\mathcal{A}_H(r_0) = \oint dx \sqrt{h} = 2\pi r_0, \quad (4.14)$$

### 4.2.2 Einstein-power-Maxwell case

Solving Einstein's field equations for  $\beta = 3/4$ , the lapse function  $f(r)$  and the electric field  $E(r)$  are found to be

$$f_0(r) = \frac{4G_0Q_0^2}{3r} - G_0M_0, \quad (4.15)$$

$$E_0(r) = \frac{Q_0}{r^2}. \quad (4.16)$$

It is worth mentioning that, unlike in the previous section, the solutions here considered do not contain the electromagnetic coupling. This is due to the fact that a dimensional analysis on the action (4.1) for  $\beta = 3/4$  reveals that the electric charge is dimensionless in this case. As a consequence, we can set the electromagnetic coupling to unity without affecting the classical action.

At classical level a horizon is present, and it is computed by requiring that  $f(r_0) = 0$ , which reads

$$r_0 = \frac{4}{3} \frac{Q_0^2}{M_0}. \quad (4.17)$$

Expressing the mass  $M_0$  in terms of the horizon one obtains

$$f_0(r) = \frac{4}{3} G_0 Q_0^2 \left[ \frac{1}{r} - \frac{1}{r_0} \right]. \quad (4.18)$$

Classical thermodynamics plays a crucial role since it provides us with valuable information about the underlying black hole physics. The Hawking temperature  $T_0$ , the Bekenstein-Hawking entropy  $S_0$  as well as the heat capacity  $C_0$  are given by

$$T_0(r_0) = \frac{1}{4\pi} \left| \frac{M_0 G_0}{r_0} \right|, \quad (4.19)$$

$$S_0(r_0) = \frac{\mathcal{A}_H(r_0)}{4G_0}, \quad (4.20)$$

$$C_0(r_0) = -\frac{\mathcal{A}_H(r_0)}{4G_0}. \quad (4.21)$$

In agreement with the notation in the previous section,  $\mathcal{A}_H(r_0)$  is the so-called horizon area.

### 4.3 Scale–dependent couplings and scale setting

This section summarizes the equations of motion for the scale dependent Einstein-Maxwell and Einstein-power-Maxwell theories. The notation follows closely [125] as well as [56, 58, 144].

The scale dependent couplings of the theories are i) the gravitational coupling  $G_k$ , and ii) the electromagnetic coupling  $1/e_k$ . Furthermore, there are three independent fields, which are the metric  $g_{\mu\nu}(x)$ , the electromagnetic four-potential  $A_\mu(x)$ , and the scale field  $k(x)$ . The effective action for the non-linear electrodynamics reads

$$\Gamma[g_{\mu\nu}, A_\mu, k] = \int d^3x \sqrt{-g} \left[ \frac{1}{2\kappa_k} R - \frac{1}{e_k^{2\beta}} \mathcal{L}(F) \right], \quad (4.22)$$

The equations of motion for the metric  $g_{\mu\nu}(x)$  are given by

$$G_{\mu\nu} = \frac{\kappa_k}{e_k^{2\beta}} T_{\mu\nu}^{\text{effec}}, \quad (4.23)$$

with

$$T_{\mu\nu}^{\text{effec}} = T_{\mu\nu}^{\text{EM}} - \frac{e_k^{2\beta}}{\kappa_k} \Delta t_{\mu\nu}. \quad (4.24)$$

Note that  $T_{\mu\nu}^{\text{EM}}$  is given by Eq. 4.3,  $\kappa_k = 8\pi G_k$  is the Einstein constant and the additional object  $\Delta t_{\mu\nu}$  is defined as follows

$$\Delta t_{\mu\nu} = G_k \left( g_{\mu\nu} \square - \nabla_\mu \nabla_\nu \right) G_k^{-1}. \quad (4.25)$$

The equations of motion for the four-potential  $A_\mu(x)$  taking into account the running of  $e_k$  are

$$D_\mu \left( \frac{\mathcal{L}_F F^{\mu\nu}}{e_k^{2\beta}} \right) = 0. \quad (4.26)$$

It is important to note that since the renormalization scale  $k$  is actually not constant any more, this set of equations of motion do not close consistently by itself. This implies that the stress energy tensor is most likely not conserved for almost any choice of functional dependence  $k = k(r)$ . This type of scenario has largely been explored in the context of renormalization group improvement of black holes in asymptotic safety scenarios [54, 69, 71,

110–112, 114, 117–121, 146, 147, 176]. The loss of a conservation laws comes from the fact that there is one consistency equation missing. This missing equation can be obtained from varying the effective action (4.22) with respect to the scale field  $k(r)$ , i.e.

$$\frac{d}{dk}\Gamma[g_{\mu\nu}, A_\mu, k] = 0, \quad (4.27)$$

which can thus be understood as variational scale setting procedure [52, 123–126]. The combination of (4.27) with the above equations of motion guarantees the conservation of the stress energy tensors. A detailed analysis of the split symmetry within the functional renormalization group equations, supports this approach of dynamic scale setting [177].

The variational procedure (4.27), however, requires the knowledge of the exact beta functions of the problem. Since in many cases the precise form of the beta functions is unknown (or at least unsure) one can, for the case of simple black holes, impose a null energy condition and solve for the couplings  $G(r)$ ,  $\Lambda(r)$ ,  $e(r)$  directly [53, 55, 56, 58]. This philosophy of assuring the consistency of the equations by imposing a null energy condition will also be applied in the following study on Einstein-Maxwell and Einstein-power-Maxwell black holes.

## 4.4 The null energy condition

The so-called Null Energy Condition (hereafter NEC) is the less restrictive of the usual energy conditions (dominant, weak, strong, and null), and it helps us to obtain desirable solutions of Einstein's field equations [33, 127]. Considering a null vector  $\ell^\mu$ , the NEC is applied on the matter stress energy tensor such as

$$T_{\mu\nu}^m \ell^\mu \ell^\nu \geq 0. \quad (4.28)$$

The application of such a condition was appropriately implemented in Ref. [56] inspired by the Jacobson idea [130]. Note that in proving fundamental black hole theorems, such as the no hair theorem [129] and the second law of black hole thermodynamics [36], the NEC is, indeed, required. For scale dependent couplings, one requires that the aforementioned condition is not violated and, therefore, the NEC is applied on the effective stress energy

tensor for a special null vector  $\ell^\mu = \{f^{-1/2}, f^{1/2}, 0\}$  such as

$$T_{\mu\nu}^{\text{effec}} \ell^\mu \ell^\nu = \left( T_{\mu\nu}^{\text{EM}} - \frac{\epsilon_k^{2\beta}}{\kappa_k} \Delta t_{\mu\nu} \right) \ell^\mu \ell^\nu \geq 0. \quad (4.29)$$

In addition, the left hand side (LHS) is null as well as  $T_{\mu\nu}^{\text{EM}} \ell^\mu \ell^\nu = 0$  and the condition reads

$$\Delta t_{\mu\nu} \ell^\mu \ell^\nu = 0. \quad (4.30)$$

One should note that Eq. 4.30 allows us to obtain the gravitational coupling  $G(r)$  easily by solving the differential equation

$$G(r) \frac{d^2 G(r)}{dr^2} - 2 \left( \frac{dG(r)}{dr} \right)^2 = 0, \quad (4.31)$$

which leads to

$$G(r) = \frac{G_0}{1 + \epsilon r}. \quad (4.32)$$

The NEC allows us to decrease the number of degrees of freedom, and thus it becomes an important tool for scale dependent black hole problems.

## 4.5 Scale dependence in Einstein-Maxwell theory

In order to get insight into non-linear electrodynamics regarding the running of couplings, one first has to discuss the effects of scale dependence in linear electrodynamics. With this in mind, one also needs to determine the set of four functions  $\{G(r), E(r), f(r), e(r)^2\}$  which are obtained by combining Einstein's effective equations of motion with the NEC taking into account the EOM for the four-potential  $A_\mu$ .

### 4.5.1 Solution

The solution for this scale dependent black hole is given by

$$\begin{aligned}
G(r) &= \frac{G_0}{1 + \epsilon r}, \\
E(r) &= \frac{Q_0}{r} e(r)^2, \\
f(r) &= -\frac{G_0 M_0}{(r\epsilon + 1)^2} - \frac{Q_0^2}{2e_0^2} \frac{(\ln(r/\tilde{r}_0) + r\epsilon)}{(r\epsilon + 1)^2}, \\
e(r)^2 &= e_0^2 \left[ \frac{1}{(1 + r\epsilon)^3} + 4 \frac{r\epsilon}{(1 + r\epsilon)^3} \right. \\
&\quad \left. - \left( 4M_0 G_0 - 5Q_0^2 + 2Q_0^2 \ln \left( \frac{r}{\tilde{r}_0} \right) \right) \frac{r^2 \epsilon^2}{(1 + r\epsilon)^3} \right].
\end{aligned} \tag{4.33}$$

where the integration constants are chosen such as the classical Einstein-Maxwell (2+1)-dimensional black hole is recovered according to [162]. It is relevant to say that the gravitational coupling  $G(r)$  is obtained by taking advantage of NEC, while the electric field  $E(r)$  is given by the covariant derivative 4.26, which depends on the electromagnetic coupling constant  $e(r)$ . Besides, the lapse function  $f(r)$  and the coupling  $e(r)$  are directly obtained by using Einstein's effective field equations combined with the solutions for  $E(r)$  and  $G(r)$ . In addition, our solution reproduces the results of the classical theory in the limit  $\epsilon \rightarrow 0$ , i.e.

$$\begin{aligned}
\lim_{\epsilon \rightarrow 0} G(r) &= G_0, \\
\lim_{\epsilon \rightarrow 0} E(r) &= \frac{Q_0}{r} e_0^2, \\
\lim_{\epsilon \rightarrow 0} f(r) &= -G_0 M_0 - \frac{Q_0^2}{2e_0^2} \ln \left( \frac{r}{\tilde{r}_0} \right), \\
\lim_{\epsilon \rightarrow 0} e(r)^2 &= e_0^2.
\end{aligned} \tag{4.34}$$

which justifies the naming of the constants aforementioned  $\{G_0, M_0, Q_0, e_0\}$  in terms of their meaning in the absence of scale dependence [56], as it should be. Besides, the parameter  $\epsilon$  controls the strength of the new scale dependence effects, and therefore it is useful to treat

it as a small expansion parameter as follows

$$G(r) \approx G_0 \left[ 1 - r\epsilon + \mathcal{O}(\epsilon^2) \right], \quad (4.35)$$

$$E(r) \approx \frac{Q_0}{r} e_0^2 \left[ 1 + \epsilon r + \mathcal{O}(\epsilon^2) \right], \quad (4.36)$$

$$f(r) \approx f_0(r) + \left[ 2G_0 M_0 - \frac{1}{2} \frac{Q_0^2}{e_0^2} + \frac{Q_0^2}{e_0^2} \ln \left( \frac{r}{\tilde{r}_0} \right) \right] r\epsilon + \mathcal{O}(\epsilon^2), \quad (4.37)$$

$$e(r)^2 \approx e_0^2 \left[ 1 + \epsilon r + \mathcal{O}(\epsilon^2) \right]. \quad (4.38)$$

In figure 4.1 the lapse function  $f(r)$  is shown for different values of  $\epsilon$  in comparison to

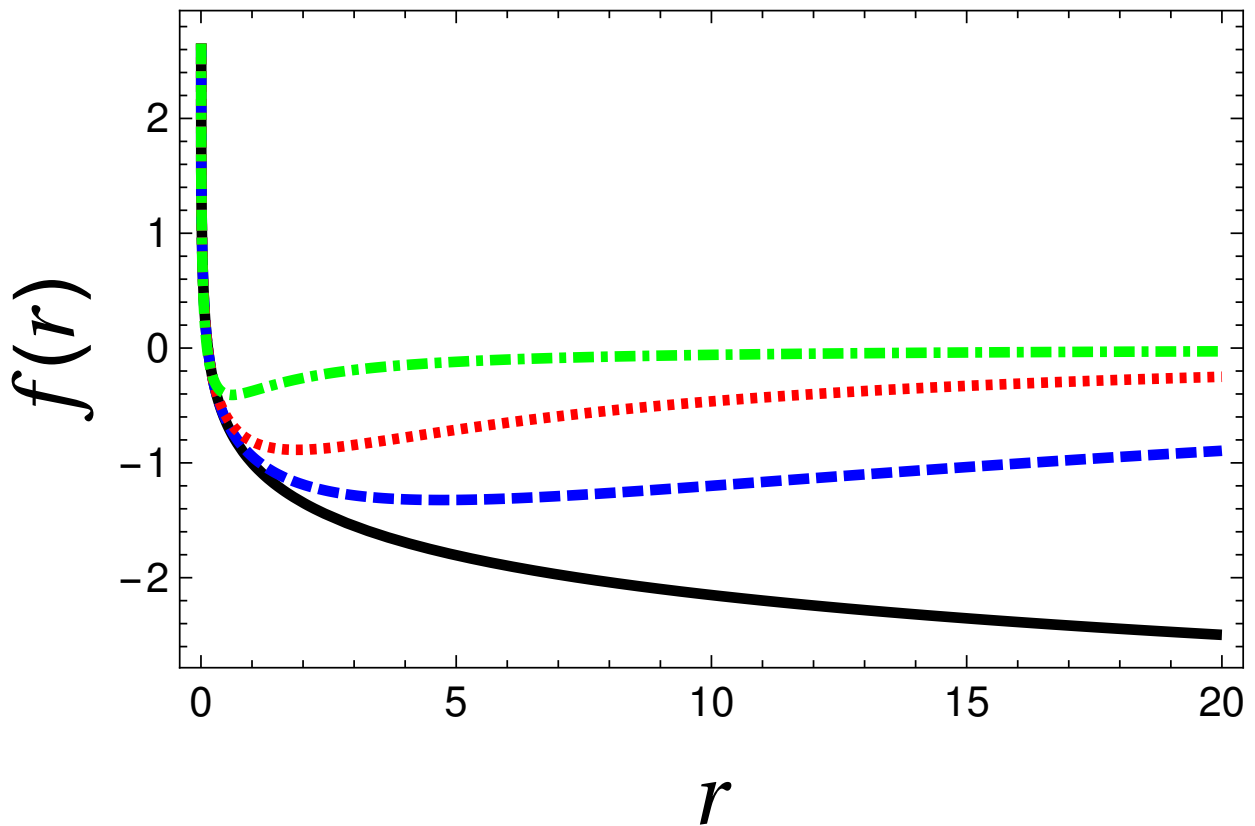


**Figure 4.1:** Lapse function  $f(r)$  for  $\epsilon = 0$  (black solid line),  $\epsilon = 0.04$  (blue dashed line),  $\epsilon = 0.15$  (dotted red line) and  $\epsilon = 1$  (dotted dashed green line). The values for the rest of the parameters have been taken as unity.

the classical (2+1)-dimensional Einstein-Maxwell solution. The figure shows that the scale dependent solution for small  $\epsilon \cdot r$  values is consistent with the classical case. However, when  $\epsilon \cdot r$  becomes sufficiently large, a deviation from the classical solution appears. The

electromagnetic coupling  $e(r)$  is shown in Figure 4.2 for different values of  $\epsilon$ . Note that when  $\epsilon$  is small the classical case is recovered, but when  $\epsilon$  increases the electromagnetic coupling tends to decrease until it is stabilized.

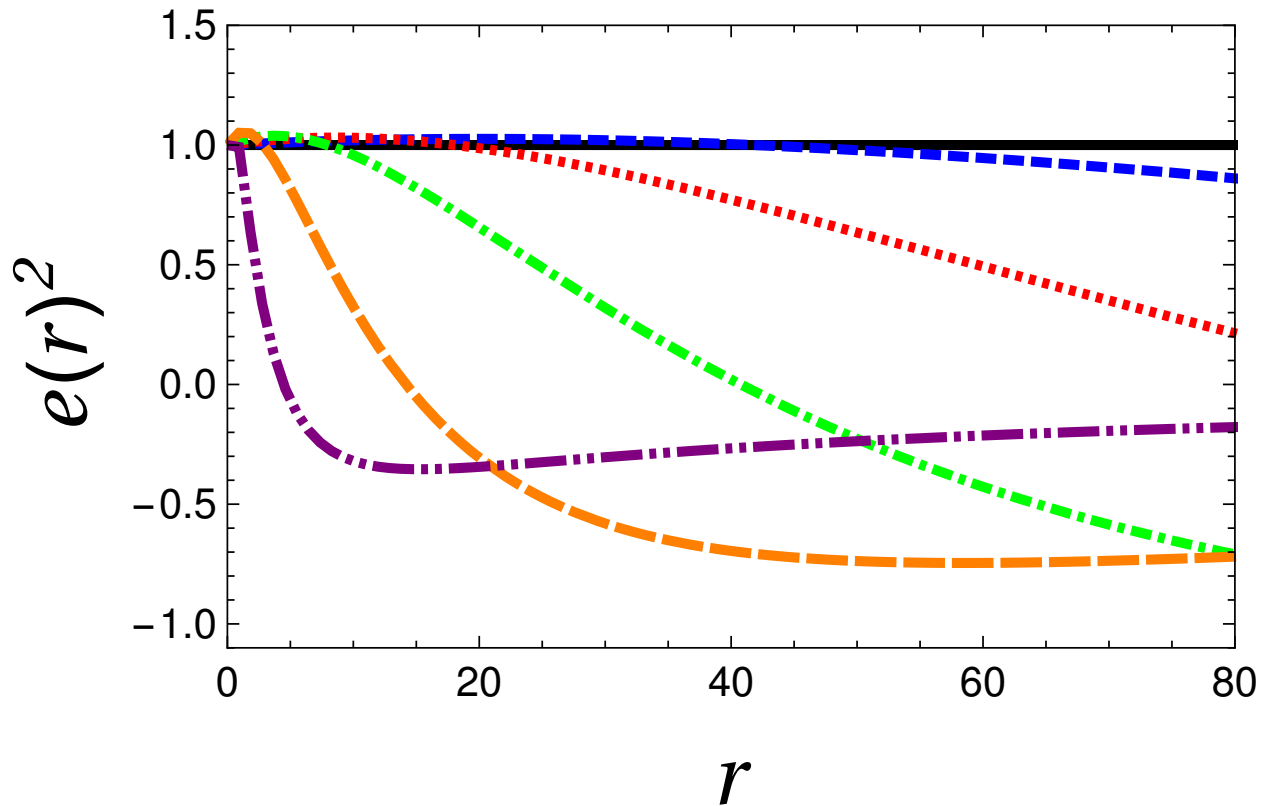


**Figure 4.2:** Electromagnetic coupling  $e(r)^2$  for  $\epsilon = 0$  (black solid line),  $\epsilon = 0.0025$  (short dashed blue line),  $\epsilon = 0.007$  (dotted red line),  $\epsilon = 0.02$  (dotted dashed green line),  $\epsilon = 0.08$  (long dashed orange line) and  $\epsilon = 0.5$  (double dotted dashed purple line). The other values have been taken as unity.

## 4.5.2 Asymptotic behaviour

In this subsection a few invariants need to be revisited. In particular we will focus on the Ricci scalar  $R$  and the Kretschmann scalar  $\mathcal{K}$ . Both of them are relevant in order to check if some additional divergences appear. For the static and circularly symmetric metric we have considered, the Ricci scalar is given by

$$R = -f''(r) - \frac{2f'(r)}{r}, \quad (4.39)$$

or more precisely

$$R = \frac{Q_0^2}{2r^2 e_0^2 (1+r\epsilon)^4} - \frac{8M_0 G_0 e_0^2 + 4Q_0^2 \ln(r/\tilde{r}_0)}{2r^2 (1+r\epsilon)^4 e_0^2} r\epsilon + \frac{4M_0 G_0 e_0^2 - 7Q_0^2 + 2Q_0^2 \ln(r/\tilde{r}_0)}{2r^2 (1+r\epsilon)^4 e_0^2} (r\epsilon)^2. \quad (4.40)$$

We require that classically the Ricci scalar reads

$$R_0 = \frac{1}{2} \frac{Q_0^2}{e_0^2 r^2}. \quad (4.41)$$

Considering  $r$  values close to zero one obtains

$$R \approx R_0 \left[ 1 - \left[ \frac{8M_0 G_0 e_0^2}{Q_0^2} + 4 \ln \left( e \frac{r}{\tilde{r}_0} \right) \right] r\epsilon + \dots \right]. \quad (4.42)$$

Thus, upon comparing Eq.4.40 with Eq.4.41 we observe that the scale dependent effect strongly distorts this invariant. Despite that, for small values of  $r$  the standard case  $R_0$  is recovered. In the same way, one expects that  $\epsilon$  should be small, therefore one can expand the Ricci scalar around  $\epsilon = 0$  but the solution is exactly the same reported for  $r \ll 1$ . Regarding the Kretschmann scalar, it is computed to be

$$\mathcal{K} = R_{\mu\nu\alpha\beta} R^{\mu\nu\alpha\beta}. \quad (4.43)$$

Thus, when  $\epsilon$  is small the Kretschmann scalar reads

$$\mathcal{K} \approx \mathcal{K}_0 \left[ 1 - \left[ \frac{16M_0 G_0 e_0^2}{3Q_0^2} + \frac{8}{3} \ln \left( \frac{r}{\tilde{r}_0} \right) \right] r\epsilon \right] + \dots \quad (4.44)$$

Note that the classical result for this invariant is indeed  $\mathcal{K}_0 = 3Q_0^4/4r^4$ , which coincides with our solution when  $\epsilon \rightarrow 0$ .

The other regime of asymptotic behaviour can be studied in a large radius expansion  $r \rightarrow \infty$ . In this limit the lapse function  $f(r)$  decays as  $r^{-1}$  which disagrees with the classical result shown in Eq.4.15. On the other hand, the electromagnetic coupling  $e(r)$  also tends to zero as  $r^{-1}$  in contrast with the expected result,  $e_0$ . Finally, one obtains that  $E(r) \sim r^{-2}$ ,  $R \sim r^{-4}$  and  $\mathcal{K} \sim r^{-6}$ , all of them going to zero as expected. However, it can be shown that these functions decay faster than those corresponding to the classical solutions. In fact, in absence

of running coupling, a straightforward calculation reveals that  $E(r) \sim r^{-1}$ ,  $R \sim r^{-2}$  and  $\mathcal{K} \sim r^{-4}$ .

### 4.5.3 Horizons

The event horizon occurs when the lapse function vanishes, i.e.  $f(r_H) = 0$ . Thus, this Einstein-Maxwell black hole solution represents a non trivial deviation from the classical solution which is manifest when we compare our solution with the corresponding black hole solution without the scale dependence. Here, the horizon read

$$r_H = \frac{1}{\epsilon} W \left( \epsilon e^{-\frac{2G_0 M_0 \epsilon_0^2}{Q_0^2}} \right), \quad (4.45)$$

where  $W(\cdot)$  is the so-called Lambert- $W$  function, which is a set of functions, namely the branches of the inverse relation of the function  $Y(r\epsilon) = r\epsilon e^{r\epsilon}$  with  $r\epsilon$  being a complex number. In particular, Eq 4.45 is also the principal solution for  $r\epsilon$ . In Figure 4.3 the scale dependent effect on horizon is shown. We can see that the deviation from the classical case is also evident for small  $M_0$  values.

In addition, one can expand the horizon around  $\epsilon = 0$  obtaining the classical solution plus corrections i.e.

$$r_H \approx r_0 \left[ 1 - \epsilon r_0 + \mathcal{O}(\epsilon^2) \right]. \quad (4.46)$$

### 4.5.4 Thermodynamic properties

After having gained experience on the horizon structure one can now move towards the usual thermodynamic properties associated with our solution shown at Eq. 4.33. Thus, the Hawking temperature of the black hole assuming the ansatz 4.5 is given by

$$T_H(r_H) = \frac{1}{4\pi} \left| \lim_{r \rightarrow r_H} \frac{\partial_r g_{tt}}{\sqrt{-g_{tt}g_{rr}}} \right|, \quad (4.47)$$

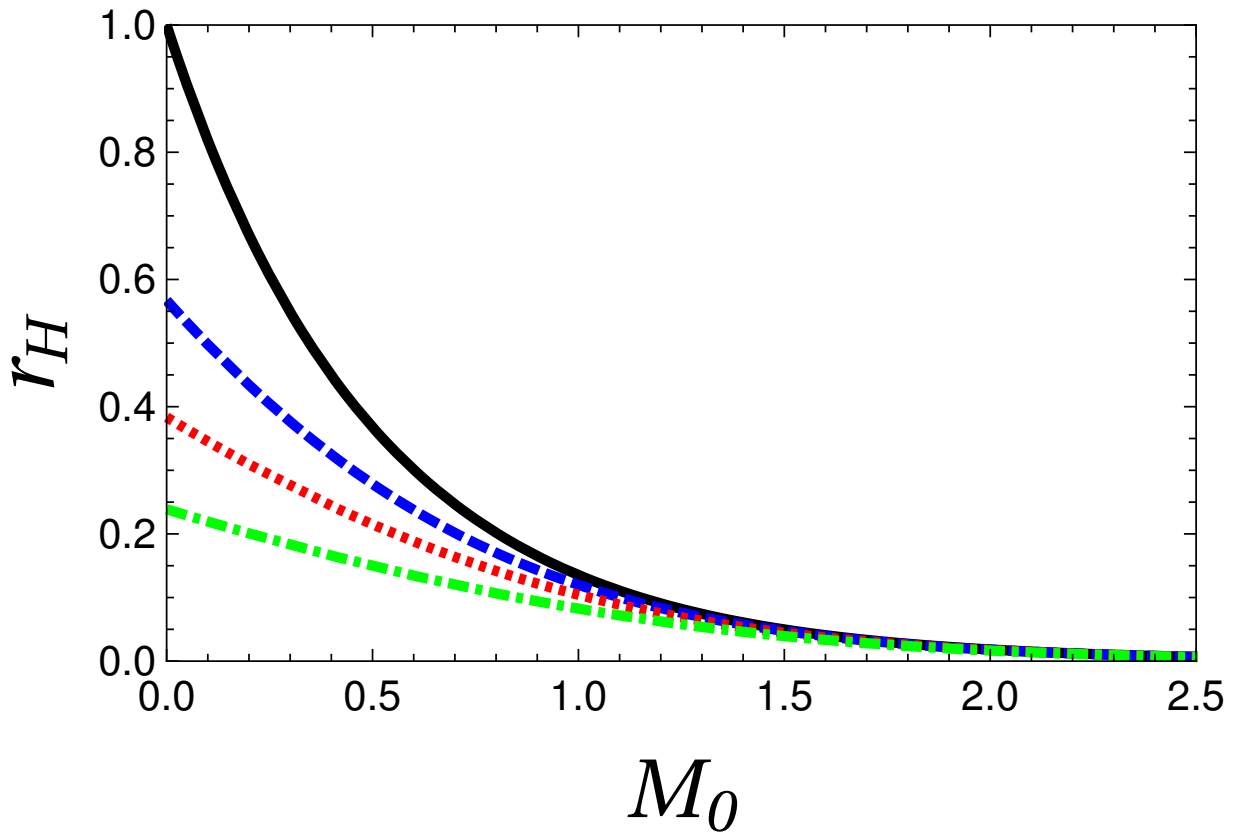


**Figure 4.3:** Black hole horizons  $r_H$  as a function of the mass  $M_0$  for  $\epsilon = 0$  (black solid line),  $\epsilon = 1$  (blue dashed line),  $\epsilon = 2.5$  (dotted red line) and  $\epsilon = 6$  (dotted dashed green line). The values of the rest of the parameters have been taken as unity.

i.e.

$$T_H(r_H) = \frac{1}{4\pi} \left| \frac{Q_0^2}{2r_H(1 + \epsilon r_H)e_0^2} \right|. \quad (4.48)$$

Taking advantage of the fact that the integration constant  $\epsilon$  should be small, one can expand around  $\epsilon = 0$  to get the well-known Hawking temperature (at leader order) i.e.

$$T_H(r_H) \approx T_0(r_0) \left| 1 + \epsilon r_0 + \mathcal{O}(\epsilon^2) \right|. \quad (4.49)$$

In Figure 4.4 we show the effective temperature which takes into account the running coupling effect.

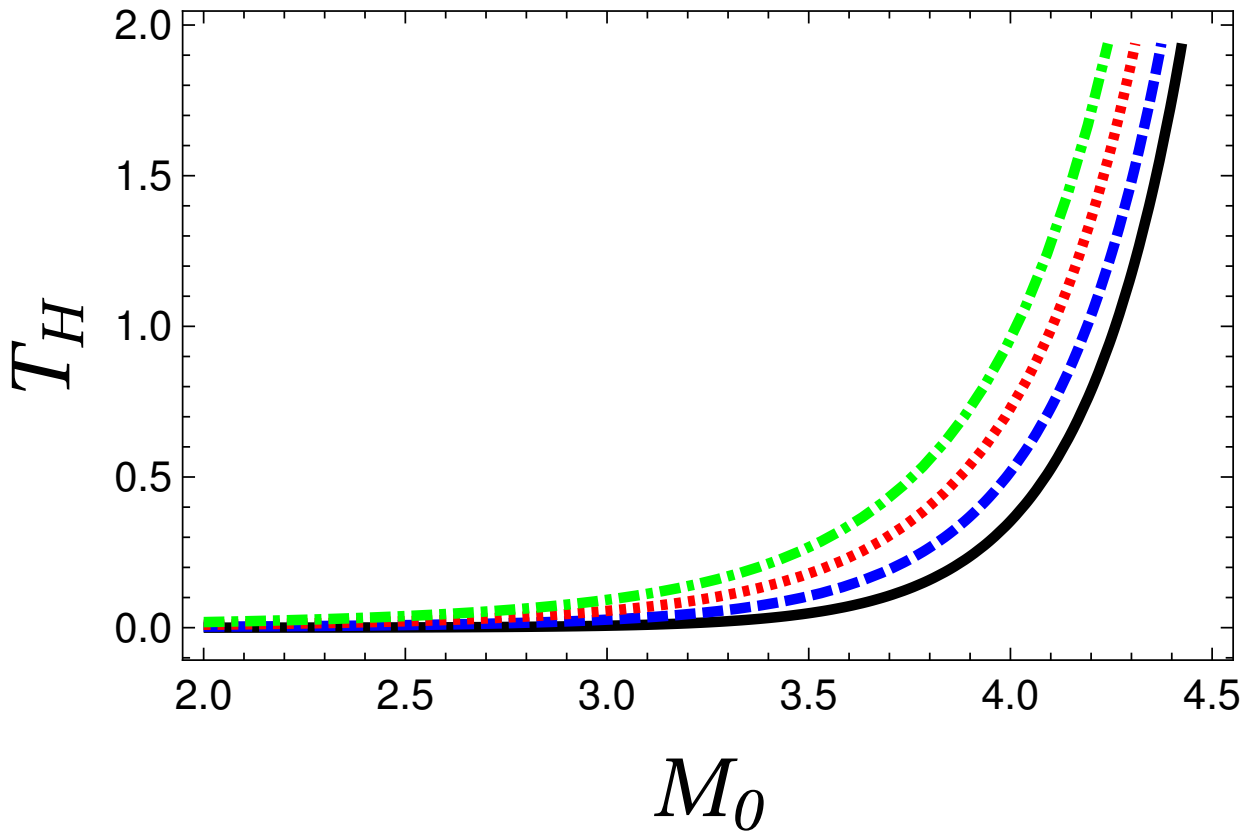


**Figure 4.4:** The Hawking temperature  $T_H$  as function of the classical mass  $M_0$  for  $\epsilon = 0$  (black solid line),  $\epsilon = 750$  (blue dashed line),  $\epsilon = 1800$  (dotted red line) and  $\epsilon = 3000$  (dotted dashed green line). The other values of the rest of the parameters have been taken as unity. Note that the vertical axis is scaled  $1 : 10^6$

Moreover, the Bekenstein-Hawking entropy for his black hole is

$$S = \frac{\mathcal{A}_H(r_H)}{4G(r_H)} = S_0(r_H)(1 + \epsilon r_H), \quad (4.50)$$

and assuming small values of  $\epsilon$  one can expand to get

$$S \approx S_0(r_0) \left[ 1 - \frac{1}{2}(\epsilon r_0)^2 + \mathcal{O}(\epsilon^3) \right]. \quad (4.51)$$

In Figure 4.5 below we show the entropy for our (2+1)-dimensional Einstein-Maxwell scale dependent black hole. It is clear that the running effect is dominant when  $\epsilon$  is not small, while for large values of  $M_0$  the effect is practically zero.

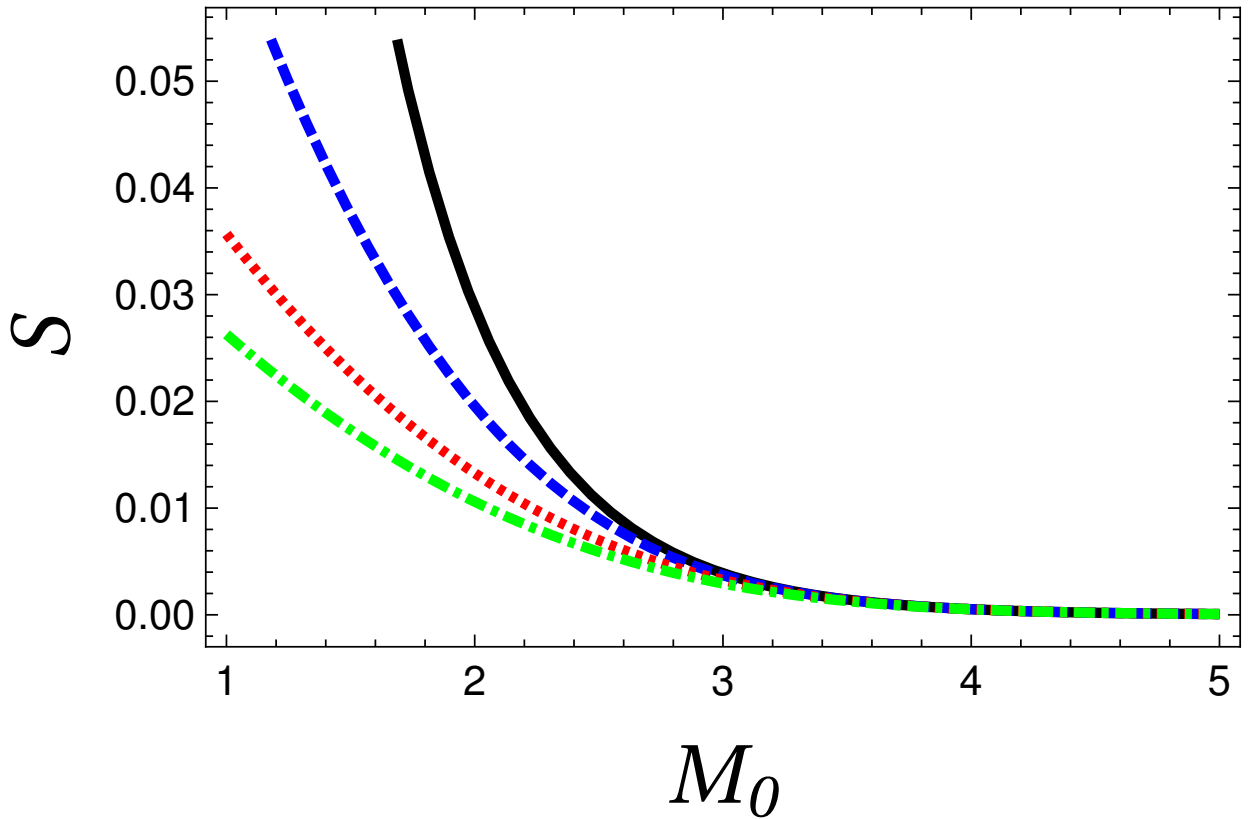


**Figure 4.5:** The Bekenstein-Hawking entropy  $S$  as function of classical mass  $M_0$  for  $\epsilon = 0$  (black solid line),  $\epsilon = 200$  (blue dashed line),  $\epsilon = 600$  (dotted red line) and  $\epsilon = 1000$  (dotted dashed green line). The other values have been taken as unity.

Finally, the heat capacity is computed in the usual way i.e.:

$$C_Q = T \left. \frac{\partial S}{\partial T} \right|_Q, \quad (4.52)$$

which read

$$C_Q = -S_0(r_H)(1 + \epsilon r_H). \quad (4.53)$$

The classical case is, of course, recovered in the  $\epsilon \rightarrow 0$  limit. Due to a weak  $\epsilon$  dependence it was necessary to plot the figure with very large values of  $\epsilon$  in order to generate a visible effect. The scale dependent effect is notoriously small for those quantities.

### 4.5.5 Total charge

The electric field is parametrized through the total charge  $Q$ , but in our previous discussion  $Q_0$  only denotes an integration constant which coincides with the charge of the classical theory. In general, we need to compute the total charge by the following relation [1]

$$Q = \int \sqrt{-g} d\Omega \left( \frac{\mathcal{L}_F F_{\mu\nu}}{e_k^{2\beta}} \right) n^\mu \sigma^\nu, \quad (4.54)$$

where  $n^\mu$  and  $\sigma^\nu$  are the unit spacelike and timelike vectors normal to the hypersurface of radius  $r$ , and they are given by  $n^\mu = (f^{-1/2}, 0, 0)$  and  $\sigma^\nu = (0, f^{1/2}, 0)$  as well as  $\sqrt{-g} d\Omega = r d\phi$ . Making use of these we obtain

$$Q = 2\pi Q_0, \quad (4.55)$$

which is proportional to the classical value and has no  $\epsilon$  dependence.

## 4.6 Einstein-power-Maxwell scale dependence

This section is devoted to the study of a  $(2+1)$  scale dependent gravity coupled to a power-Maxwell source. As mentioned before, the case  $\beta = 3/4$  leads to a dimensionless electromagnetic coupling which was set to the unity in the section 4.2.2. However, if one considers a scale dependent gravity, the electromagnetic coupling has a non-trivial scale dependence. Therefore, in this section we shall hold the electromagnetic coupling dependence of the action 4.1. In this way, the solution consists of a set of four functions  $\{G(r), E(r), f(r), e(r)^3\}$ , which are obtained by combining Einstein's effective equations of motion with the NEC taking advantage of the EOM for the four-potential  $A_\mu$ . In what follows we shall obtain the solutions of the system in terms of the functions mentioned above.

### 4.6.1 Solution

The integration constants have been chosen such as the scale dependent solution reduces to the classical NLED case when the appropriate limit is taken. Thus, our solution reads

$$\begin{aligned}
G(r) &= \frac{G_0}{1 + \epsilon r}, \\
E(r) &= \frac{Q_0}{r^2} \left( \frac{e(r)}{e_0} \right)^3, \\
f(r) &= \frac{4G_0Q_0^2}{3r(r\epsilon + 1)^3} - \frac{M_0G_0(r^3\epsilon^2 + 3r^2\epsilon + 3r)}{3r(r\epsilon + 1)^3}, \\
e(r)^3 &= e_0^3 \left[ \frac{(2r\epsilon(3r\epsilon + 2) + 1)}{(r\epsilon + 1)^4} - \frac{M_0r^3\epsilon^2(r\epsilon + 4)}{4Q_0^2(r\epsilon + 1)^4} \right].
\end{aligned} \tag{4.56}$$

In the limit  $\epsilon \rightarrow 0$  we obtain

$$\begin{aligned}
\lim_{\epsilon \rightarrow 0} G(r) &= G_0, \\
\lim_{\epsilon \rightarrow 0} E(r) &= \frac{Q_0}{r^2}, \\
\lim_{\epsilon \rightarrow 0} f(r) &= \frac{4G_0Q_0^2}{3r} - G_0M_0, \\
\lim_{\epsilon \rightarrow 0} e(r)^3 &= e_0^3.
\end{aligned} \tag{4.57}$$

Note that if we set  $e_0 = 1$ , the classical solution in section 4.2.2 is recovered. Even more, if one demands that  $G_0 = 1$  (which is the standard lore) then we are in complete agreement with the classical solution given at Ref. [158].

### 4.6.2 Asymptotic behaviour

The asymptotic behaviour of this solution can be studied by computing geometrical invariants i.e. the Ricci scalar, which for our solution is

$$R = -4G_0\epsilon \left[ \frac{M_0 + 4Q_0^2\epsilon}{r(r\epsilon + 1)^5} \right], \tag{4.58}$$

where the classical case (with a null cosmological constant) is clearly  $R_0 = 0$ . For  $r \rightarrow 0$  one obtains

$$R \approx -4G_0\epsilon \left[ \frac{M_0 + 4Q_0^2\epsilon}{r} \right] + \mathcal{O}(r). \quad (4.59)$$

We observe that the Ricci scalar is altered in presence of scale dependent coupling. In addition, one note that an unexpected  $r^6$  divergence appears, which is controlled by  $\epsilon$ . Another geometrical invariant is the Kretschmann scalar  $\mathcal{K}$  which is given by

$$\mathcal{K} = R_{\mu\nu\alpha\beta}R^{\mu\nu\alpha\beta}. \quad (4.60)$$

For  $r \rightarrow 0$  one can obtain the first terms which are

$$\mathcal{K} \approx \frac{32G_0^2Q_0^4}{3r^6} \left[ 1 - \left( \frac{M_0}{Q_0^2}\epsilon + 4\epsilon^2 \right) r^2 \right] + \mathcal{O}(r^{-3}). \quad (4.61)$$

Taking into account that the  $\epsilon$  should be small we have

$$\mathcal{K} \approx \frac{32G_0^2Q_0^4}{3r^6} \left[ 1 - \frac{M_0r^2}{Q_0^2}\epsilon + \mathcal{O}(\epsilon^2) \right], \quad (4.62)$$

where the standard value  $\mathcal{K}_0$  has been obtained demanding that  $\epsilon$  goes to zero. Classically, the Ricci scalar for null cosmological constant is identically zero, however in presence of scale dependent couplings it exhibits a singularity. The Kretschmann scalar exhibits a singularity at  $r \rightarrow 0$  for both the classical and the scale dependent case. On the other hand, the opposite regime of asymptotic behaviour is studied in the large radius expansion  $r \rightarrow \infty$  both for the Ricci and the Kretschmann scalar. The Ricci scalar as well as the Kretschmann scalar are asymptotically close to zero.

Regarding the limit  $r \rightarrow \infty$  the lapse function goes as  $r^{-1}$  in agreement with the asymptotic behaviour of the classical solution. In addition, note the unusual behaviour of the electromagnetic coupling in the light of scale dependent framework in Fig. 4.8. Starting from  $e_0^3$  the electromagnetic coupling decays softly and it stabilizes when

$$\lim_{r \rightarrow \infty} e(r)^3 = - \left( \frac{1}{3r_0\epsilon} \right) e_0^3, \quad (4.63)$$

instead of reach the classical value. The electric field tends to zero as expected but slowly

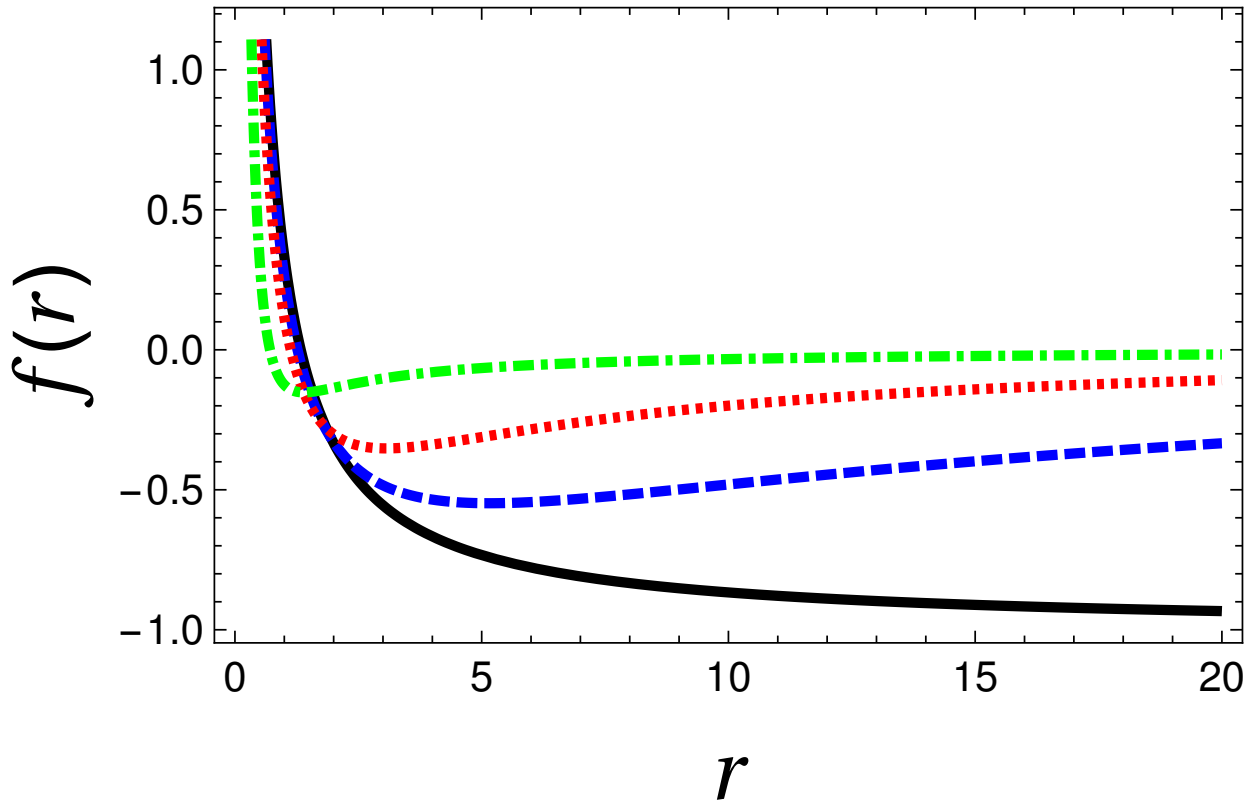


**Figure 4.6:** Lapse function  $f(r)$  for  $\epsilon = 0$  (black solid line),  $\epsilon = 0.04$  (blue dashed line),  $\epsilon = 0.15$  (dotted red line) and  $\epsilon = 1$  (dotted dashed green line). The values of the rest of the parameters have been taken as unity.

compared with the classical case. In fact,  $E(r)$  behaves as  $r^{-1}$  in clearly deviation with respect to the result shown in Eq.4.16. Finally, the curvature and Kretschmann scalars hold the same asymptotic behaviour of the results obtained in absence of running, i.e.  $R \sim r^{-4}$  and  $\mathcal{K} \sim r^{-6}$ .

### 4.6.3 Horizons

Applying the condition  $f(r_H) = 0$  one obtains the scale dependent horizon which reads

$$r_H = -\frac{1}{\epsilon} \left[ 1 - \left[ 1 + 3\epsilon r_0 \right]^{1/3} \right], \quad (4.64)$$

$$r_{\pm} = -\frac{1}{\epsilon} \left[ 1 + \frac{1}{2}(1 \pm i\sqrt{3}) \left[ 1 + 3\epsilon r_0 \right]^{1/3} \right]. \quad (4.65)$$

where  $r_0$  is the classical value given by Eq. 4.17. Note that one obtains three horizons, out of which one is real (physical horizon) and two  $r_{\pm}$  are complex (non-physical).

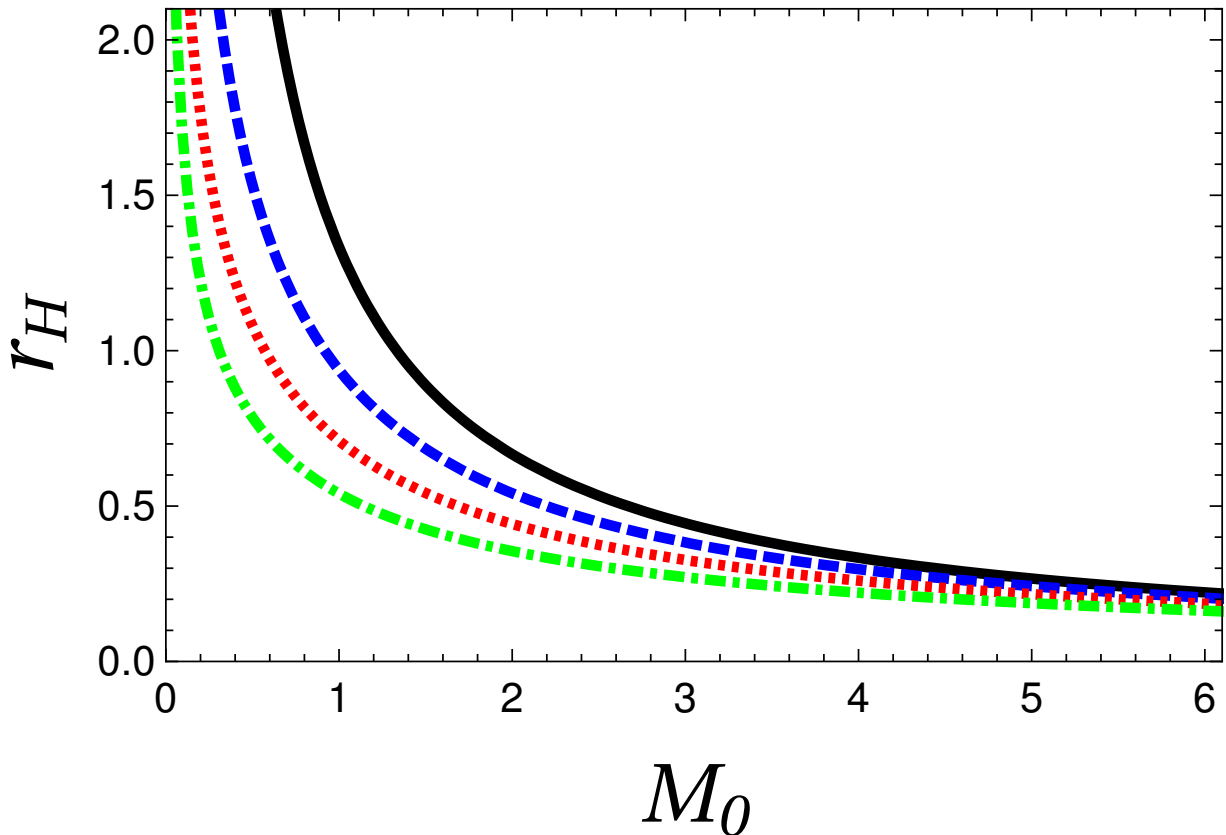


**Figure 4.7:** Black hole horizons  $r_H$  as a function of the mass  $M_0$  for  $\epsilon = 0$  (black solid line),  $\epsilon = 0.4$  (blue dashed line),  $\epsilon = 1$  (dotted red line) and  $\epsilon = 2$  (dotted dashed green line). The values of the rest of the parameters have been taken as unity.

In addition, since the scale dependence of coupling constants is usually assumed to be weak, it is reasonable to consider the dimensionful parameter  $\epsilon$  as small compared to the other scales and, therefore, one can expand around  $\epsilon$  close to zero, which gives us

$$r_H \cong r_0 \left[ 1 - \epsilon r_0 + \frac{5}{3} (\epsilon r_0)^2 + \dots \right]. \quad (4.66)$$

One should note that when  $\epsilon$  tends to zero the classical case is recovered. Besides, although  $\epsilon$  could take positive or negative values, here in order to obtain desirable physical results we require that  $\epsilon > 0$ . In our set of solutions  $\{G(r), E(r), f(r), e(r)^3\}$  we can expand around

zero for small values of  $\epsilon$ , i.e.

$$G(r) \approx G_0 \left[ 1 - r\epsilon + \mathcal{O}(\epsilon^2) \right], \quad (4.67)$$

$$E(r) \approx E_0(r) + \mathcal{O}(\epsilon^2), \quad (4.68)$$

$$f(r) \approx f_0(r) + \left[ 2G_0M_0 - \frac{4G_0Q_0^2}{r} \right] r\epsilon + \mathcal{O}(\epsilon^2), \quad (4.69)$$

$$e^3(r) \approx e_0^3 \left[ 1 + \mathcal{O}(\epsilon^2) \right]. \quad (4.70)$$

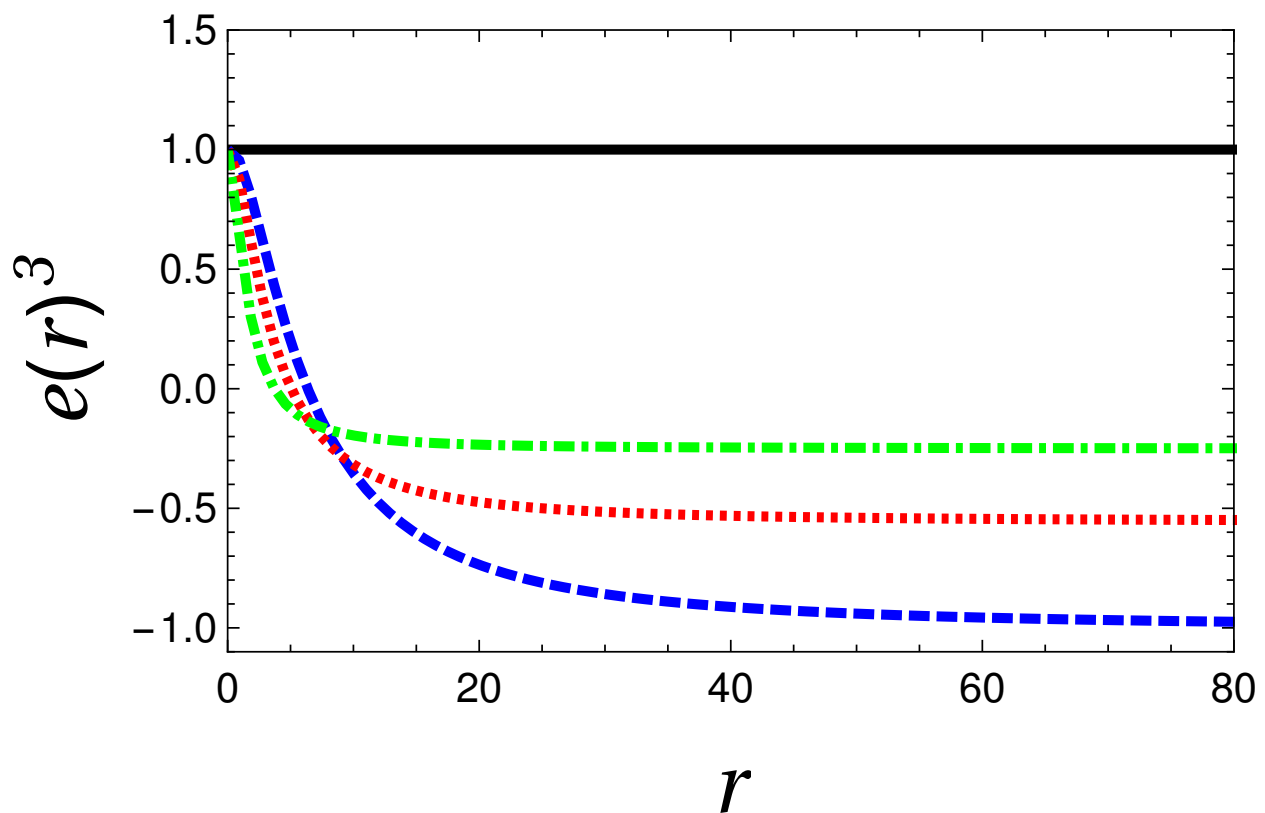


**Figure 4.8:** Electromagnetic coupling  $e(r)^3$  for  $\epsilon = 0$  (black solid line),  $\epsilon = 0.25$  (dashed blue line),  $\epsilon = 0.45$  (dotted red line) and  $\epsilon = 1$  (dotted dashed green line). The values of the rest of the parameters have been taken as unity.

#### 4.6.4 Thermodynamic properties

Using the horizon structure and the lapse function (which is given by Eq. 4.56) one can calculate the Hawking temperature of the corresponding scale dependent black hole. At the

outer horizon this temperature is given by the simple formula

$$T_H = \frac{1}{4\pi} \left| \lim_{r \rightarrow r_H} \frac{\partial_r g_{tt}}{\sqrt{-g_{tt}g_{rr}}} \right|, \quad (4.71)$$

which reads in term of the horizon radius

$$T_H = \frac{1}{4\pi} \left| \frac{M_0 G_0}{r_H(1 + \epsilon r_H)} \right|. \quad (4.72)$$

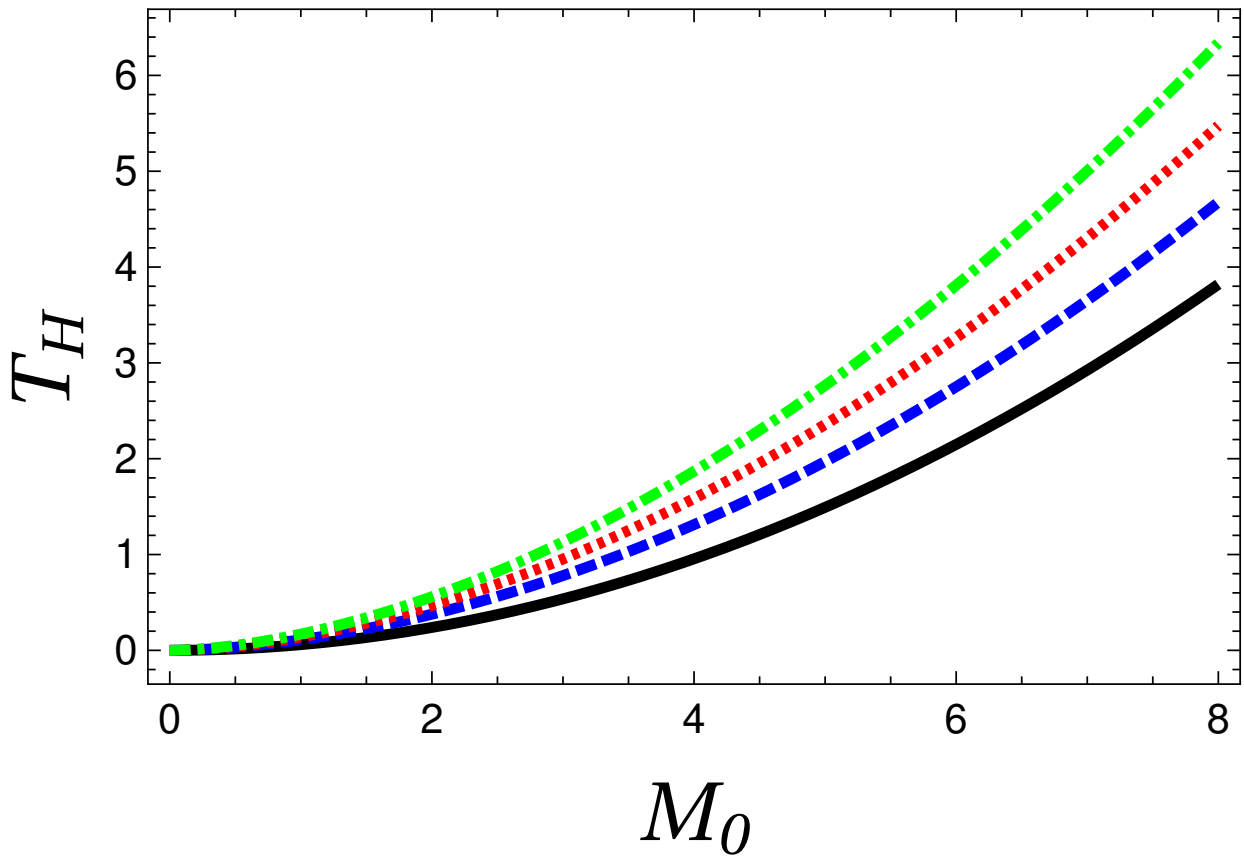


**Figure 4.9:** Hawking temperature  $T_H$  as a function of the classical mass  $M_0$  for  $\epsilon = 0$  (black solid line),  $\epsilon = 20$  (blue dashed line),  $\epsilon = 50$  (dotted red line) and  $\epsilon = 100$  (dotted dashed green line). The values of the rest of the parameters have been taken as unity.

In order to recover the classical result we expand around  $\epsilon = 0$  and upon evaluating at the classical horizon we obtain

$$T_H(r_H) \approx T_0(r_0) \left| 1 + \frac{1}{3}(\epsilon r_0)^2 + \mathcal{O}(\epsilon^3) \right|, \quad (4.73)$$

where it is clear that  $\epsilon \rightarrow 0$  coincides with Eq. 4.19 as it should be.

In addition, the Bekenstein-Hawking entropy obeys the well-known relation heritage of Brans-Dickey theory applied to the (2+1)-dimensional case

$$S = \frac{1}{4} \oint dx \frac{\sqrt{h}}{G(x)}, \quad (4.74)$$

where  $h_{ij}$  is the induced metric at the horizon. For the present circularly symmetric solution this integral is trivial because the induced metric for constant  $t$  and  $r$  slices is  $ds = r d\phi$  and moreover  $G(x) = G(r_H)$  is constant along the horizon. Using these facts, the entropy for this solution is found to be [56, 58]

$$S = \frac{\mathcal{A}_H}{4G(r_H)} = S_0(r_H)(1 + \epsilon r_H), \quad (4.75)$$

while for small values of  $\epsilon$  one obtains

$$S \approx S_0(r_0) \left[ 1 - \frac{1}{3}(\epsilon r_0)^2 + \mathcal{O}(\epsilon^3) \right], \quad (4.76)$$

which, of course, coincides with the classical results in the limit  $\epsilon \rightarrow 0$ . In addition, the heat capacity (at constant charge)  $C_Q$  can be calculated by

$$C_Q = T \left. \frac{\partial S}{\partial T} \right|_Q. \quad (4.77)$$

Combining Eq. 4.72 with 4.75 one obtains the simple relation

$$C_Q = -\frac{1}{8} \frac{M_0}{T_H} = -S_0(r_H)(1 + \epsilon r_H). \quad (4.78)$$

Note that the black hole is unstable since  $C_Q < 0$ , and it coincides with the classical result in the limit  $\epsilon \rightarrow 0$ .

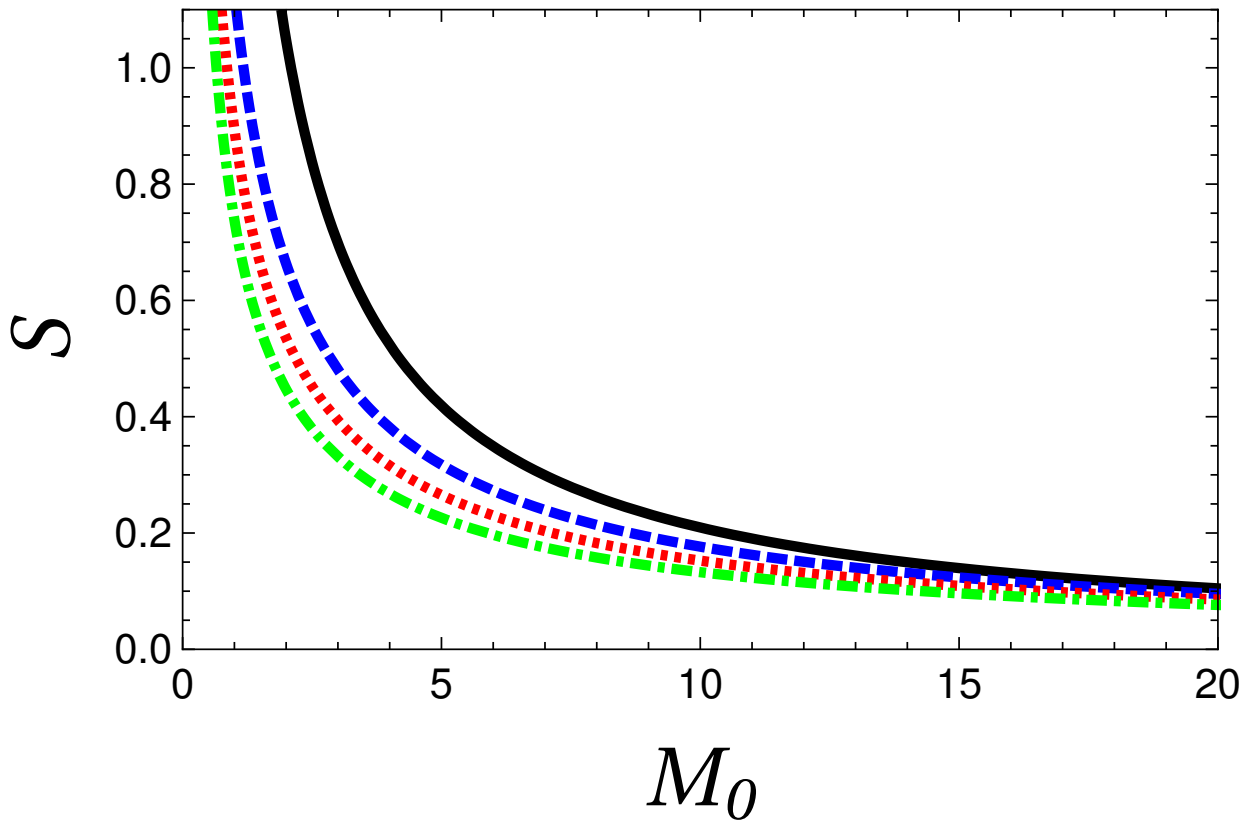


**Figure 4.10:** The Bekenstein-Hawking entropy  $S$  as a function of the classical mass  $M_0$  for  $\epsilon = 0$  (black solid line),  $\epsilon = 20$  (blue dashed line),  $\epsilon = 50$  (dotted red line) and  $\epsilon = 100$  (dotted dashed green line). The other values have been taken as unity.

#### 4.6.5 Total charge

As in the previous case, the total charge  $Q$  needs to be computed by the relation [1]

$$Q = \int \sqrt{-g} d\Omega \left( \frac{\mathcal{L}_F F_{\mu\nu}}{e_k^{2\beta}} \right) n^\mu \sigma^\nu. \quad (4.79)$$

In this case we obtain

$$Q = \frac{Q_0}{2e_0^{3/2}}, \quad (4.80)$$

which also is proportional to the classical value and does not have  $\epsilon$  dependence.

## 4.7 Discussion

Scale dependent gravitational couplings can induce non-trivial deviations from classical Black Holes solutions. We have studied two cases, first Einstein-Maxwell and second Einstein-power-Maxwell case. Both of them have a common feature: the lapse function tends to zero when  $r \rightarrow \infty$ , characteristic which is absent in the classical solutions. In addition, the total charge is modified as a consequence of our scale dependent framework. Moreover, we have found that, for the same value of the classical black hole mass, the event horizon radius (and the Bekenstein-Hawking entropy) decreases when the strength of the scale dependence increases. This is in agreement with the findings in [54, 69, 71, 110–112, 114, 117–121, 146, 147, 176]. On the other hand, the Hawking temperature increases with  $\epsilon$ . Please, note that the effect of the scale dependence in the Einstein-power-Maxwell case is stronger than the Einstein-Maxwell case. The behaviour of the electromagnetic coupling  $e(r)$  depends on the choice of the electromagnetic Lagrangian density. While  $e(r)$  goes to zero in the limit  $r \rightarrow \infty$  for a Maxwell Lagrangian density, it approaches a constant value for the power-Maxwell case. Finally, it is well known that a black hole (as a thermodynamical system) is locally stable if its heat capacity is positive [178]. In both scale dependent cases it is found that these black holes are unstable ( $C_Q < 0$ ), like their classical counterparts.

## 4.8 Conclusion

In this chapter we have studied the scale dependence of charged black holes in three-dimensional spacetime both in linear (Einstein-Maxwell) and non-linear (Einstein-power-Maxwell) electrodynamics. In the second case we have considered the case where the electromagnetic energy momentum tensor is traceless, which happens for  $\beta = 3/4$ . After presenting the models and the classical black hole solutions, we have allowed for a scale dependence of the electromagnetic as well as the gravitational coupling, and we have solved the corresponding generalized field equations by imposing the “null energy condition” in three-dimensional spacetimes with static circular symmetry. Horizon structure, asymptotic spacetimes and thermodynamics have been discussed in detail.

## 4.9 Appendix

In this appendix we study some features of the scale dependent  $(2+1)$  gravity coupled to a power-Maxwell source for an arbitrary  $\beta$ . For this system the action is given by

$$\Gamma = \int d^3x \sqrt{-g} \left[ \frac{1}{16\pi G(r)} R - \frac{1}{e(r)^{2\beta}} \mathcal{L}(F) \right], \quad (4.81)$$

where  $G(r)$  and  $e(r)$  are the gravitational and the electromagnetic scale-dependent couplings,  $R$  is the Ricci scalar,  $\mathcal{L}(F) = C^\beta |F|^\beta$  is the electromagnetic Lagrangian density,  $F = (1/4)F_{\mu\nu}F^{\mu\nu}$  is the Maxwell invariant, and  $C$  is a dimensionless constant which depends on the choice of  $\beta$ . Metric signature  $(-, +, +)$  and natural units ( $c = \hbar = k_B = 1$ ) are used in our computations.

Variations of the Eq.4.81 with respect to the metric field lead to the modified Einstein's equations

$$R_{\mu\nu} - \frac{1}{2}g_{\mu\nu}R = 8\pi \frac{G(r)}{e^{2\beta}(r)} T_{\mu\nu} - \Delta t_{\mu\nu}, \quad (4.82)$$

where  $T_{\mu\nu}$  stands for the power-Maxwell energy momentum tensor and

$$\Delta t_{\mu\nu} = G(r) \left( g_{\mu\nu} \square - \nabla_\mu \nabla_\nu \right) G(r)^{-1}, \quad (4.83)$$

is the non-material energy momentum tensor which arises as a consequence of the scale dependence of the gravitational coupling. On the other hand, after variations of the action Eq.4.81 with respect to the electromagnetic four-potential,  $A_\mu$ , one obtains the modified Maxwell equations

$$D_\mu \left( \frac{\mathcal{L}_F F^{\mu\nu}}{e(r)^{2\beta}} \right) = 0. \quad (4.84)$$

Henceforth, only static and circularly symmetric solutions will be considered. Therefore we shall assume the ansatz

$$ds^2 = -f(r)dt^2 + f(r)^{-1}dr^2 + r^2 d\Omega^2, \quad (4.85)$$

$$F_{\mu\nu} = (\delta_\mu^t \delta_\nu^r - \delta_\mu^r \delta_\nu^t) E(r), \quad (4.86)$$

for the metric and the electromagnetic tensor, respectively. With the former prescription is straightforward to prove, from Eq.4.84, that the electric field is given in terms of the electromagnetic coupling by

$$E(r) = \frac{2^{\frac{\beta-1}{2\beta-1}} C^{-\frac{\beta}{2\beta-1}} Q_0^{\frac{1}{2\beta-1}} e(r)^{\frac{2\beta}{2\beta-1}}}{\beta^{\frac{1}{2\beta-1}} r^{\frac{1}{2\beta-1}}}, \quad (4.87)$$

or, in a more convenient way

$$E(r) = \left[ \left( \frac{2^{\beta-1} C^{-\beta}}{\beta} \right) \left( \frac{Q_0}{r} e(r)^{2\beta} \right) \right]^{\frac{1}{2\beta-1}}. \quad (4.88)$$

Please, note that setting  $\beta = 1$  and  $C = 1$  the electric field reported in Eq.4.33 is recovered

$$E(r) = \frac{Q_0}{r} e(r)^2. \quad (4.89)$$

In the same way, for  $\beta = 3/4$  and  $C^{3/4} = 2^{7/3} 3^{-\frac{4}{3}} e_0^2 Q_0^{2/3}$  one obtain

$$E(r) = \frac{Q_0}{r^2} \left( \frac{e(r)}{e_0} \right)^3, \quad (4.90)$$

in complete agreement with Eq.4.56. It is worth noting that, even in the general case the electric field depends on an specific power of the charge as a consequence of the non-linear electrodynamics, in the cases  $\beta = 1$  and  $\beta = 3/4$ , this behaviour is not observed due to a particular setting of  $C$ .

If the null energy condition is used as an additional condition, we obtain that the scale-dependent gravitational coupling reads

$$G(r) = \frac{G_0}{1 + \epsilon r}, \quad (4.91)$$

where  $G_0$  is Newton's constant and  $\epsilon$  is the running parameter. Note that the classical limit is recovered in the limit  $\epsilon \rightarrow 0$ . Finally, Eq.4.82 reduces to a pair of differential equations

for  $\{f(r), e(r)^{2\alpha}\}$  given by

$$2^\alpha \kappa_0 C^{-\alpha} Q_0^{2\alpha} (2\beta - 1) r e(r)^{2\alpha} + \beta^{2\alpha} r^{2\alpha} \left( (2r\epsilon + 1) f'(r) + 2\epsilon f(r) \right) = 0, \quad (4.92)$$

$$2^\alpha \kappa_0 C^{-\alpha} Q_0^{2\alpha} e(r)^{2\alpha} - \beta^{2\alpha} r^{2\alpha} \left( (r\epsilon + 1) f''(r) + 2\epsilon f'(r) \right) = 0, \quad (4.93)$$

where  $\alpha = \frac{\beta}{2\beta-1}$  and  $\kappa_0 = 8\pi G_0$ . It can be checked by the reader that, in the case  $\beta = 3/4$ , the solutions of the set of equations 4.92, 4.93, 4.91 and 4.87 coincide with those listed in Eq.4.56 after an appropriate choice of the integration constants.

# Chapter 5

## Generalized scale–dependent charged solutions

This chapter was published in *The European Physical Journal C* [61]

### 5.1 Introduction

Three-dimensional gravity is attracting a lot of attention for several reasons. On one hand due to the deep connection to Yang-Mills and Chern-Simons theory [73–75]. On the other hand in this lower dimensional gravitational theory, there are no propagating degrees of freedom, which makes analytic manipulations much more accessible. Furthermore, three-dimensional black holes are characterized by properties also found in their four-dimensional counterparts, such as horizon radius, temperature, entropy etc. Therefore, three-dimensional gravity allows to get deep insight into the corresponding systems that live in four-dimensions.

The main motivation to study non-linear electrodynamics (NLED) was to overcome certain problems present in the standard Maxwell’s theory. Initially, the so called Born-Infeld non-linear electrodynamics was introduced in the 30’s in order to obtain a finite self-energy of point-like charges [149]. During the last decades, these type of models reappear in the open sector of superstring theories [150, 151] as their describe the dynamics of D-branes [152]. Similarly, in heterotic string theory a Gauss-Bonnet term coupled to quartic contractions of the Maxwell field strength appears. [179–183].

Also, this kind of electrodynamics has been coupled to gravity in order to obtain, for example, regular black hole solutions [153–155], semiclassical corrections to the black hole entropy [156], and novel exact solutions with a cosmological constant acting as an effective Born-Infeld cut-off [157].

A particularly interesting class of NLED theories is the so called power-Maxwell theory (EpM hereafter). There are several reasons to study the Einstein-power-Maxwell electrodynamics, as it was recently pointed out in [160]: "In recent years, the use of power Maxwell fields has attracted considerable interest. It has been used for obtaining solutions in d-spacetime dimensions [164], Ricci flat rotating black branes with a conformally Maxwell source [184], Lovelock black holes [185], Gauss-Bonnet gravity [166], and the effect of power Maxwell field on the magnetic solutions in Gauss-Bonnet gravity [186]."

The EpM theory is described by a Lagrangian density of the form  $\mathcal{L}(F) = F^\beta$ , where  $F = F_{\mu\nu}F^{\mu\nu}/4$  is the Maxwell invariant, and  $\beta$  is an arbitrary rational number. When  $\beta = 1$  one recovers the standard linear electrodynamics, while for  $\beta = D/4$ , with  $D$  being the dimensionality of space time, the electromagnetic energy momentum tensor is traceless [158, 159]. In three dimensions the generic black hole solution without imposing the traceless condition has been found in [160], while black hole solutions in linear Einstein-Maxwell theory are given in [161, 162]. Other interesting solutions and properties of black holes in the presence of power-Maxwell theory have been found in [39, 40, 163–166], whereas some topological black hole solutions with power-law Maxwell fields have been investigated in [167–169], as well as Born-Infeld theory in [38, 187]. Interesting features arise from a study of the thermodynamic properties of EpM black holes, as discussed in [165].

It is well-known that one of the open issues in modern theoretical physics is a consistent formulation of quantum gravity. Although there are several approaches to the problem (for an incomplete list see e.g. [84, 86, 88–90, 92, 96–98] and references therein), most of them have something in common, namely that the basic parameters that enter into the action, such as Newton's constant, the cosmological constant or the electromagnetic coupling, become scale-dependent quantities. As scale dependence at the level of the effective action is a generic result of quantum field theory, the resulting effective action of scale-dependent gravity is expected to modify the properties of classical black hole backgrounds.

It is the aim of this chapter to study the scale dependence at the level of the effective action of three-dimensional charged black holes in the presence of the Einstein-power-Maxwell non-linear electrodynamics for any value of the power parameter, extending and generalizing

previous chapter, where we imposed the traceless condition  $\beta = 3/4$ . We will use the formalism and notation of [57].

Our work is organized as follows. After this introduction we present the model and the field equations. Section 5.3 is devoted to introduce the classical black hole background. In sections 5.4 and 5.5 we allow for scale dependent couplings, we impose the “null energy condition”, and after that we present our solution for the metric lapse function as well as for the couplings in the scale dependent scenario. In section 5.7 we briefly discuss our main findings, concluding in the same section.

## 5.2 Classical Einstein-power-Maxwell theory

In this section we will present the classical theory of non-linear electrodynamics in (2+1) dimensional spacetimes for an arbitrary EpM theory (namely, for an arbitrary index  $\beta$ ). Those theories will then be investigated in the context of scale-dependent couplings. Our starting point is the so-called Einstein-power-Maxwell action without cosmological constant ( $\Lambda_0 = 0$ ), assuming the EpM Lagrangian density, i.e.  $\mathcal{L}(F) = \gamma|F|^\beta$ , which reads

$$I_0[g_{\mu\nu}, A_\mu] = \int d^3x \sqrt{-g} \left[ \frac{1}{2\kappa_0} R - \frac{1}{e_0^{2\beta}} \mathcal{L}(F) \right], \quad (5.1)$$

where  $\kappa_0 \equiv 8\pi G_0$  is the gravitational coupling,  $G_0$  is Newton’s constant,  $e_0$  is the electromagnetic coupling constant,  $R$  is the Ricci scalar,  $\mathcal{L}(F)$  is the electromagnetic Lagrangian density,  $\gamma$  is a proportionality constant,  $F$  is the Maxwell invariant previously defined, and  $F_{\mu\nu} = \partial_\mu A_\nu - \partial_\nu A_\mu$  is the electromagnetic field strength tensor. We use the metric signature  $(-, +, +)$ , and natural units ( $c = \hbar = k_B = 1$ ) such that the action is dimensionless. Note that  $\beta$  is an arbitrary rational number, which also appears in the exponent of the electromagnetic coupling in order to maintain the action dimensionless. It is easy to check that the special case  $\beta = 1$  reproduces the classical Einstein-Maxwell action, and thus the standard electrodynamics is recovered. For  $\beta \neq 1$  one can obtain Maxwell-like solutions. In the following we shall consider the general case, so that  $\beta$  is taken to be a free parameter. As our solution should reproduce the classical one, we restrict the values of this parameter by demanding the energy conditions to be satisfied. According to [160], we will only take into account the (naive) range  $\beta \in \mathfrak{R}^+$  (our solution, however, could have additional forbidden values of the parameter  $\beta$ ). The classical equations of motion for the metric field are given

by Einstein's field equations

$$G_{\mu\nu} = \frac{\kappa_0}{e_0^{2\beta}} T_{\mu\nu}. \quad (5.2)$$

The energy momentum tensor  $T_{\mu\nu}$  is associated to the electromagnetic field strength  $F_{\mu\nu}$  through

$$T_{\mu\nu} \equiv T_{\mu\nu}^{\text{EM}} = \mathcal{L}(F)g_{\mu\nu} - \mathcal{L}_F F_{\mu\gamma} F_{\nu}{}^{\gamma}, \quad (5.3)$$

remembering that  $\mathcal{L}_F = d\mathcal{L}/dF$ . Besides, for static circularly symmetric solutions the electric field  $E(r)$  is given by

$$F_{\mu\nu} = (\delta_{\mu}^r \delta_{\nu}^t - \delta_{\nu}^r \delta_{\mu}^t) E(r). \quad (5.4)$$

Taking the variation of the classical action with respect to the field  $A_{\mu}(x)$  one obtains

$$D_{\mu} \left( \frac{\mathcal{L}_F F^{\mu\nu}}{e_0^{2\beta}} \right) = 0, \quad (5.5)$$

where  $e_0^{2\beta}$  is a constant. Combining Eq. (5.2) with Eq. (5.5) we are able to determine the set of functions  $\{f(r), E(r)\}$ . It should be noted that the general solution of this problem was previously appointed in Ref. [160] by computing the lapse function and the electric field, as well as the corresponding thermodynamic properties.

### 5.3 Black hole solution for Einstein-Maxwell model of arbitrary power

The general metric ansatz assuming circular symmetry is given by

$$ds^2 = -f(r)dt^2 + g(r)dr^2 + r^2d\phi^2. \quad (5.6)$$

Note that, in the classical solution, it is possible to deduce the Schwarzschild relation, namely  $g(r) = f(r)^{-1}$ . The classical (2+1)-dimensional Einstein-Maxwell black hole solution (for an arbitrary index  $\beta$ ) is obtained after solving  $f_0(r)$  and  $E_0(r)$  and was previously found in Ref. [160]. As we will compare these results with the scale-dependent solution provided

in Section 5.6, here we will briefly comment the main features of the classical case. Then, solving the Einstein field equations we obtain:

$$f_0(r) = Br^{1-\alpha} + \frac{C}{\alpha - 1}, \quad (5.7)$$

$$E_0(r) = A \left[ \frac{e_0^{\alpha+1}}{r^\alpha} \right]. \quad (5.8)$$

where the set  $\{A, B, C\}$  are constants of integration which must be fixed. According to Ref. [160], the parameter  $C$  is related with the mass of the black hole  $M_0$  while  $B$  takes into account the classical charge  $Q_0$  (the same for the parameter  $A$ ). In addition, note that the auxiliary parameter  $\alpha$  is defined as follow:

$$\alpha = \frac{1}{2\beta - 1}. \quad (5.9)$$

The next step consists in computing the horizon of this black hole, which is

$$r_0 = \left( \frac{C}{B(1 - \alpha)} \right)^{\frac{1}{1-\alpha}}. \quad (5.10)$$

By writing the lapse function in terms of the classical horizon we have

$$f_0(r) = \frac{C}{\alpha - 1} \left[ 1 - \left( \frac{r_0}{r} \right)^{\alpha-1} \right]. \quad (5.11)$$

Another important point is the thermodynamics of the system. We can then define three quantities, i. e., the Hawking temperature,  $T_H$ , the Bekenstein-Hawking entropy,  $S$ , and the specific heat,  $C_Q$ . Their corresponding expressions are given by

$$T_0(r_0) = \frac{1}{4\pi} \left| \frac{C}{r_0} \right|, \quad (5.12)$$

$$S_0(r_0) = \frac{\mathcal{A}_0}{4G_0}, \quad (5.13)$$

$$C_0(r_0) = T \left. \frac{\partial S}{\partial T} \right|_{r_0}, \quad (5.14)$$

being  $\mathcal{A}_0$  the horizon area defined as

$$\mathcal{A}_0 = \oint dx \sqrt{h} = 2\pi r_0. \quad (5.15)$$

where  $h_{ij}$  is the induced metric at the horizon  $r_0$ .

## 5.4 Scale–dependent coupling and scale setting

This section summarizes the equations of motion for the scale–dependent Einstein–power–Maxwell theory with arbitrary index. The idea and notation follows [56–58, 60, 64, 65, 67, 125, 144, 145]. The scale–dependent couplings of the theory are i) the Newton’s coupling  $G_k$  (which can be related with the gravitational coupling by  $\kappa_k \equiv 8\pi G_k$ ), and ii) the electromagnetic coupling  $1/e_k$ . Furthermore, there are three independent fields, which are the metric  $g_{\mu\nu}(x)$ , the electromagnetic four-potential  $A_\mu(x)$ , and the scale field  $k(x)$ . The effective action for this theory reads

$$\Gamma[g_{\mu\nu}, A_\mu, k] = \int d^3x \sqrt{-g} \left[ \frac{1}{2\kappa_k} R - \frac{1}{e_k^{2\beta}} \mathcal{L}(F) \right]. \quad (5.16)$$

The equations of motion obtained from a variation of (5.16) with respect to  $g_{\mu\nu}(x)$  are

$$G_{\mu\nu} = \frac{\kappa_k}{e_k^{2\beta}} T_{\mu\nu}^{\text{eff}}, \quad (5.17)$$

where

$$T_{\mu\nu}^{\text{eff}} = T_{\mu\nu}^{\text{EM}} - \frac{e_k^{2\beta}}{\kappa_k} \Delta t_{\mu\nu}. \quad (5.18)$$

Note that  $T_{\mu\nu}^{\text{EM}}$  is given by (5.3) and the additional contribution  $\Delta t_{\mu\nu}$  is

$$\Delta t_{\mu\nu} = G_k \left( g_{\mu\nu} \square - \nabla_\mu \nabla_\nu \right) G_k^{-1}. \quad (5.19)$$

The equations of motion for the four-potential  $A_\mu(x)$  taking into account the running of  $e_k$  are

$$D_\mu \left( \frac{\mathcal{L}_F F^{\mu\nu}}{e_k^{2\beta}} \right) = 0. \quad (5.20)$$

It is important to note that, in any quantum field theory the renormalization scale  $k$  has to be set to a quantity characterizing the physical system under consideration. Thus, for background solutions of the gap equations, it is not constant anymore. However, having an

arbitrarily chosen non-constant  $k = k(x)$  implies that the set of equations of motion does not close consistently. This implies that the stress energy tensor is most likely not conserved for almost any choice of the functional dependence  $k = k(x)$ . This type of scenario has been largely explored in the context of renormalization group improvement of black holes in asymptotic safety scenarios [54, 69, 71, 110–112, 114, 117–121, 146, 147, 176]. The loss of a conservation laws comes from the fact that there is one consistency equation missing. This missing equation can be obtained from varying the effective action (5.16) with respect to the scale field  $k(r)$ , i.e.

$$\frac{d}{dk}\Gamma[g_{\mu\nu}, A_\mu, k] = 0, \quad (5.21)$$

which can thus be understood as variational scale setting procedure [52, 123–126]. The combination of (5.21) with the above equations of motion guarantees the conservation of the stress energy tensor. A detailed analysis of the split symmetry within the functional renormalization group equations supports this approach of dynamic scale setting [177]. To apply the variational procedure (5.21), however, the knowledge of the exact beta functions of the problem is required. Since in many cases the precise form of these functions is unknown (or at least uncertain) one can, for the case of simple black holes, impose a null energy condition and solve for the couplings  $G(r)$ ,  $\Lambda(r)$ ,  $e(r)$  directly [53, 55, 56, 58–60, 67]. This philosophy of assuring the consistency of the equations by imposing a null energy condition will also be applied in the following study on Einstein-Maxwell and Einstein-power-Maxwell black holes.

## 5.5 The null energy condition

An energy condition is, basically, an additional relation one imposes on the matter stress-energy tensor e.g. in order to try to capture the idea that “energy should be positive” [188]. There are typically four energy conditions (dominant, weak, strong, and null) which help to obtain desirable solutions of Einstein’s field equations [33, 127]. Among those conditions, the null energy condition (NEC) is particularly interesting since it is a crucial assumption of the Penrose(-Hawking) singularity theorem [148], valid in General Relativity. Thus, for matter obeying the NEC, there is always a singularity that gets formed inside a black hole horizon, and any contracting Universe ends up in a singularity, provided its spatial curvature is dynamically negligible [127]. Thus, we will focus our attention to the NEC. Our starting point is to consider certain null vector, called  $\ell^\mu$ , and to contract it with the matter stress

energy tensor as NEC demands, i.e. :

$$T_{\mu\nu}^m \ell^\mu \ell^\nu \geq 0. \quad (5.22)$$

This “trick” was used in Ref. [56] inspired by the Jacobson idea [130] on getting acceptable physical solutions. Note that in proving fundamental black hole theorems, such as the no hair theorem [129], and the second law of black hole thermodynamics [36], the NEC is, indeed, required. In the scale dependent scenario, we maintain the same condition in a more restrictive and thus more useful form by making the inequality an equality

$$T_{\mu\nu}^{\text{eff}} \ell^\mu \ell^\nu = \left( T_{\mu\nu}^{\text{EM}} - \frac{e_k^{2\beta}}{\kappa_k} \Delta t_{\mu\nu} \right) \ell^\mu \ell^\nu = 0. \quad (5.23)$$

For the null vector we choose a radial null vector  $\ell^\mu = \{f^{-1/2}, f^{1/2}, 0\}$ . Since the electromagnetic contribution to the effective stress energy tensor (5.3) satisfies the NEC (5.23) by construction, the same has to hold for the additional contribution introduced due to the scale dependence of the gravitational coupling i.e.

$$\Delta t_{\mu\nu} \ell^\mu \ell^\nu = 0. \quad (5.24)$$

## 5.6 Scale dependent Einstein-power-Maxwell theory

### 5.6.1 Solution

In order to obtain the full solution with circular symmetry, we need to find the set  $\{G(r), E(r), f(r), e(r)^{\alpha+1}\}$ . We first start by considering the constraint given by the NEC. The Eq. (5.24) gives an explicit differential equation for the gravitational coupling  $G(r)$ , i.e.

$$G(r) \frac{d^2 G(r)}{dr^2} - 2 \left( \frac{dG(r)}{dr} \right)^2 = 0, \quad (5.25)$$

which allows us to obtain

$$G(r) = \frac{G_0}{1 + \epsilon r}. \quad (5.26)$$

After that, we use equation of motion for the 4-potential given by Eq. (5.20) to get

$$\frac{dE(r)}{dr} - \left[ (\alpha + 1) \frac{e'(r)}{e(r)} - \frac{\alpha}{r} \right] E(r) = 0, \quad (5.27)$$

which gives a relation between the electric field  $E(r)$  and the electromagnetic coupling  $e(r)^{\alpha+1}$ . Then, we have

$$E(r) = A \left[ \frac{e(r)^{1+\alpha}}{r^\alpha} \right]. \quad (5.28)$$

Here,  $\epsilon$  is an integration constant which controls the strength of the scale dependence, and which is thus called “running parameter”. As (5.26) shows, the NEC is a useful tool in order to decrease the number of degrees of freedom of the problem. The Einstein field

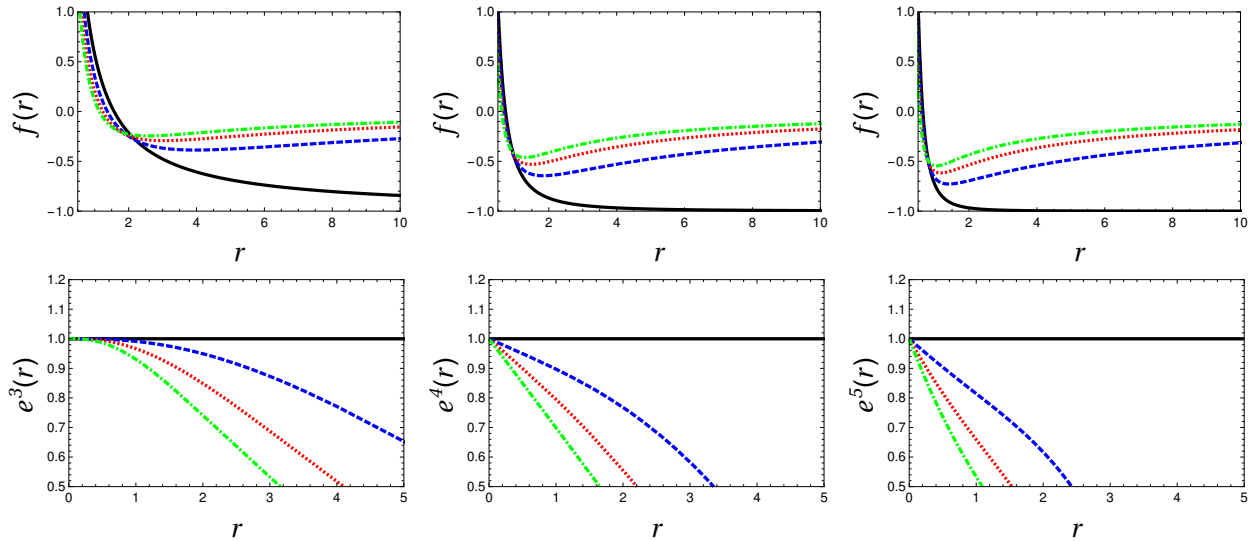


**Figure 5.1:** The lapse function  $f(r)$  and the electromagnetic coupling  $e(r)^{\alpha+1}$  versus radial coordinate  $r$  for three cases. The first line correspond to the lapse function while the second line correspond to the electromagnetic coupling. The first (left), second (center) and third (right) column correspond to the cases  $\alpha = \{2, 3, 4\}$  respectively. We show the classical model (solid black line) and three different cases for each figure: i)  $\epsilon = 0.1$  (dashed blue line), ii)  $\epsilon = 0.2$  (dotted red line) and iii) for  $\epsilon = 0.3$  (dotted dashed green line). We have used the set  $\{Q_0, M_0, \gamma, G_0\} = \{1, 1, 1, 1/8\}$  in both set of figures. Besides, to complete the scale setting we have used certain  $A$  values such as  $e_0^{\alpha+1}$  remains as unity. They are  $\{A(\alpha = 2), A(\alpha = 3), A(\alpha = 4)\} = \{0.891, 0.841, 0.812\}$ .

equations give:

$$\begin{aligned} \pi 2^{\frac{7}{2}-\frac{1}{2\alpha}} \gamma G_0 A^{\frac{1}{\alpha}+1} r^{-\alpha} e(r)^{\alpha+1} + \\ \alpha(2r\epsilon + 1)f'(r) + 2\alpha\epsilon f(r) = 0 \end{aligned} \quad (5.29)$$

$$\begin{aligned} \pi 2^{\frac{7}{2}-\frac{1}{2\alpha}} \gamma G_0 A^{\frac{1}{\alpha}+1} r^{-\alpha} e(r)^{\alpha+1} - \\ r\left((r\epsilon + 1)f''(r) + 2\epsilon f'(r)\right) = 0 \end{aligned} \quad (5.30)$$

where the lapse function  $f(r)$  and the electromagnetic coupling  $e(r)^{\alpha+1}$  gives the solution:

$$\begin{aligned} f(r) = r^{-\alpha}(1 + \epsilon r)^{-\alpha-1} \left[ Br + C\Gamma(\alpha - 1)r^\alpha \right. \\ \left. \times {}_2\tilde{F}_1(\alpha - 1, -\alpha; \alpha; -r\epsilon) \right], \end{aligned} \quad (5.31)$$

$$\begin{aligned} e(r)^{\alpha+1} = \frac{D}{r(1 + r\epsilon)^{\alpha+2}} \left[ (1 - \alpha)Cr^\alpha(1 + 2\epsilon r) \right. \\ \left. (1 + \epsilon r)^{\alpha+1} + \left[ \alpha(1 + 2\epsilon r)^2 - \right. \right. \\ \left. \left. 2\epsilon r(2 + \epsilon r) - 1 \right] \times \left[ (\alpha - 1)Br + C \times \right. \right. \\ \left. \left. r^\alpha {}_2F_1(\alpha - 1, -\alpha; \alpha; -r\epsilon) \right] \right], \end{aligned} \quad (5.32)$$

where  $D$  is an auxiliary parameter given by

$$D = \frac{2^{\frac{1}{2}(\frac{1}{\alpha}-7)} \alpha A^{-\frac{\alpha+1}{\alpha}}}{\pi(\alpha - 1)\gamma G_0}, \quad (5.33)$$

and  ${}_2\tilde{F}_1(\cdot, \cdot; \cdot; \cdot)$  is the so-called Hypergeometric Regularized function defined as follows:

$${}_2\tilde{F}_1(a, b; c; z) = \sum_{s=0}^{\infty} \frac{1}{\Gamma(c + s)} (a)_s (b)_s \frac{z^s}{s!}, \quad (5.34)$$

where  $(c)_n$  is the (rising) Pochhammer symbol, i.e.

$$(c)_s = \begin{cases} 1 & \text{if } s = 0 \\ c(c + 1) \cdots (c + s - 1) & \text{if } s > 0 \end{cases} \quad (5.35)$$

Please, note that  ${}_2\tilde{F}_1(a, b; c; z)$  is finite for all finite values of  $a$ ,  $b$ ,  $c$ , and  $z$  as long as  $|z| < 1$ . Outside the circle  $|z| < 1$ , the function is defined as the analytic continuation with respect to  $z$  of this sum, the parameters  $a$ ,  $b$ ,  $c$  held fixed [189]. Besides, the special case  ${}_2\tilde{F}_1(a, b; c; z) = 0$  is forbidden because we assume a non-null  ${}_2\tilde{F}_1$  in the computation of thermodynamic quantities. In general, the constants are chosen such that the solution matches the classical case when the running parameter is switched off  $\epsilon \rightarrow 0$ . However, as the final result depends on the value of the free index  $\beta$  (or  $\alpha$ ), we first need to take some particular values of these parameters. We must emphasize the number of integration constants involved into the problem. Firstly, the scale-dependent gravitational coupling introduce two of them, i.e.  $G_0$  and  $\epsilon$ . This is because we are in the presence of a second order differential equation. The electromagnetic field gives an additional integration constant  $A$  whereas the solution for the lapse function implies two additional integration constants  $B$  and  $C$  (for the same reason as is the gravitational coupling case). Thus, the integration constant  $C$  can be associated with the classical mass of the black hole  $M_0$ , and the constant  $B$  encodes the classical charge  $Q_0$ . Following Ref. [160] we can set the relation between our integration constants and the classical counterpart as:

$$C \rightarrow \eta M_0 = -8G_0 M_0 (\alpha - 1), \quad (5.36)$$

$$B \rightarrow \xi Q_0^{\frac{1+\alpha}{\alpha}} = \frac{8\pi G_0}{(\alpha - 1)\alpha} Q_0^{\frac{1+\alpha}{\alpha}}. \quad (5.37)$$

Thus, we have a link between the usual solution and the scale-dependent one. We emphasize that  $M_0$  is the classical mass, not to be confused with the mass of the scale-dependent black hole. The  $M_0$  identification is made when we take the limit  $\epsilon \rightarrow 0$ , since the scale-dependent solution tends to the classical one in that limit. According to the previous expressions we observe that the parameters of the theory depend on the power  $\beta$  of the theory, in total agreement with the classical one. Furthermore, an important check is that our solution reproduces the results of the classical theory in the limit  $\epsilon \rightarrow 0$ , i.e.

$$\begin{aligned} \lim_{\epsilon \rightarrow 0} G(r) &= G_0, \\ \lim_{\epsilon \rightarrow 0} E(r) &= E_0(r) = A \left[ \frac{BD(1-\alpha)^2}{r^\alpha} \right], \\ \lim_{\epsilon \rightarrow 0} f(r) &= f_0(r) = -\frac{C}{1-\alpha} + Br^{1-\alpha}, \\ \lim_{\epsilon \rightarrow 0} e(r)^{\alpha+1} &= e_0^{\alpha+1} = BD(1-\alpha)^2. \end{aligned} \quad (5.38)$$

where the parameters  $\{A, B, C, D\}$  have fixed values according to [160] in terms of their meaning in the absence of scale dependence [56]. The scale dependent scenario introduces small corrections to the fixed-scale background, as can be easily seen by

$$G(r) \approx G_0 [1 - \epsilon r] + \mathcal{O}(\epsilon^2), \quad (5.39)$$

$$E(r) \approx E_0(r) [1 - (\alpha - 2)r\epsilon] + \mathcal{O}(\epsilon^2), \quad (5.40)$$

$$f(r) \approx f_0(r) + \left[ \frac{2Cr}{1 - \alpha} - \frac{(\alpha + 1)B}{r^{\alpha-2}} \right] \epsilon + \mathcal{O}(\epsilon^2), \quad (5.41)$$

$$e(r)^{\alpha+1} \approx e_0^{\alpha+1} [1 - (\alpha - 2)r\epsilon] + \mathcal{O}(\epsilon^2). \quad (5.42)$$

Finally, we should remark that certain values of the power  $\alpha$  are forbidden. As our solution must be valid indeed in the classical case, the first step is to analyze this solution. In order to avoid singularities in the classical lapse function,  $\alpha = 1$  is excluded. Following the same line of thought, the scale-dependent lapse function implies that  $\alpha \neq 0$  is forbidden. Hence, the two parameters  $\alpha = \{0, 1\}$  are not permitted. Besides, all complex numbers except the non-positive integers (where the function has simple poles), are, in principle, possible. Despite that, we will focus on cases where  $\alpha \geq 2$ . In Fig 5.1 we observe the behaviour of the lapse function and the electromagnetic coupling for different values of the parameter  $\beta$ .

## 5.6.2 Asymptotic behaviour

The asymptotic behaviour will be studied using two curvature invariants, i.e. the Ricci scalar as well as the Kretschmann scalar. These invariants give information related to possible divergences, which is crucial for the diagnostic of our solution. To complete the analysis, we will include in our discussion the coordinate dependent (not invariant) asymptotic lapse function. Given the metric function (5.6), the scalars are given by

$$R = -f''(r) - 2\frac{f'(r)}{r}, \quad (5.43)$$

$$\mathcal{K} \equiv R_{\mu\nu\alpha\beta}R^{\mu\nu\alpha\beta} = f''(r)^2 + 2\left(\frac{f'(r)}{r}\right)^2, \quad (5.44)$$

which, in our particular case, take the form:

$$\begin{aligned}
 R = & \frac{C(\alpha + 2\alpha r\epsilon - 2)}{r^2(r\epsilon + 1)^2} - r^{-\alpha-2}(r\epsilon + 1)^{-\alpha-3} \times \\
 & \left[ (\alpha + 2\alpha r\epsilon)^2 - \alpha(2r\epsilon(r\epsilon + 4) + 3) + 2 \right] \times \\
 & Br + C\Gamma(\alpha - 1)r^\alpha {}_2\tilde{F}_1(\alpha - 1, -\alpha; \alpha; -r\epsilon),
 \end{aligned} \tag{5.45}$$

$$\begin{aligned}
 \mathcal{K} = & \frac{r^{-2(\alpha+2)}(r\epsilon + 1)^{-2(\alpha+3)}}{\Gamma(\alpha)^2} \left[ 2(r\epsilon + 1)^2 \left\{ Br \right. \right. \\
 & \times \Gamma(\alpha)(\alpha + 2\alpha r\epsilon - 1) - C\Gamma(\alpha - 1)r^\alpha \left( (\alpha - 1) \right. \\
 & \times (r\epsilon + 1)^{\alpha+1} - \Gamma(\alpha)(\alpha + 2\alpha r\epsilon - 1) \\
 & \left. \left. \times {}_2\tilde{F}_1(\alpha - 1, -\alpha; \alpha; -r\epsilon) \right) \right\}^2 + \left\{ Br\Gamma(\alpha) \right. \\
 & \left. \times \left[ \alpha(-2r^2\epsilon^2 + 2r\epsilon + 1) - (\alpha + 2\alpha r\epsilon)^2 + 2r\epsilon \right] \right. \\
 & + C\Gamma(\alpha - 1)r^\alpha \left[ \Gamma(\alpha)(\alpha(-2r^2\epsilon^2 + 2r\epsilon + 1) \right. \\
 & \left. - (\alpha + 2\alpha r\epsilon)^2 + 2r\epsilon) {}_2\tilde{F}_1(\alpha - 1, -\alpha; \alpha; -r\epsilon) \right. \\
 & \left. \left. \left. + (\alpha - 1)(\alpha + 2\alpha r\epsilon + 2r\epsilon)(r\epsilon + 1)^{\alpha+1} \right] \right\}^2 \right].
 \end{aligned} \tag{5.46}$$

Thus, the classical values for the scalars are

$$R_0 \equiv \lim_{\epsilon \rightarrow 0} R = \frac{(\alpha - 2)(1 - \alpha)B}{r^{\alpha+1}}, \tag{5.47}$$

$$\mathcal{K}_0 \equiv \lim_{\epsilon \rightarrow 0} \mathcal{K} = \frac{(\alpha - 1)^2 (\alpha^2 + 2) B^2}{r^{2(\alpha+1)}}. \tag{5.48}$$

### 5.6.2.1 Asymptotics for $r \rightarrow 0$

First, the lapse function in this regime is given by

$$f(r \rightarrow 0) = f_0(r) - \frac{2C\epsilon r}{\alpha - 1} + \mathcal{O}(r^2), \quad (5.49)$$

whereas the invariants take the form:

$$R(r \rightarrow 0) = R_0 + \frac{4C\epsilon}{(\alpha - 1)r} + \mathcal{O}(r^{-\alpha}), \quad (5.50)$$

$$\mathcal{K}(r \rightarrow 0) = \mathcal{K}_0 + 8BC\epsilon r^{-(\alpha+2)} + \mathcal{O}\left(r^{-(1+2\alpha)}\right). \quad (5.51)$$

We see that the scalars have singularities in the scale dependent scenario, i.e. when we include the running of the coupling constants, just like their scale-independent counterpart. It would be interesting to investigate how and to which extent those singularities could be cancelled by an additional contribution from the effective stress energy tensor as discussed in [67].

### 5.6.2.2 Asymptotics for $r \rightarrow \infty$

As before, it is very useful compute the lapse function for this regime, i.e.

$$\begin{aligned} f(r \rightarrow \infty) = & \frac{r^{-\alpha}}{(r\epsilon + 1)^{\alpha+1}} \left[ Br + \frac{1}{2}C\epsilon^\alpha r^{2\alpha} \times \right. \\ & \left. \left[ \frac{2}{2\alpha - 1} + \frac{\alpha}{(\alpha - 1)r\epsilon} \right] + Cr\epsilon^{1-\alpha} \times \right. \\ & \left. \frac{\Gamma(1 - 2\alpha)\Gamma(\alpha - 1)}{\Gamma(-\alpha)} \right] + \mathcal{O}\left(\frac{1}{r}\right)^2 \end{aligned} \quad (5.52)$$

Besides, we have that the Ricci scalar can be written up to zeroth order as:

$$\begin{aligned}
R(r \rightarrow \infty) = & \frac{1}{(r\epsilon + 1)^{\alpha+3}} \left[ R_0(r \rightarrow \infty) - 4(\alpha - 2) \right. \\
& \times \alpha B \epsilon r^{-\alpha} + 2(1 - 2\alpha) \alpha B \epsilon^2 r^{1-\alpha} - \\
& \alpha C \epsilon^{\alpha+1} r^{\alpha-1} \left[ \frac{4\alpha^3 - 11\alpha + 8}{2\alpha^2 - 3\alpha + 1} + 2r\epsilon \right] \\
& \frac{-C \epsilon^{1-\alpha}}{r^{1+\alpha} \Gamma(-\alpha)} \left( (\alpha + 2\alpha r\epsilon)^2 - \alpha(2r\epsilon(r\epsilon \right. \\
& \left. + 4) + 3) + 2 \right) \Gamma(1 - 2\alpha) \Gamma(\alpha - 1) \left. \right] \quad (5.53)
\end{aligned}$$

The Kretschmann scalar has a complicated expansion, and it is avoided for simplicity. It is remarkable that the invariants in that limit maintain the singularity present in the classical theory.

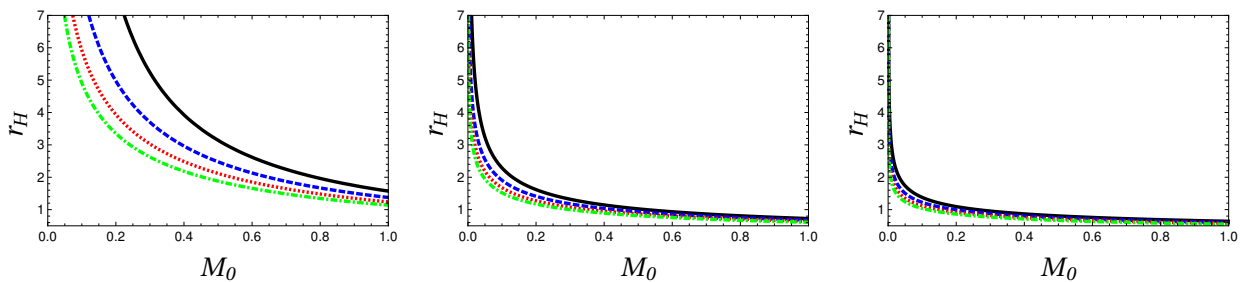


**Figure 5.2:** The evolution of event horizon  $r_H$  versus the classical black hole mass  $M_0$  for three cases. The first (left), second (center) and third (right) column correspond to the cases  $\alpha = \{2, 3, 4\}$ , respectively. We show the classical model (solid black line) and three different cases for each figure: i)  $\epsilon = 0.1$  (dashed blue line), ii)  $\epsilon = 0.2$  (dotted red line) and iii) for  $\epsilon = 0.3$  (dotted dashed green line). We have used the set  $\{Q_0, G_0\} = \{1, 1/8\}$  in all set of figures.

### 5.6.3 Horizons

The event horizon is given when the lapse function vanishes, i.e.  $f(r_H) = 0$ . Given the functional structure of  $f(r)$ , it is required to select a certain value of the index  $\beta$  (or  $\alpha$ ). Note that the effect of scale dependence ( $\epsilon \neq 0$ ) can be understood as a non-trivial deviation from the classical solution ( $\epsilon = 0$ ). As we commented before, we will focus on models where  $\alpha \geq 2$ . The corresponding lapse functions in that regime has a polynomial structure and the roots usually have a complex form. As a benchmark point, we will revisit the solution

for  $\alpha = 2$  which was previously discussed in Ref. [57]. Note that, although we are able to produce physical solutions for  $\alpha \geq 2$ , only a single case will be shown here explicitly. Fig. 5.2 show the behavior of that solution plus two additional cases assuming  $\alpha = \{3, 4\}$ . The scale dependent lapse function  $f(r; \alpha)$  is, for  $\alpha = 2$ ,

$$f(r; 2) = \frac{3B + Cr(r\epsilon(r\epsilon + 3) + 3)}{3r(r\epsilon + 1)^3}, \quad (5.54)$$

whereas the corresponding classical solution is:

$$f_0(r) = C + \frac{B}{r}. \quad (5.55)$$

In order to connect the classical with the scale-dependent counterpart, we compute the classical horizon, i.e.  $r_0 = -B/C$ . Then we obtain the scale-dependent horizon  $r_H(\epsilon; \alpha)$  using the classical value, as

$$r_H(\epsilon; 2) = -\frac{1}{\epsilon} \left[ 1 - (1 + 3\epsilon r_0)^{1/3} \right]. \quad (5.56)$$

Finally, we recover the classical case expanding the solution for small values of  $\epsilon$ , that is

$$r_H(\epsilon; 2) \approx r_0 \left[ 1 - \epsilon r_0 + \mathcal{O}(\epsilon^2) \right]. \quad (5.57)$$

One notes that the horizon radius in the scale dependent scenario  $r_H$  is reduced with respect to its classical counterpart  $r_0$ , this effect can also be appreciated from the graphical analysis in figure 5.2.

#### 5.6.4 Thermodynamic properties

The horizon structure provides the required information in order to obtain thermodynamic properties like temperature and entropy. On one hand, the Hawking temperature for the ansatz (5.6) is given by

$$T_H(r_H) = \frac{1}{4\pi} \left| \lim_{r \rightarrow r_H} \frac{\partial_r g_{tt}}{\sqrt{-g_{tt}g_{rr}}} \right|, \quad (5.58)$$

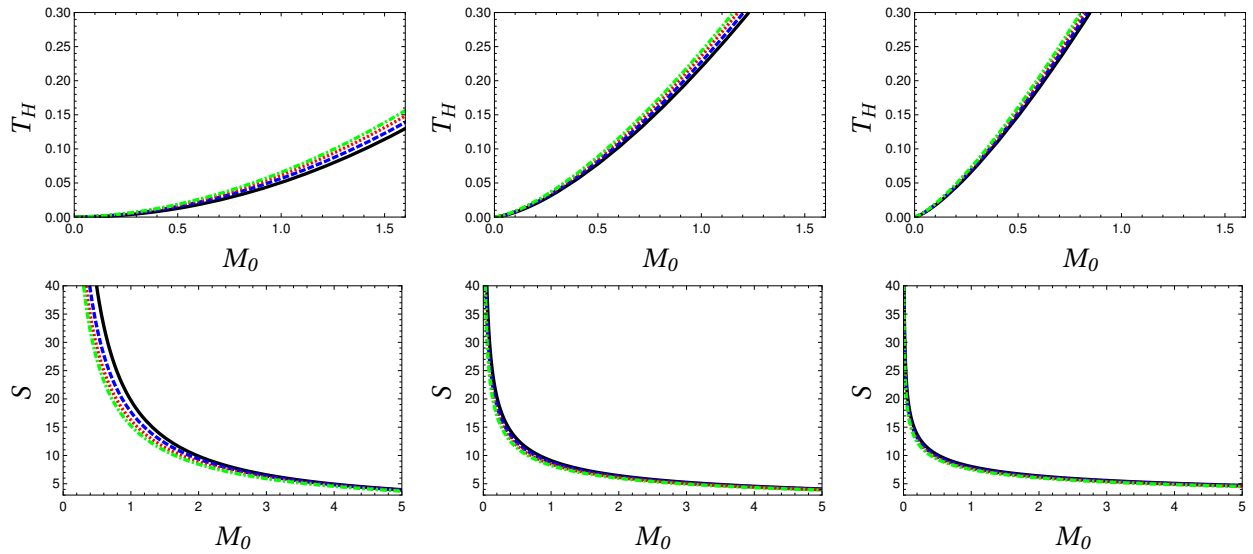


**Figure 5.3:** The Hawking temperature  $T_H$  and Bekenstein-Hawking entropy  $S$  versus the classical mass  $M_0$  for three cases. The first line correspond to the Hawking temperature while the second line correspond to the Bekenstein-Hawking entropy. The first (left), second (center) and third (right) column correspond to the cases  $\alpha = \{2, 3, 4\}$ , respectively. We show the classical model (solid black line) and three different cases for each figure: i)  $\epsilon = 1$  (dashed blue line), ii)  $\epsilon = 2$  (dotted red line) and iii) for  $\epsilon = 3$  (dotted dashed green line). We have used the set  $G_0 = 1/8$  in all set of figures.

i.e.

$$T_H(r_H) = \frac{1}{4\pi} \left| \frac{C}{r_H(1 + \epsilon r_H)} \right|. \quad (5.59)$$

One notes that the functional structure of Hawking temperature remains invariant under changes of the parameter  $\alpha$ . In addition, note that we recover the classical solution after demanding  $\epsilon \rightarrow 0$ . Taking into account the scale-dependent philosophy, the solution can be expanded around  $\epsilon = 0$

$$T_H(r_H) \approx T_0(r_0) \left| 1 + \epsilon r_0 + \mathcal{O}(\epsilon^2) \right|, \quad (5.60)$$

where  $r_0$  is the classical horizon. Clearly, the classical result  $T_0$  is recovered for  $\epsilon \rightarrow 0$ . In Figure 5.3 we show the scale-dependent temperature which takes into account the running coupling effect. On the other hand, the Bekenstein-Hawking entropy for Brans-Dicke type theories is known to be

$$S = \frac{1}{4} \oint dx \frac{\sqrt{h}}{G(x)}, \quad (5.61)$$

where  $h_{ij}$  is the induced metric at the horizon. In presence of circularly symmetric solution and taking advantage of the fact that  $G(x) = G(r_H)$  is constant along the horizon, this integral takes the form [56, 58]

$$S = \frac{\mathcal{A}_H(r_H)}{4G(r_H)} = S_0(r_H)(1 + \epsilon r_H). \quad (5.62)$$

Note that the relation (5.62) naively suggests that the entropy increases for increasing  $\epsilon$ , this effect is however overcompensated by the decrease in the black hole horizon  $r_H$  as it can be appreciated from e.g. (5.57). In the lower part of Figure 5.3 we show the entropy for the generalized (2+1)-dimensional Einstein-power-Maxwell scale dependent black hole. It is evident that the running effect is important when  $\epsilon r$  is large, however, we remain small values of the parameter  $\epsilon$  following the idea that quantum correction should be just small corrections to the classical solution. To conclude, the heat capacity can be obtained from the usual relation

$$C_Q = T \left. \frac{\partial S}{\partial T} \right|_Q, \quad (5.63)$$

which gives

$$C_Q = -S_0(r_H)(1 + \epsilon r_H), \quad (5.64)$$

where we have used the chain rule through the relation  $\partial S/\partial T = (\partial S/\partial r_H)(\partial r_H/\partial T)$ . It is important to note that solution (5.64) is an exact result and, indeed, gives us the classical solution after demanding  $\epsilon \rightarrow 0$ . Besides, due to a weak  $\epsilon$  dependence it was necessary to plot all the figures with very large values of  $\epsilon$  in order to generate an appreciable effect. The scale dependent effect is notoriously small for those quantities.

Regarding the Smarr formula and the first law of black hole mechanics, we remark a couple of facts first: given that we work in the framework of non-linear electrodynamics, we expect to have a modified relation compared to Maxwell's linear theory, as it has been shown in [190]. Furthermore, the Smarr formula requires knowledge of the total mass  $M$ , which unfortunately in the present work is unknown. In spite of that, to get some insight into the underlying physics, we take the case where  $\alpha = 2$  to exemplify how the new Smarr-like

relation looks like. It is straightforward to check that in the classical theory one obtains:

$$M_0 = T_0 S_0, \quad (5.65)$$

while in the scale-dependent scenario, to leading order in  $\epsilon$ , we find

$$M \approx M_0 \approx T_H S_H - \epsilon \left( \frac{1}{2} \pi Q_0^{3/2} \right). \quad (5.66)$$

Note that in the weak regime ( $r\epsilon \ll 1$ ) we have approximated the total mass as the classical one. This should be a good approximation, as we expect that any deviations from the classical value will be small. A more detailed analysis of the Smarr formula is beyond the purpose of this study, and we hope to be able to address this issue in more detail in a future work.

Before we conclude our work a final comment is in order here. The no-go theorem of [191], which links the existence of smooth black hole horizons to the presence of a negative cosmological constant, does not apply in the given case. First, the theorem is based on unmodified classical Einstein Field equations, which is not the case in scale-dependent scenarios. Second, the no-go theorem assumes the dominant energy condition which is not part of our assumptions. Instead, we take advantage of the so-called null energy condition. Furthermore, and most importantly, given the solutions previously presented one can check that they do have smooth horizons and well behaved asymptotic spacetimes, and therefore they are black holes. Note that even the classical solution in [160] was shown to be a black hole in this sense, even for a vanishing cosmological constant.

## 5.7 Conclusions

In the present chapter we have studied the effect of scale dependent couplings on charged black holes in the presence of three-dimensional Einstein-power-Maxwell non-linear electrodynamics for any value of the power parameter, extending and generalizing a previous work. First we presented the model and the classical black hole solution assuming static circular symmetry, and then we allowed for a scale dependence of the couplings, both the electromagnetic and the gravitational one. We solved the corresponding effective field equations applying the same formalism already used in our previous work, namely by imposing the

“null energy condition”. Black hole properties, such as horizon structure, Hawking temperature, Bekenstein-Hawking entropy as well as asymptotic properties, are discussed in detail. In order to show how the scale-dependent scenario modifies the classical solution, we have considered three different benchmark cases taking  $\alpha = \{2, 3, 4\}$  which are shown in Fig. 5.1, 5.2 and 5.3. The aforementioned solutions have a manageable mathematical structure which allows to obtain analytical expressions for the physical quantities. The solutions obtained in this work and our main numerical results show that the scale-dependent scenario allows us to induce deviations from classical black hole solutions, confirming a result already reported in [160]. In particular, it is worth mentioning that the behavior of the electromagnetic coupling depends drastically on the choice of the parameter  $\alpha$ . Regarding the basic black hole properties, we have found that for a fixed classical black hole mass, the Hawking temperature increases with  $\epsilon$ , while both the event horizon radius and the Bekenstein-Hawking entropy decrease when the strength of the scale dependence increases. Our findings imply that quantum corrections may have a remarkable effect, i.e. the black hole becomes hotter and at the same time loses less information compared to its classical counterpart. This is in agreement with the findings in [54, 69, 71, 110–112, 114, 117–121, 146, 147, 176]. Finally, it is well-known that a black hole, viewed as a thermodynamical system, is locally stable if its heat capacity is positive [178]. We have found that the black holes studied here are unstable ( $C_Q < 0$ ), both classically and in the scale dependent scenario. To conclude, our results allow us to gain a solid understanding of the most important modifications that a possible scale dependence would imply for the Einstein-Maxwell black holes of arbitrary power in  $2 + 1$  dimensions.

# Chapter 6

## Discussion and final remarks

### 6.1 Discussion

Before summarizing the main results of this thesis, we wish to point out several aspects related to theories beyond Einstein's GR to establish the contribution of this work within the context of different approaches to quantum gravity.

#### 6.1.1 Quantum gravity inspired classical theory

It should be clarified that the scale-dependent scenario is not derived from some underlying fundamental theory. Instead, it is only based on the idea that the classical action is promoted to an effective action when quantum effects are taken into account. In this sense, we remark that our framework certainly assumes an effective version of the classical action where the scale dependence arises via the running of the couplings. This feature appears in several approaches to quantum gravity. However, we formally do not use quantum gravity to attack any particular situation. Instead, we only allow the action to evolve (with certain scale) and, incorporating certain acceptable assumptions, we analyze how this inclusion modifies Einstein's classical GR.

### 6.1.2 Wetterich equation as tool in scale–dependent gravity?

We emphasize that one of the advantages of our formalism is precisely the fact that we avoid the use of the Wetterich equation. Our approach basically uses the modified version of Einstein’s field equations (with some additional constraints) to derive the solution. The Wetterich equation does not supplement our approach but certainly in the RG improvement method, one uses the function  $G(k)$  obtained by solving the corresponding  $\beta_g$  function. The additional information required to solve our problem is taken imposing the appropriate physical conditions.

### 6.1.3 Comparison: Scale–Dependence vs Brans–Dicke theory

As it was briefly commented in the introduction of this thesis, the Brans–Dicke theory was one of the most popular deviations to classical Einstein’s gravity. In such a theory, as it was pointed out before, one assumes  $\phi \rightarrow G^{-1}$  and derives the new Einstein’s field equations. Thus, one only assumes the running of the Newton coupling whereas other couplings remain as fixed values. This idea is technically similar to the scale–dependent scenario although the conceptual foundation is completely different. To supplement our previous subsection, we remark that BD theory is still a classical theory (i.e., any quantum inspiration is used to derive it) and the scale–dependent scenario can be formally considered as “quantum gravity inspired classical theory” given that we do not use the Wetterich flow equation in any part of our approach.

### 6.1.4 Comparison: Scale–Dependence vs RG improving solutions

One apparent misconception in our formalism emerges when one naively identifies it with the well–known “renormalization group improvement” technique [110]. The scale–dependent scenario was successfully discussed along with this thesis, but the renormalization group improved formalism was circumvented. Now, we briefly summarize how this idea works to differentiate it from our approach. The seminal work of Bonanno and Reuter [110] improved the Schwarzschild metric taking as main motivation the running of Newton’s constant (which is obtained from the exact evolution equation for the effective average action). Again, this idea is borrowed from particle physics and subsequently applied to gravitational theories.

Notice that a crucial aspect of this approach is the appropriate identification of the renormalization point  $k$  with the inverse of the distance  $r$ . Thus, as it was commented in the aforementioned paper, such an identification is possible because  $r$  is a dimensionful quantity which could define a scale. What is more, the relation  $k \propto 1/r$  retains the dominant effects of quantum fluctuations on the problem.

Roughly speaking, the meaning of “improve” a black hole is translated as follows: one replaces the Newton constant by its running counterpart  $G(k)$  with a suitable position-dependent scale  $k = k(r)$  where  $r$  is the radial coordinate [110]. Precisely, a non-perturbative solution for  $G(k)$  is used, obtained from the “Einstein Hilbert truncation”.

#### 6.1.4.1 Technical points

One should start by writing down the effective Einstein Hilbert action avoiding ghosts:

$$\Gamma_k = \frac{1}{16\pi G(k)} \int d^d x \sqrt{g} (-R(g) + 2\bar{\lambda}(k)), \quad (6.1)$$

where  $G(k)$  and  $\bar{\lambda}(k)$  denote the running Newton constant and cosmological constant, respectively. Taking this action, we combine it with the Wetterich equation

$$\partial_t \Gamma_k = \frac{1}{2} \text{Tr} \left( \frac{\partial_t \mathcal{R}_k}{\Gamma_k^{(2)}[\phi] + \mathcal{R}_k} \right), \quad (6.2)$$

where  $t = \ln(k)$ . To carry out this computation, it is required to choose certain arbitrary smooth function  $\mathcal{R}_k$ . For comparison, one will follow [110] and then inserting  $\Gamma_k$  into the Wetterich equation and project the flow onto the subspace spanned by the Einstein-Hilbert truncation one obtains a system of coupled differential equations for the dimensionless Newton’s constant. In the four-dimensional case, the corresponding evolution of the dimensionless gravitational coupling is given by

$$\frac{dg(t)}{dt} = \left[ 2 + \left( \frac{B_1 g}{1 - B_2 g} \right) \right] g(t) = \beta(g(t)), \quad (6.3)$$

where  $B_1$  and  $B_2$  are defined in Ref. [110]. Solving the last equation one is able to integrate it to obtain an explicit form of  $g(k)$  (or equivalently  $G(k)$ ) which is

$$G(k) = \frac{G_0}{1 + \omega G_0 k^2}. \quad (6.4)$$

Up to now, the procedure is restricted to taking a particular action and using the Wetterich equation to obtain the beta function for the gravitational coupling. But the crucial point in the “improve” approach is the connection of  $k$  with some physical parameter. Indeed, for black hole physics, the standard identification to be made is

$$k(P) = \frac{\xi}{d(P)}, \quad (6.5)$$

where  $\xi$  is a numerical factor (to be fixed later) and  $d(P)$  is the distance scale which provides the relevant cut-off for Newton’s constant when the test particle is located at the point  $P$  of the black hole spacetime [110]. The above relation then introduces the connection between  $k$  and  $r$ , however, it is not clear the precise way in which those parameters are connected. In particular, the main feature which is preserved when one takes  $k \propto 1/r$  is that the deviations with respect to the classical counterpart emerge in the expected sector. Thus, for large black hole masses, the effects of the running of the gravitational coupling are insignificant, whereas for light black holes such the new features are predominant.

In the four-dimensional case, and for the Schwarzschild metric, the implementation of these ideas is used at the level of solutions, i.e., one accepts the Schwarzschild solution and promotes the classical couplings to scale dependent quantities, which, in this case, is only the gravitational coupling. In this sense, the metric preserves the classical properties and one only needs to revisit some quantities to see how this modification introduces deviations with respect to the standard solution. Thus, we assume that  $G_0 \rightarrow G(r)$  which implies

$$ds^2 = -f(r)dt^2 + f(r)^{-1}dr + r^2d\Omega^2, \quad (6.6)$$

with

$$f(r) = 1 - \frac{2M_0 G(r)}{r^2}. \quad (6.7)$$

Finally, we can conclude that the RG improvement is motivated by asymptotic safety, as it takes advantage of the computation of the running gravitational coupling. Besides, it is

worth-noticing that the parameter  $k$  (which is in principle arbitrary) should be connected with some dimensionful scale of the problem, as Bonanno says.

Now, in light of the GR improved formalism, the differences between the latter and the scale-dependent scenario are clear. First, in our approach, we do not solve the Wetterich equation, and therefore we do not find the specific form of the gravitational coupling computing the corresponding beta function for this coupling. Secondly, our solution is obtained starting from the truncated Einstein-Hilbert action, and then derived from the effective equations which include an additional term given, of course, by the running of the gravitation coupling via the effective contribution  $\Delta t_{\mu\nu}$ . Third, our approach does not assume any particular form for the scale  $k$ , instead, we only take advantage of the fact that it should depend on the radial coordinate (inspired by Bonanno and Reuter). The logic behind the reparameterization of  $k$  in terms of  $r$  or invariants can be understood taking seriously the principle of minimal sensitivity, or the corresponding modern version called Variational Parameter Setting VPS which claims that the problem should be insensitive to changes of the scale  $k$ , i.e.,

$$\left. \frac{d\Gamma_k}{dk} \right|_{k=k_{\text{opt}}} = 0. \quad (6.8)$$

Imposing this condition, one gets a special value  $k = k_{\text{opt}}$ . As a consequence, the solutions only depend on the scales and on the parameters of the original action (i.e,  $R, G(r), \Lambda(r), r, \dots$ ) and not on any unphysical scale. Equation (6.8) is satisfied in our formalism and therefore implies that  $k$  can be written in terms of the parameters of the action.

#### 6.1.4.2 Scale setting and its importance

As we have already mentioned, the arbitrary scale  $k$  is usually a source of uncertainties since one does not have any reason to choose one or another particular form of that. Commonly one takes advantage of that  $l \sim k^{-1}$  gives a natural resolution noticed by an observer who uses an experimental apparatus as was undoubtedly pointed out in Ref.[110]. In problems with certain degree of symmetry, the identification of  $k$  is given in terms of the radial coordinate (for instance, when we are in presence of spherical, circular or cylindrical symmetry). Usually, the relation between  $k$  and  $r$  is reciprocal, because it guarantees the suitable effects at high energy. Particular problems take different parameterization for the scale  $k$ , for instance, another choice which is still valid is  $k(r) \propto 1/r^{3/2}$ . Similar identification has been made in Cosmology [192], where Bonanno and Reuter used the natural choice  $k(t) = 1/t$ . In addition,

when one is following the evolution of the scale factor  $a(t)$  of the Universe; another natural identification is  $k(a(t)) \sim 1/a(t)$  as was pointed out by Floreanini and Percacci [193]. Over the years, progress in the context of RG improvement in black hole physics has been made, but the same assumption appears as a common factor: the functional form of the scale  $k$  is usually linked to the reciprocal of length [194].

Irrespective of the uncertainties, the distance  $d(P)$ , which appears in Eq. (6.5), can be motivated in a variety of ways inspired by the Schwarzschild metric (in four-dimensional spacetimes), flat space metric, dimensional analysis, and interpolations. The most relevant ways to fix  $d(P)$  are: i) Dimensional analysis, ii) Proper distance, which is obtained by identifying the RG momentum scale  $k$  with the inverse diffeomorphism invariant distance  $d_{\text{diff}}(r)^{-1}$  solving

$$d_{\text{diff}}(r) = \int \sqrt{|ds^2|}, \quad (6.9)$$

iii) IR matching (approximation made if the black hole mass  $M$  is sufficiently large compared to the Planck mass), iv) UV matching (which is taken into account when the radius is smaller than the classical counterpart), and v) Interpolations (which introduce an interpolation function between IR and UV matching) [70]. These different manners of taking  $d(P)$  or  $k(r)$  ensure a good behavior at high energy level, which is suitable, but the price to pay is that one introduces “by hand” this effect. In principle, one does not have a fundamental derivation of  $k(r)$  which is always a problem. What is more, the invariance under diffeomorphism is, in general, violated when we fix  $k(r)$ . The scale-dependent scenario does not assume any form of  $k(r)$  reason why the invariance under diffeomorphism is not violated in our case. There is, however, a price to be paid: we need to impose an additional condition in order to close the system of equations, and thus to be able to solve the problem. We have used in a variety of cases the null energy condition because it satisfies the constraint  $f(r) \cdot g(r) = 1$ , which is a common feature, at least in the black holes analyzed along with this thesis.

Finally, in the context of theories beyond General Relativity, we can visualize, via the following flow chart (6.1), the different ways to achieve a consistent theory of “quantum gravity”. The level I corresponds to the suitable ingredients to construct the theory, which are: i) the metric field and ii) diffeomorphism invariance (i.e., despite the metric change, the Einstein field equations remain the same form). At this point, we can include in our theory both ingredients or only one of them. The level II is devoted to the plausible theories available to investigate problems in quantum gravity. We unquestionably do not comment about other

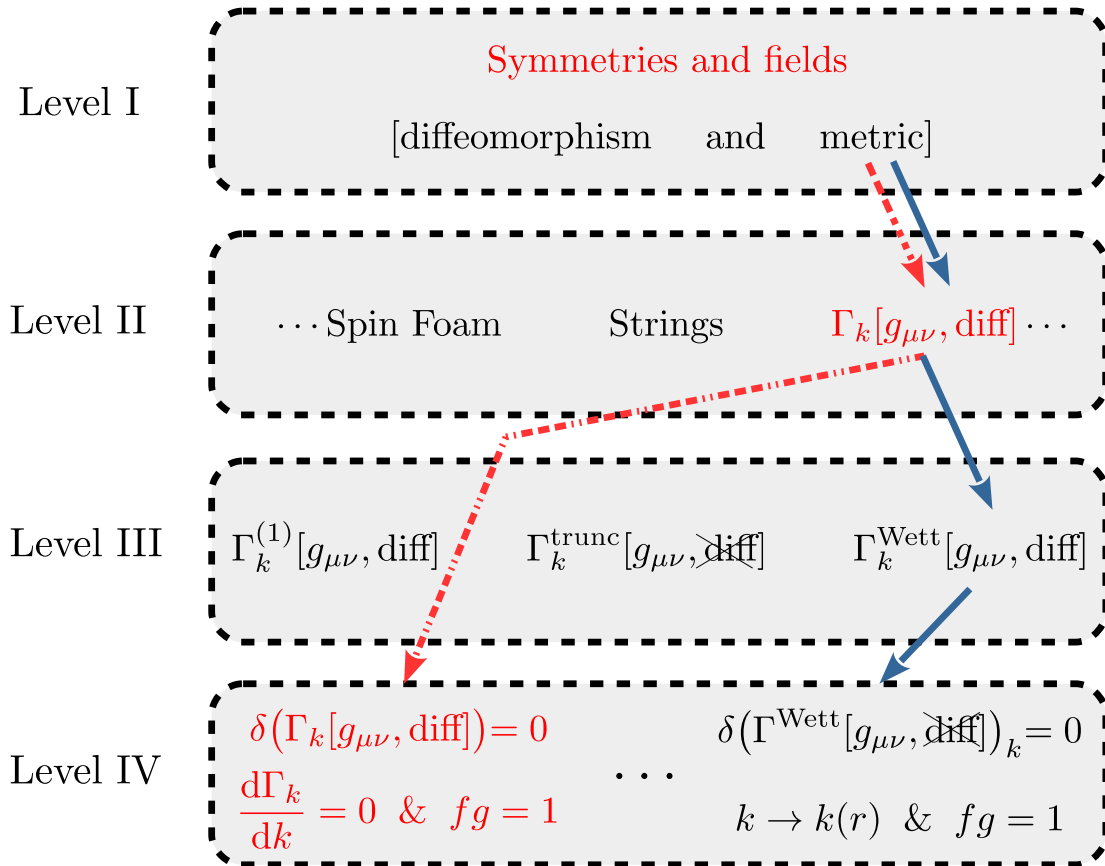


**Figure 6.1:** Illustrative image explaining the top-down structure, from symmetry considerations to observables of quantum gravity.

interesting angles as loop quantum gravity or string theories, however, different approaches can be found at [84, 195, 196]. In level III we have the methods typically used to solve problems in quantum gravity. We focus on the cases where the effective action plays a crucial role. Finally, in level IV we have the observables that, in our case, are black holes. In this final step, we can follow the Wetterich and related approaches, or our idea, which is similarly inspired but not the same. So, following a path and adding certain conditions, we can make progress. In the flow chart, we follow the double dotted-dashed red arrows.

We first start by taking, in Level I, a metric field. Then, we select a theory that preserves diffeomorphism invariance in Level II and finally, in Level IV, we use the effective action and physical conditions to get information about observables. An alternative route is, for example, obtained following the solid blue arrows. In that last case, one, unfortunately, loses diffeomorphism reason why we use our approach (which preserves it).

### 6.1.5 Comparison: with and without NEC

As we discussed, our solutions take advantage of the NEC as a supplementary ingredient. The application of the NEC in classical black holes is typically misinterpreted. It is due many times the Schwarzschild ansatz is used, and one does not consider the physical consequences of that assumption. We remark that, as Jacobson said [130], the NEC leads to  $f(r) \cdot g(r) = 1$ . Frequently, such condition is not valid, but in simple black holes solutions, the Schwarzschild ansatz is correct and therefore the NEC is, of course, true too. In the scale-dependent scenario, the energy above condition emerges due we try to mimic the behavior present in the classical solution. In case we violate that, we will have an additional function to solve and extra information will be needed.

One can try to map the same idea towards the Brands–Dicke theory but, in that case, it is better to take advantage of the Klein Gordon equation which is, of course, a more natural way to complete the set of equations. In case we insist on the use of the NEC, it can be on DB theory when the  $\omega_{\text{BD}}$  is taken to be zero. Different circumstances were not analyzed in this thesis.

Additionally, and following the discussion regarding the null energy condition, the use of NEC introduces strong effects at large distances. The effect appears due we do not ensure the suitable behavior at high energy. We, however, can reconcile the use of NEC with the expected effect at high energy taking an extended version of it. As we can see in the appendix, the differential equation for the gravitational coupling is

$$2 \left[ \frac{dG(r)}{dr} \right]^2 - G(r) \frac{d^2 G(r)}{dr^2} = -\frac{1}{2} G(r) \frac{dG(r)}{dr} \left[ \left( f(r) \cdot g(r) \right)^{-1} \frac{d}{dr} \left( f(r) \cdot g(r) \right) \right], \quad (6.10)$$

which is obtained taking a minimum version of NEC, namely

$$T_{\mu\nu}^{\text{effec}} \ell^\mu \ell^\nu = \alpha(r) = 0. \quad (6.11)$$

In order to fix the discrepancy in the running of the gravitational coupling, respect the asymptotic safety program, a possibility is to take  $\alpha(r)$  in such way that  $G(r)$  mimics the suitable high energy effect, in this sense, we still do not take a particular form of  $k(r)$ . The crucial point here is, similar to the RG improvement approach, that  $G(r)$  is taken consistently at large energies. Formally, if we assume a certain form for  $G(r)$ , we do not need to use the

NEC because now we can obtain all the functions involved. The price to pay is that now the relation between the metric components change from  $f(r) \cdot g(r) = 1$  to  $f(r) \cdot g(r) = h(r)$ .

To explore this possibility, we take as an example the well-known BTZ black hole assuming a suitable form for the gravitational coupling given by

$$G(r) = G_0 \left[ 1 + \left( \frac{\xi}{r} \right)^2 \right]^{-1}, \quad (6.12)$$

where we will take  $G_0 = 1$  for simplicity. Please, note that  $G(r)$  introduces relevant corrections for small values of radial coordinate (in agreement with the RG improvement technique). The line element is written as follows:

$$ds^2 = -A(r)dt^2 + B(r)dr^2 + r^2d\phi^2, \quad (6.13)$$

Naturally, we recover the nondeformed solution demanding that  $\xi$  goes to zero. The problem has three unknown functions, namely, two metric components  $A(r)$  and  $B(r)$  and the cosmological coupling  $\Lambda(r)$ . Solving the effective Einstein field equations we get

$$A(r) = A_0(r) + \frac{1}{3}M_0 \left[ 24 - 6 \left( \frac{\xi}{r} \right)^2 + \left( \frac{\xi}{r} \right)^4 - 24 \left( \frac{\xi}{r} \right)^{-2} \ln \left( 1 + \left( \frac{\xi}{r} \right)^2 \right) \right], \quad (6.14)$$

$$B(r) = \left[ 1 - \left( \frac{\xi}{r} \right)^2 \right]^6 A(r)^{-1}, \quad (6.15)$$

$$\Lambda(r) = - \frac{A(r) \left( 1 + \frac{\xi^2}{r^2} \right) \left( 1 - 3\frac{\xi^2}{r^2} \right) + M_0 \left( 1 - \frac{\xi^2}{r^2} \right)^4}{r^2 \left( 1 - \frac{\xi}{r} \right)^6 \left( 1 + \frac{\xi}{r} \right)^6 \left( 1 + \frac{\xi^2}{r^2} \right)^2}. \quad (6.16)$$

Taking this suitable form for the gravitational coupling we can: i) obtain analytic solutions for the functions involved, ii) introduce corrections for small values of  $r$  and iii) get consistent thermodynamics. Indeed, the temperature for this case acquires the simple form:

$$T_H(r_H) = T_0(r_H) \left[ 1 + \left( \frac{\xi}{r_H} \right)^2 \right]^{-1}, \quad (6.17)$$

where  $r_H$  is the event horizon and  $T_0$  is the classical temperature. In light of this solution, we confirm that if we want to obtain correction at small values of  $r$ , we need to choose a  $\alpha(r)$  such that  $G(r)$  mimics the desirable behavior. Just, in this case, the NEC reconciles with

the solutions obtained in RG improvement. In the next subsection, we will briefly comment about the thermodynamics of scale-dependent black holes.

### 6.1.6 About Thermodynamics

Now we will briefly comment on the thermodynamics of the problems treated in this thesis. The classical theory, i.e., Einstein's gravity, can describe black hole physics due to the scales in which these objects appear are appropriated. When we accept deviations from classical gravity, we have three possibilities: i) correction at small length scale, ii) correction at large length scale and finally iii) correction at both scales. In principle, we should expect corrections in the high energy sector, which means small  $r$  values. Fig. (6.2) schematically shows the regime in which classical Einstein's gravity works. The left-hand side corresponds to the quantum region (where we are interested in), and the right-hand side represents a large length scale.

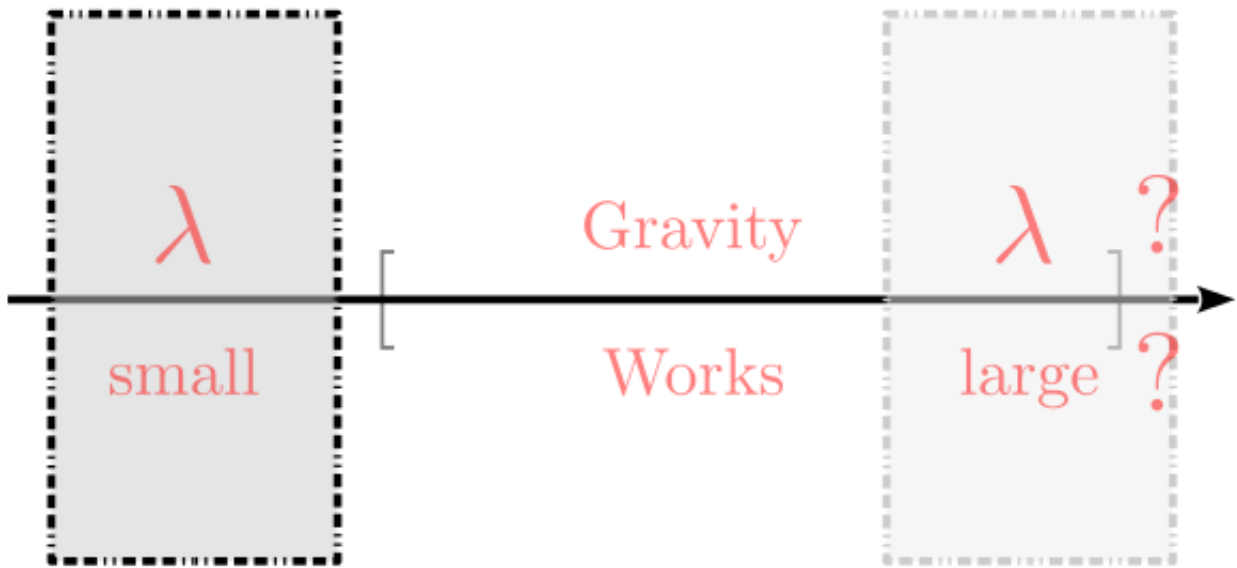


**Figure 6.2:** Illustrative image where gravity works. Notice that  $\lambda$  is a length scale.

Conventional approaches to quantum gravity (as RG improved or the Wetterich approach) introduce significant corrections at small length scales and intermediate scales. Our approach extends the standard classical solutions, although the significant corrections emerge in the opposite sector. We remark that, at small scale physics, the corrections introduce quantum

features suitable to get a quantum theory of gravity. Physics at large (length) scale is modeled by GR but, indeed, one has alternative approaches to (modified) theories of gravity where dark matter is not required. In this sense, although our results are quantum inspired, unquestionably the study of gravity at large scale is essential too. Thus, formally it is interesting to study corrections to gravity at large and small length scales. The same occurs when the thermodynamics is examined. In our approach, the temperature and the entropy acquire corrections due to the radial coordinate where the real impact of corrections is collected at large scale.

Given that our solutions are quantum inspired, although our results are mathematically correct, they are only valid when the deviations, respect the classical counterpart, are small, the reason why we trust in our results just when the combination  $\epsilon r$  is taken to be small.

In particular, the combination  $\epsilon r_H$  reveals where the effects are more significant. In cases where the corrections are important, should be noticed that as the scale-dependent parameter  $\epsilon$  is small by construction, the horizon becomes large. In such circumstances, given that the horizon is typically related with the black hole mass by  $r_H \sim M_0^\alpha$  (with  $\alpha > 0$ ), the corrections appear for large values of  $M_0$ .

In the cases treated here we have computed the entropy for the new scale-dependent black hole. We observed, in figures, how the deviation respect the classical case, appears. We indeed have plotted (when it is possible) two values for the entropy. This fact blurred the landscape because the meaning of a multi-valued entropy is not clear. The explanation, however, is quite simple: the lesson from physics is that entropy will increase reason why, of the two solutions, the physical one will be the bigger between them (i.e. taking  $r_H = r_+$  as it should be).

### 6.1.7 Charged solutions

One relevant aspect which should be commented before to conclude is concerning to the charged black holes. Firstly, we recognize that the electric field  $E(r)$  has an unusual behavior respect to the standard Maxwell solution in (2+1) dimensional spacetime. Our formalism does not introduce this effect. Indeed, in the context of non-linear electrodynamics, we expect to have variations due to the non-linearity. Our cases are only devoted to the Einstein-power-Maxwell electrodynamics which is one of the most economical non-lineal electrodynamics, and it only introduces a deviation in the power law of the electric field as

we pointed out in previous chapters. We remark that the standard EpM gives an electric field  $E(r) \propto r^{-\alpha}$  in the classical regimen (where  $\alpha$  is an arbitrary rational number). This electric field is associated with some charge which we naively identify as  $Q_0$  in the traditional case. The scale-dependent approach, however, does not make the charge a scale-dependent quantity, and therefore any fundamental change appears (at the level of the charge) in our solutions.

Just to make the situation clearer, we recall that Maxwell equations relate the electromagnetic field strength tensor  $F^{\mu\nu}$  to the electric current four-vector  $J_\mu$  by  $D_\mu(F^{\mu\nu}) = J^\mu$ . The situation is slightly different in the presence of non-linear electrodynamics, where we have  $D_\mu(\mathcal{L}_F F^{\mu\nu}) = J^\mu$ . We start with the calculation of the black hole electric charge  $Q$ , as a conserved quantity, by calculating the flux of the electromagnetic field at infinity which means

$$Q \equiv \int \sqrt{-g} d\Omega \left( \mathcal{L}_F F_{\mu\nu} \right) n^\mu \sigma^\nu, \quad (6.18)$$

where  $n^\mu$  and  $u^\nu$  are the unit spacelike and timelike normals to the hypersurface of radius  $r$  defined as  $n^\mu = (f(r)^{-1/2}, 0, 0)$  and  $u^\nu = (0, f(r)^{1/2}, 0)$ . We then observe that  $Q$  is a constant and it is directly related to the power of the Einstein-power-Maxwell law [178, 197].

Regarding the dependence of our solutions on the  $\alpha$  index we comment that: i) given that we only analyze the (2+1) case, we are not able to establish any bound on the parameter  $\alpha$ . The situation is quite different in the four-dimensional case where one can study the static equilibrium of a charged massive particle around a charged black hole [198] as a tool to put constraints on the parameter  $\alpha$ .

### 6.1.8 Possible reconciliation

Recent publications give evidence that a “gravitational instability” could introduce modifications of Asymptotic safety theories in the deep infrared [199, 200]. In this sense, this infrared instability can lead to significant deviations from classical gravity. In such cases, the gravitational coupling grows (for small values of  $\ln(k)$ ) up to a certain point (at intermediate  $\ln(k)$ ) maintaining the same value. After certain scale, the function  $G_k$  decreases (for large values of  $\ln(k)$ ) and tends to zero. This behavior is quite similar to our results, and therefore, our solutions can be considered as a prediction.

Further evidence for such behavior in AS close to the separatrix flow line has been pointed out in [201]. It would be fascinating to investigate whether our findings reflect those qualitatively agreeing results also quantitatively.

## 6.2 Final remarks

By developing this thesis, we have noticed several general features that always appear in the different subtopics treated here. We briefly sum them up below:

- ▶ We can always introduce self-consistent quantum corrections via the scale-dependent scenario, which is inspired by the asymptotic safety program.
- ▶ Starting from the effective action, the corresponding scale-dependent solutions effectively include the classical subdomain of solutions. This feature ensures we generalize a classical problem.
- ▶ Symmetry plays a crucial role. Taking advantage of spherical/circumferential symmetry, we can transform the equations to obtain a simpler set of field equations to solve.
- ▶ The integration constants are crucial in this approach. The correct choice of them allows us to i) identify the parameter which introduces the quantum features and ii) turn it off to test if the classical solution is recovered.
- ▶ Black hole thermodynamics matches in classical and scale-dependent regime, under the replacement  $G_0 \rightarrow G(r)$ . It is worth-noticing that the event horizon is smaller than its classical counterpart.
- ▶ The null energy condition allows us to complete the set of equations without introducing further assumptions. Thus, taking advantage of this, we can always obtain a specific form of gravitational coupling.

Finally, we can conclude that using the scale-dependent scenario we are able to improve classical solutions incorporating quantum corrections. In addition, all the solutions reported here boil down to the classical ones when the running parameter is taken to be zero.



# Appendix A

## On the null energy condition in scale dependent frameworks

This Appendix was published in the proceedings of 20th Chilean Physics Symposium [144]

### A.1 Introduction

Nowadays, different alternatives exist to obtain an unified theory of quantum gravity. Loop quantum gravity [45] as well as string theory [195, 196] are famous candidates to achieve this unification. Besides, a self-consistent theory of quantum gravity is still lacking, being studied assuming different points of view [82–98]. Many quantum extensions of general relativity present a common feature: a scale dependence appearing at the level of the effective action of gravity. The classical couplings are not constants any more, instead, they depend on arbitrary scale  $k$ . The physics of a black hole strongly depends on the scale setting e.g. the connection between  $k$  and  $r$ . For the case of spherically symmetric black holes, it can be expected that  $k = k(r)$  and thus  $\{G_k, \Lambda_k, e_k, \mathcal{O}_k\} \rightarrow \{G(r), \Lambda(r), e(r), \mathcal{O}(r)\}$  [123, 125]. Those  $r$ -dependent couplings can be obtained directly from the quantum gap equations, if one assumes certain energy conditions.

Recent papers have shown that the so-called “Null Energy Condition” (NEC) plays a crucial role in this context [53, 56, 58]. Thus, in this Appendix we analyze the link between the

so-called Schwarzschild ansatz and the NEC, in the light of scale dependent couplings. We show farther the important role played by the NEC in determining the gravitational running coupling  $G(r)$ . The present work is organized as follows: after this short introduction, we explain the main idea of this letter in Section A.2, whereas the technique and results are collected at Section A.3. Finally, the conclusions are given at Section A.4.

## A.2 Main idea

The so-called Null Energy Condition is one of the usual energy conditions (dominant, weak, strong, and null) and, besides, the least restrictive of them. It helps to obtain suitable solutions of the Einstein field equation and it is usually applied to discern whether a solution has physical validity or not. We will explore this condition in the context of spherical symmetry where the line element reads

$$ds^2 = -f(r)dt^2 + g(r)dr^2 + r^2d\Omega, \quad (\text{A.1})$$

which have to be determined by theorems. Here  $f(r)$  and  $g(r)$  are arbitrary functions, and  $d\Omega$  is the solid angle (which depends on the studied dimension). In many cases the task of solving the EOM's is simplified by the so called Schwarzschild ansatz  $f(r) \cdot g(r) = 1$ . As was explained by Jacobson [130], the aforementioned ansatz can be seen as a consequence of NEC. This finding follows from the fact that the Ricci tensor is proportional to the metric in the  $t - r$  subspace. In addition, and regarding the application of this condition, one should note that validity of NEC was guaranteed at Ref. [130], and it applies in spherical symmetry with either Maxwell electrodynamics (i.e. the Reissner-Nordstrom solution) or Born-Infeld non-linear electrodynamics [202], and persists in the presence of a cosmological constant.

In the present work, Jacobson's argument is applied to black holes in the light of the running couplings, analysing the effect of this on the underlying physics as well as the implications associated with the specific form of gravitational coupling  $G(r)$ . Thus, for an effective Einstein-Hilbert action with cosmological constant, one has the effective Einstein field equations which read [56, 58]

$$G_{\mu\nu} + \Lambda(r)g_{\mu\nu} = 8\pi G(r)T_{\mu\nu}^{\text{effec}}, \quad (\text{A.2})$$

and the effective energy momentum tensor is defined according to

$$8\pi G(r)T_{\mu\nu}^{\text{effec}} = 8\pi G(r)T_{\mu\nu}^m - \Delta t_{\mu\nu}. \quad (\text{A.3})$$

Here,  $T_{\mu\nu}^m$  is the matter energy momentum tensor (which for simplicity is taken to be zero) and the additional term  $\Delta t_{\mu\nu}$  is related to the scale dependence of the gravitational running coupling  $G(r)$  as shown in next section.

### A.3 Technique and results

In spherical symmetry [A.1](#) and according to Jacobson's idea [[130](#)], the Null Energy Condition reads

$$T_{\mu\nu}^{\text{effec}}\ell^\mu\ell^\nu = 0, \quad \therefore \quad R_{\mu\nu}\ell^\mu\ell^\nu = 0, \quad (\text{A.4})$$

where, in three dimensional spacetime,  $\ell^\mu$  is a null vector given by

$$\ell^\mu \equiv \left( \sqrt{g(r)}, \sqrt{f(r)}, 0 \right), \quad (\text{A.5})$$

For arbitrary dimension, one always can define appropriate a null vector such as  $\ell^\mu = (g^{1/2}, f^{1/2}, \mathbf{0})$ , where  $\mathbf{0}$  encoded the zero component for an arbitrary dimension of this null vector. Using the aforementioned  $\ell^\mu$  combined with Eq. [A.4](#), it is ever possible to obtain a simple differential equation which is straightforward to solve.

Besides, note that in the Einstein-Hilbert truncation [[203](#)] the field equation of motion are consistent with Eq. [A.2](#). Thus, from [A.4](#) one sees that

$$\left[ R_{\mu\nu} - \left( \frac{1}{2}R - \Lambda(r) \right) g_{\mu\nu} \right] \ell^\mu \ell^\nu = \left[ 8\pi G(r)T_{\mu\nu}^m - \Delta t_{\mu\nu} \right] \ell^\mu \ell^\nu, \quad (\text{A.6})$$

where the additional object  $\Delta t_{\mu\nu}$  is defined as follows

$$\Delta t_{\mu\nu} \equiv G_k \left( g_{\mu\nu} \square - \nabla_\mu \nabla_\nu \right) G_k^{-1}. \quad (\text{A.7})$$

Note that, by definition, a null vector satisfies that  $g_{\mu\nu}\ell^\mu\ell^\nu = 0$ , which allows getting the simple equation

$$R_{\mu\nu}\ell^\mu\ell^\nu = 0, \quad \therefore \quad \Delta t_{\mu\nu}\ell^\mu\ell^\nu = 0, \quad (\text{A.8})$$

which produces the following ordinary differential equation:

$$2 \left[ \frac{dG(r)}{dr} \right]^2 - G(r) \frac{d^2G(r)}{dr^2} = -\frac{1}{2}G(r) \frac{dG(r)}{dr} \left[ \left( f(r) \cdot g(r) \right)^{-1} \frac{d}{dr} \left( f(r) \cdot g(r) \right) \right], \quad (\text{A.9})$$

thereby, one finds without even solving the set of equations [A.2](#) that

$$G(r) = a \left[ \int_{r_0}^r \sqrt{f(r') \cdot g(r')} dr' \right]^{-1}, \quad (\text{A.10})$$

independent of the actual form of  $f(r)$  and  $g(r)$ . In addition,  $a$  is a real value which is taken such as one recovering  $G(r) \rightarrow G_0$  in some limit. Particular attention must be dedicated to case when the Schwarzschild ansatz is used. Under this assumption, the aforementioned differential equation is simplified to be

$$2 \left[ \frac{dG(r)}{dr} \right]^2 = G(r) \frac{d^2G(r)}{dr^2}, \quad (\text{A.11})$$

which gives the following scale dependent gravitational coupling

$$G(r) = \frac{G_0}{1 + \epsilon r}. \quad (\text{A.12})$$

The running coupling found in [\[55–58\]](#) corresponds to  $f(r) \cdot g(r) = 1$ , which is consistent with [Eq. A.12](#). Please, note that the relation  $f(r) \cdot g(r) = 1$  is actually independent of the truncation and form of E.O.M.'s since by [A.8](#) alone one finds the solution.

## A.4 Conclusion

In the present appendix, the role of Null Energy Condition [\[130\]](#) is analyzed in the context of running couplings. It is found that the NEC allows to obtain a justification of the Schwarzschild ansatz (by the virtue of [\[56\]](#)). By imposing non-generation of stress energy

tensor due to scale dependent gravitational coupling [56, 58] it allows to determine the form of  $G(r)$ .



# Bibliography

- [1] Sean M. Carroll. *Spacetime and geometry: An introduction to general relativity*. 2004. ISBN 0805387323, 9780805387322. URL <http://www.slac.stanford.edu/spires/find/books/www?cl=QC6:C37:2004>.
- [2] Adam G. Riess et al. Observational evidence from supernovae for an accelerating universe and a cosmological constant. *Astron. J.*, 116:1009–1038, 1998. doi: 10.1086/300499.
- [3] Oeyvind Groen and Sigbjorn Hervik. *Einstein's general theory of relativity: With modern applications in cosmology*. 2007. URL <http://www.springer.com/978-0-387-69199-2>.
- [4] K. Schwarzschild. Über das Gravitationsfeld eines Massenpunktes nach der Einsteinschen Theorie. *Sitzungsberichte der Königlich Preußischen Akademie der Wissenschaften (Berlin)*, 1916, Seite 189-196, 1916.
- [5] Roy P. Kerr. Gravitational field of a spinning mass as an example of algebraically special metrics. *Phys. Rev. Lett.*, 11:237–238, 1963. doi: 10.1103/PhysRevLett.11.237.
- [6] F. W. Dyson, A. S. Eddington, and C. Davidson. A Determination of the Deflection of Light by the Sun's Gravitational Field, from Observations Made at the Total Eclipse of May 29, 1919. *Philosophical Transactions of the Royal Society of London Series A*, 220:291–333, 1920. doi: 10.1098/rsta.1920.0009.
- [7] S. S. Shapiro, J. L. Davis, D. E. Lebach, and J. S. Gregory. Measurement of the Solar Gravitational Deflection of Radio Waves using Geodetic Very-Long-Baseline Interferometry Data, 1979-1999. *Phys. Rev. Lett.*, 92:121101, 2004. doi: 10.1103/PhysRevLett.92.121101.

- [8] Clifford M. Will. The Confrontation between general relativity and experiment. *Living Rev. Rel.*, 9:3, 2006. doi: 10.12942/lrr-2006-3.
- [9] Slava G. Turyshev. Experimental Tests of General Relativity. *Ann. Rev. Nucl. Part. Sci.*, 58:207–248, 2008. doi: 10.1146/annurev.nucl.58.020807.111839.
- [10] Irwin I. Shapiro, Gordon H. Pettengill, Michael E. Ash, Richard P. Ingalls, D. B. Campbell, and R. B. Dyce. Mercury’s Perihelion Advance: Determination by Radar. *Phys. Rev. Lett.*, 28:1594–1597, 1972. doi: 10.1103/PhysRevLett.28.1594.
- [11] Estelle Asmodelle. *Tests of General Relativity: A Review*. PhD thesis, Central Lancashire U., 2017.
- [12] A. Friedmann. Über die Krümmung des Raumes. *Zeitschrift für Physik*, 10:377–386, 1922. doi: 10.1007/BF01332580.
- [13] Timothy Clifton, Chris Clarkson, and Philip Bull. The isotropic blackbody CMB as evidence for a homogeneous universe. *Phys. Rev. Lett.*, 109:051303, 2012. doi: 10.1103/PhysRevLett.109.051303.
- [14] W. Hasse and V. Perlick. On spacetime models with an isotropic Hubble law. *Classical and Quantum Gravity*, 16:2559–2576, August 1999. doi: 10.1088/0264-9381/16/8/301.
- [15] C.W. Misner, K.S. Thorne, and J.A. Wheeler. *Gravitation*. W.H. Freeman and Company, 1973.
- [16] E. W. Kolb and M. S. Turner. *The early universe*. 1990.
- [17] Jorge L. Cervantes-Cota and George Smoot. Cosmology today-A brief review. *AIP Conf. Proc.*, 1396:28–52, 2011. doi: 10.1063/1.3647524.
- [18] J. A. Peacock. *Cosmological Physics*. January 1999.
- [19] V. Mukhanov. *Physical Foundations of Cosmology*. Cambridge University Press, Oxford, 2005. ISBN 0521563984, 9780521563987. URL <http://www-spires.fnal.gov/spires/find/books/www?cl=QB981.M89::2005>.
- [20] Pierre-Henri Chavanis. Relativistic stars with a linear equation of state: analogy with classical isothermal spheres and black holes. *Astron. Astrophys.*, 483:673, 2008. doi: 10.1051/0004-6361:20078287.

- [21] Heinz-Jurgen Schmidt and Felix Homann. Photon stars. *Gen. Rel. Grav.*, 32:919–931, 2000. doi: 10.1023/A:1001989125318.
- [22] J. Ponce de Leon and Norman Cruz. Hydrostatic equilibrium of a perfect fluid sphere with exterior higher dimensional Schwarzschild space-time. *Gen. Rel. Grav.*, 32:1207–1216, 2000. doi: 10.1023/A:1001982402392.
- [23] J. R. Oppenheimer and G. M. Volkoff. On Massive neutron cores. *Phys. Rev.*, 55: 374–381, 1939. doi: 10.1103/PhysRev.55.374.
- [24] C. W. Misner and H. S. Zeplosky. High-Density Behavior and Dynamical Stability of Neutron Star Models. *Phys. Rev. Lett.*, 12:635–637, 1964. doi: 10.1103/PhysRevLett.12.635.
- [25] L. Herrera. Cracking of self-gravitating compact objects. *Phys. Lett.*, A165:206–210, 1992. doi: 10.1016/0375-9601(92)90036-L.
- [26] L. Herrera and N. O. Santos. Local anisotropy in self-gravitating systems. *Phys. Rept.*, 286:53–130, 1997. doi: 10.1016/S0370-1573(96)00042-7.
- [27] R. J. Trumpler. Observational Evidence of a Relativity Red Shift in Class O Stars. , 47:249, October 1935. doi: 10.1086/124604.
- [28] Nikolaos Stergioulas. Rotating Stars in Relativity. *Living Rev. Rel.*, 6:3, 2003. doi: 10.12942/lrr-2003-3.
- [29] B. P. Abbott et al. Observation of Gravitational Waves from a Binary Black Hole Merger. *Phys. Rev. Lett.*, 116(6):061102, 2016. doi: 10.1103/PhysRevLett.116.061102.
- [30] B. P. Abbott et al. GW151226: Observation of Gravitational Waves from a 22-Solar-Mass Binary Black Hole Coalescence. *Phys. Rev. Lett.*, 116(24):241103, 2016. doi: 10.1103/PhysRevLett.116.241103.
- [31] Benjamin P. Abbott et al. GW170104: Observation of a 50-Solar-Mass Binary Black Hole Coalescence at Redshift 0.2. *Phys. Rev. Lett.*, 118(22):221101, 2017. doi: 10.1103/PhysRevLett.118.221101,10.1103/PhysRevLett.121.129901. [Erratum: *Phys. Rev. Lett.*121,no.12,129901(2018)].
- [32] B. P. Abbott et al. GW170814: A Three-Detector Observation of Gravitational Waves from a Binary Black Hole Coalescence. *Phys. Rev. Lett.*, 119(14):141101, 2017. doi: 10.1103/PhysRevLett.119.141101.

- [33] Robert M. Wald. *General Relativity*. Chicago, Usa: Univ. Pr. 491p, 1984. doi: 10.7208/chicago/9780226870373.001.0001.
- [34] S. W. Hawking. Black hole explosions. *Nature*, 248:30–31, 1974. doi: 10.1038/248030a0.
- [35] S. W. Hawking. Particle Creation by Black Holes. *Commun. Math. Phys.*, 43:199–220, 1975. doi: 10.1007/BF02345020,10.1007/BF01608497. [,167(1975)].
- [36] James M. Bardeen, B. Carter, and S. W. Hawking. The Four laws of black hole mechanics. *Commun. Math. Phys.*, 31:161–170, 1973. doi: 10.1007/BF01645742.
- [37] Jacob D. Bekenstein. Black holes and entropy. *Phys. Rev.*, D7:2333–2346, 1973. doi: 10.1103/PhysRevD.7.2333.
- [38] Grigoris Panotopoulos and Ángel Rincón. Greybody factors for a minimally coupled massless scalar field in Einstein-Born-Infeld dilaton spacetime. *Phys. Rev.*, D96(2):025009, 2017. doi: 10.1103/PhysRevD.96.025009.
- [39] Grigoris Panotopoulos and Ángel Rincón. Greybody factors for a minimally coupled scalar field in three-dimensional Einstein-power-Maxwell black hole background. *Phys. Rev.*, D97(8):085014, 2018. doi: 10.1103/PhysRevD.97.085014.
- [40] Grigoris Panotopoulos and Ángel Rincón. Quasinormal modes of black holes in Einstein-power-Maxwell theory. *Int. J. Mod. Phys.*, D27(03):1850034, 2017. doi: 10.1142/S0218271818500347.
- [41] Edvige Corbelli and Paolo Salucci. The Extended Rotation Curve and the Dark Matter Halo of M33. *Mon. Not. Roy. Astron. Soc.*, 311:441–447, 2000. doi: 10.1046/j.1365-8711.2000.03075.x.
- [42] C. Brans and R. H. Dicke. Mach’s principle and a relativistic theory of gravitation. *Phys. Rev.*, 124:925–935, 1961. doi: 10.1103/PhysRev.124.925. [,142(1961)].
- [43] B. Bertotti, L. Iess, and P. Tortora. A test of general relativity using radio links with the Cassini spacecraft. , 425:374–376, September 2003. doi: 10.1038/nature01997.
- [44] K. Becker, M. Becker, and J. H. Schwarz. *String theory and M-theory: A modern introduction*. Cambridge University Press, 2006. ISBN 9780511254864, 9780521860697.

- [45] Carlo Rovelli. *Quantum gravity*. Cambridge Monographs on Mathematical Physics. Univ. Pr., Cambridge, UK, 2004. doi: 10.1017/CBO9780511755804. URL <http://www.cambridge.org/uk/catalogue/catalogue.asp?isbn=0521837332>.
- [46] Steven Weinberg. General Relativity: An Einstein centenary survey. *Cambridge University Press.*, chapter 16:790–831, 1979.
- [47] Bertrand Delamotte. An Introduction to the nonperturbative renormalization group. *Lect. Notes Phys.*, 852:49–132, 2012. doi: 10.1007/978-3-642-27320-9\_2.
- [48] Alessandro Codello, Roberto Percacci, and Christoph Rahmede. Investigating the Ultraviolet Properties of Gravity with a Wilsonian Renormalization Group Equation. *Annals Phys.*, 324:414–469, 2009. doi: 10.1016/j.aop.2008.08.008.
- [49] Martin Reuter and Frank Saueressig. Functional Renormalization Group Equations, Asymptotic Safety, and Quantum Einstein Gravity. In *Geometric and topological methods for quantum field theory*, pages 288–329, 2010. doi: 10.1017/CBO9780511712135.008.
- [50] M. Reuter and Frank Saueressig. Renormalization group flow of quantum gravity in the Einstein-Hilbert truncation. *Phys. Rev.*, D65:065016, 2002. doi: 10.1103/PhysRevD.65.065016.
- [51] Kevin Falls, Daniel F. Litim, Konstantinos Nikolakopoulos, and Christoph Rahmede. Further evidence for asymptotic safety of quantum gravity. *Phys. Rev.*, D93(10): 104022, 2016. doi: 10.1103/PhysRevD.93.104022.
- [52] M. Reuter and H. Weyer. Renormalization group improved gravitational actions: A Brans-Dicke approach. *Phys. Rev.*, D69:104022, 2004. doi: 10.1103/PhysRevD.69.104022.
- [53] Carlos Contreras, Benjamin Koch, and Paola Rioseco. Black hole solution for scale-dependent gravitational couplings and the corresponding coupling flow. *Class. Quant. Grav.*, 30:175009, 2013. doi: 10.1088/0264-9381/30/17/175009.
- [54] Benjamin Koch, Carlos Contreras, Paola Rioseco, and Frank Saueressig. Black holes and running couplings: A comparison of two complementary approaches. *Springer Proc. Phys.*, 170:263–269, 2016. doi: 10.1007/978-3-319-20046-0\_31.

- [55] Benjamin Koch and Paola Rioseco. Black Hole Solutions for Scale Dependent Couplings: The de Sitter and the Reissner-Nordström Case. *Class. Quant. Grav.*, 33:035002, 2016. doi: 10.1088/0264-9381/33/3/035002.
- [56] Benjamin Koch, Ignacio A. Reyes, and Ángel Rincón. A scale dependent black hole in three-dimensional spacetime. *Class. Quant. Grav.*, 33(22):225010, 2016. doi: 10.1088/0264-9381/33/22/225010.
- [57] Ángel Rincón, Ernesto Contreras, Pedro Bargueo, Benjamin Koch, Grigoris Panotopoulos, and Alejandro Hernández-Arboleda. Scale dependent three-dimensional charged black holes in linear and non-linear electrodynamics. *Eur. Phys. J.*, C77(7):494, 2017. doi: 10.1140/epjc/s10052-017-5045-9.
- [58] Ángel Rincón, Benjamin Koch, and Ignacio Reyes. BTZ black hole assuming running couplings. *J. Phys. Conf. Ser.*, 831(1):012007, 2017. doi: 10.1088/1742-6596/831/1/012007.
- [59] Ángel Rincón and Grigoris Panotopoulos. Quasinormal modes of scale dependent black holes in  $(1+2)$ -dimensional Einstein-power-Maxwell theory. *Phys. Rev.*, D97(2):024027, 2018. doi: 10.1103/PhysRevD.97.024027.
- [60] Ernesto Contreras, Ángel Rincón, Benjamin Koch, and Pedro Bargueo. Scale-dependent polytropic black hole. *Eur. Phys. J.*, C78(3):246, 2018. doi: 10.1140/epjc/s10052-018-5709-0.
- [61] Ángel Rincón, Ernesto Contreras, Pedro Bargueño, Benjamin Koch, and Grigoris Panotopoulos. Scale-dependent  $(2+1)$ -dimensional electrically charged black holes in Einstein-power-Maxwell theory. *Eur. Phys. J.*, C78(8):641, 2018. doi: 10.1140/epjc/s10052-018-6106-4.
- [62] Ernesto Contreras, Ángel Rincón, and J. M. Ramírez-Velasquez. Relativistic dust accretion onto a scale-dependent polytropic black hole. *Eur. Phys. J.*, C79(1):53, 2019. doi: 10.1140/epjc/s10052-019-6601-2.
- [63] E. Contreras and P. Bargueño. Scale-dependent Hayward black hole and the generalized uncertainty principle. *Mod. Phys. Lett.*, A33(32):1850184, 2018. doi: 10.1142/S0217732318501845.
- [64] Ángel Rincón and Benjamin Koch. Scale-dependent BTZ black hole. *Eur. Phys. J.*, C78(12):1022, 2018. doi: 10.1140/epjc/s10052-018-6488-3.

- [65] Ernesto Contreras and Pedro Bargueño. A self-sustained traversable scale-dependent wormhole. *Int. J. Mod. Phys.*, D27(09):1850101, 2018. doi: 10.1142/S0218271818501018.
- [66] Ángel Rincón, Ernesto Contreras, Pedro Bargueño, and Benjamin Koch. Scale-dependent planar Anti-de Sitter black hole. 2019.
- [67] Ernesto Contreras, Ángel Rincón, Benjamin Koch, and Pedro Bargueño. A regular scale-dependent black hole solution. *Int. J. Mod. Phys.*, D27(03):1850032, 2017. doi: 10.1142/S0218271818500323.
- [68] Ángel Rincón and J. R. Villanueva. The Sagnac effect on a scale-dependent rotating BTZ black hole background. 2019.
- [69] Kevin Falls, Daniel F. Litim, and Aarti Raghuraman. Black Holes and Asymptotically Safe Gravity. *Int. J. Mod. Phys.*, A27:1250019, 2012. doi: 10.1142/S0217751X12500194.
- [70] Kevin Falls. *Asymptotic safety and black holes*. PhD thesis, Sussex U., New York, 2012. URL <http://sro.sussex.ac.uk/45249/>.
- [71] Thomas Burschil and Benjamin Koch. Renormalization group improved black hole space-time in large extra dimensions. *Zh. Eksp. Teor. Fiz.*, 92:219–225, 2010. doi: 10.1134/S0021364010160010. [JETP Lett.92,193(2010)].
- [72] Cristopher González and Benjamin Koch. Improved ReissnerNordström(A)dS black hole in asymptotic safety. *Int. J. Mod. Phys.*, A31(26):1650141, 2016. doi: 10.1142/S0217751X16501414.
- [73] Edward Witten. (2+1)-Dimensional Gravity as an Exactly Soluble System. *Nucl. Phys.*, B311:46, 1988. doi: 10.1016/0550-3213(88)90143-5.
- [74] A. Achúcarro and P. K. Townsend. A Chern-Simons Action for Three-Dimensional anti-De Sitter Supergravity Theories. *Phys. Lett.*, B180:89, 1986. doi: 10.1016/0370-2693(86)90140-1.
- [75] Edward Witten. Three-Dimensional Gravity Revisited. 2007.
- [76] Maximo Banados, Claudio Teitelboim, and Jorge Zanelli. The Black hole in three-dimensional space-time. *Phys. Rev. Lett.*, 69:1849–1851, 1992. doi: 10.1103/PhysRevLett.69.1849.

- [77] Maximo Banados, Marc Henneaux, Claudio Teitelboim, and Jorge Zanelli. Geometry of the (2+1) black hole. *Phys. Rev.*, D48:1506–1525, 1993. doi: 10.1103/PhysRevD.48.1506,10.1103/PhysRevD.88.069902. [Erratum: *Phys. Rev.D*88,069902(2013)].
- [78] Juan Martin Maldacena. The Large N limit of superconformal field theories and supergravity. *Int. J. Theor. Phys.*, 38:1113–1133, 1999. doi: 10.1023/A:1026654312961. [Adv. Theor. Math. Phys.2,231(1998)].
- [79] Andrew Strominger. Black hole entropy from near horizon microstates. *JHEP*, 02:009, 1998. doi: 10.1088/1126-6708/1998/02/009.
- [80] Vijay Balasubramanian and Per Kraus. A Stress tensor for Anti-de Sitter gravity. *Commun. Math. Phys.*, 208:413–428, 1999. doi: 10.1007/s002200050764.
- [81] Ofer Aharony, Steven S. Gubser, Juan Martin Maldacena, Hirosi Ooguri, and Yaron Oz. Large N field theories, string theory and gravity. *Phys. Rept.*, 323:183–386, 2000. doi: 10.1016/S0370-1573(99)00083-6.
- [82] John A. Wheeler. On the Nature of quantum geometrodynamics. *Annals Phys.*, 2: 604–614, 1957. doi: 10.1016/0003-4916(57)90050-7.
- [83] Stanley Deser and B. Zumino. Consistent Supergravity. *Phys. Lett.*, B62:335, 1976. doi: 10.1016/0370-2693(76)90089-7.
- [84] Carlo Rovelli. Loop quantum gravity. *Living Rev. Rel.*, 1:1, 1998.
- [85] Luca Bombelli, Joohan Lee, David Meyer, and Rafael Sorkin. Space-Time as a Causal Set. *Phys. Rev. Lett.*, 59:521–524, 1987. doi: 10.1103/PhysRevLett.59.521.
- [86] Abhay Ashtekar. Gravity and the quantum. *New J. Phys.*, 7:198, 2005. doi: 10.1088/1367-2630/7/1/198.
- [87] A. D. Sakharov. Vacuum quantum fluctuations in curved space and the theory of gravitation. *Sov. Phys. Dokl.*, 12:1040–1041, 1968. [Gen. Rel. Grav.32,365(2000)].
- [88] Ted Jacobson. Thermodynamics of space-time: The Einstein equation of state. *Phys. Rev. Lett.*, 75:1260–1263, 1995. doi: 10.1103/PhysRevLett.75.1260.
- [89] Erik P. Verlinde. On the Origin of Gravity and the Laws of Newton. *JHEP*, 04:029, 2011. doi: 10.1007/JHEP04(2011)029.

- [90] M. Reuter. Nonperturbative evolution equation for quantum gravity. *Phys. Rev.*, D57: 971–985, 1998. doi: 10.1103/PhysRevD.57.971.
- [91] Daniel F. Litim. Fixed points of quantum gravity. *Phys. Rev. Lett.*, 92:201301, 2004. doi: 10.1103/PhysRevLett.92.201301.
- [92] Petr Horava. Quantum Gravity at a Lifshitz Point. *Phys. Rev.*, D79:084008, 2009. doi: 10.1103/PhysRevD.79.084008.
- [93] Christos Charmousis, Gustavo Niz, Antonio Padilla, and Paul M. Saffin. Strong coupling in Horava gravity. *JHEP*, 08:070, 2009. doi: 10.1088/1126-6708/2009/08/070.
- [94] A. Ashtekar. Asymptotic Quantization of the Gravitational Field. *Phys. Rev. Lett.*, 46:573–576, 1981. doi: 10.1103/PhysRevLett.46.573.
- [95] R. Penrose and W. Rindler. *SPINORS AND SPACE-TIME. VOL. 2: SPINOR AND TWISTOR METHODS IN SPACE-TIME GEOMETRY*. Cambridge University Press, 1988. ISBN 9780521347860, 9780511868429.
- [96] Alain Connes. Gravity coupled with matter and foundation of noncommutative geometry. *Commun. Math. Phys.*, 182:155–176, 1996. doi: 10.1007/BF02506388.
- [97] Piero Nicolini. Noncommutative Black Holes, The Final Appeal To Quantum Gravity: A Review. *Int. J. Mod. Phys.*, A24:1229–1308, 2009. doi: 10.1142/S0217751X09043353.
- [98] Rodolfo Gambini and Jorge Pullin. Consistent discretization and loop quantum geometry. *Phys. Rev. Lett.*, 94:101302, 2005. doi: 10.1103/PhysRevLett.94.101302.
- [99] Claus Kiefer. Quantum gravity: General introduction and recent developments. *Annalen Phys.*, 15:129–148, 2005. doi: 10.1002/andp.200510175. [Annalen Phys.518,129(2006)].
- [100] Christof Wetterich. Exact evolution equation for the effective potential. *Phys. Lett.*, B301:90–94, 1993. doi: 10.1016/0370-2693(93)90726-X.
- [101] Djamel Dou and Roberto Percacci. The running gravitational couplings. *Class. Quant. Grav.*, 15:3449–3468, 1998. doi: 10.1088/0264-9381/15/11/011.
- [102] Wataru Souma. Nontrivial ultraviolet fixed point in quantum gravity. *Prog. Theor. Phys.*, 102:181–195, 1999. doi: 10.1143/PTP.102.181.

- [103] Peter Fischer and Daniel F. Litim. Fixed points of quantum gravity in extra dimensions. *Phys. Lett.*, B638:497–502, 2006. doi: 10.1016/j.physletb.2006.05.073.
- [104] Roberto Percacci. Asymptotic Safety. 2007.
- [105] Daniel F. Litim. Fixed Points of Quantum Gravity and the Renormalisation Group. 2008. [PoSQG-Ph,024(2007)].
- [106] I. G. Avramidi. Heat kernel and quantum gravity. *Lect. Notes Phys.*, M64:1–149, 2000. doi: 10.1007/3-540-46523-5.
- [107] Maximilian Demmel, Frank Saueressig, and Omar Zanusso. Fixed-Functionals of three-dimensional Quantum Einstein Gravity. *JHEP*, 11:131, 2012. doi: 10.1007/JHEP11(2012)131.
- [108] Shin’ichi Nojiri and Sergei D. Odintsov. Effective Lagrangian and static black holes in 2-D dilatonic gravity. *Mod. Phys. Lett.*, A12:925–936, 1997. doi: 10.1142/S0217732397000959.
- [109] Alfio Bonanno and Martin Reuter. Quantum gravity effects near the null black hole singularity. *Phys. Rev.*, D60:084011, 1999. doi: 10.1103/PhysRevD.60.084011.
- [110] Alfio Bonanno and Martin Reuter. Renormalization group improved black hole spacetimes. *Phys. Rev.*, D62:043008, 2000. doi: 10.1103/PhysRevD.62.043008.
- [111] A. Bonanno and M. Reuter. Spacetime structure of an evaporating black hole in quantum gravity. *Phys. Rev.*, D73:083005, 2006. doi: 10.1103/PhysRevD.73.083005.
- [112] M. Reuter and E. Tuiran. Quantum Gravity Effects in Rotating Black Holes. In *Recent developments in theoretical and experimental general relativity, gravitation and relativistic field theories. Proceedings, 11th Marcel Grossmann Meeting, MG11, Berlin, Germany, July 23-29, 2006. Pt. A-C*, pages 2608–2610, 2006. doi: 10.1142/9789812834300\_0473.
- [113] Benjamin Koch. Renormalization group and black hole production in large extra dimensions. *Phys. Lett.*, B663:334–337, 2008. doi: 10.1016/j.physletb.2008.04.025.
- [114] Yi-Fu Cai and Damien A. Easson. Black holes in an asymptotically safe gravity theory with higher derivatives. *JCAP*, 1009:002, 2010. doi: 10.1088/1475-7516/2010/09/002.

- [115] Daniel F. Litim. Renormalisation group and the Planck scale. *Phil. Trans. Roy. Soc. Lond.*, A369:2759–2778, 2011. doi: 10.1098/rsta.2011.0103.
- [116] Piero Nicolini and Elizabeth Winstanley. Hawking emission from quantum gravity black holes. *JHEP*, 11:075, 2011. doi: 10.1007/JHEP11(2011)075.
- [117] Daniel Becker and Martin Reuter. Running boundary actions, Asymptotic Safety, and black hole thermodynamics. *JHEP*, 07:172, 2012. doi: 10.1007/JHEP07(2012)172.
- [118] D. Becker and M. Reuter. Asymptotic Safety and Black Hole Thermodynamics. In *Proceedings, 13th Marcel Grossmann Meeting on Recent Developments in Theoretical and Experimental General Relativity, Astrophysics, and Relativistic Field Theories (MG13)*, pages 2230–2232, 2015. doi: 10.1142/9789814623995\_0405. URL <https://inspirehep.net/record/1207865/files/arXiv:1212.4274.pdf>.
- [119] Kevin Falls and Daniel F. Litim. Black hole thermodynamics under the microscope. *Phys. Rev.*, D89:084002, 2014. doi: 10.1103/PhysRevD.89.084002.
- [120] Benjamin Koch and Frank Saueressig. Structural aspects of asymptotically safe black holes. *Class. Quant. Grav.*, 31:015006, 2014. doi: 10.1088/0264-9381/31/1/015006.
- [121] Benjamin Koch and Frank Saueressig. Black holes within Asymptotic Safety. *Int. J. Mod. Phys.*, A29(8):1430011, 2014. doi: 10.1142/S0217751X14300117.
- [122] Davi C. Rodrigues, Benjamin Koch, Oliver F. Piattella, and Ilya L. Shapiro. The bending of light within gravity with large scale renormalization group effects. *AIP Conf. Proc.*, 1647:57–61, 2015. doi: 10.1063/1.4913338.
- [123] Benjamin Koch and Israel Ramirez. Exact renormalization group with optimal scale and its application to cosmology. *Class. Quant. Grav.*, 28:055008, 2011. doi: 10.1088/0264-9381/28/5/055008.
- [124] Silvije Domazet and Hrvoje Stefancic. Renormalization group scale-setting from the action - a road to modified gravity theories. *Class. Quant. Grav.*, 29:235005, 2012. doi: 10.1088/0264-9381/29/23/235005.
- [125] Benjamin Koch, Paola Rioseco, and Carlos Contreras. Scale Setting for Self-consistent Backgrounds. *Phys. Rev.*, D91(2):025009, 2015. doi: 10.1103/PhysRevD.91.025009.

- [126] Carlos Contreras, Benjamin Koch, and Paola Rioseco. Setting the Renormalization Scale in QFT. *J. Phys. Conf. Ser.*, 720(1):012020, 2016. doi: 10.1088/1742-6596/720/1/012020.
- [127] V. A. Rubakov. The Null Energy Condition and its violation. *Phys. Usp.*, 57:128–142, 2014. doi: 10.3367/UFNe.0184.201402b.0137.
- [128] Maulik Parikh and Andrew Svesko. Thermodynamic Origin of the Null Energy Condition. 2015.
- [129] Markus Heusler. No hair theorems and black holes with hair. *Helv. Phys. Acta*, 69:501–528, 1996.
- [130] Ted Jacobson. When is  $g_{(tt)} g_{(rr)} = -1$ ? *Class. Quant. Grav.*, 24:5717–5719, 2007. doi: 10.1088/0264-9381/24/22/N02.
- [131] Ted Jacobson, Gungwon Kang, and Robert C. Myers. On black hole entropy. *Phys. Rev.*, D49:6587–6598, 1994. doi: 10.1103/PhysRevD.49.6587.
- [132] Vivek Iyer and Robert M. Wald. A Comparison of Noether charge and Euclidean methods for computing the entropy of stationary black holes. *Phys. Rev.*, D52:4430–4439, 1995. doi: 10.1103/PhysRevD.52.4430.
- [133] Matt Visser. Dirty black holes: Entropy as a surface term. *Phys. Rev.*, D48:5697–5705, 1993. doi: 10.1103/PhysRevD.48.5697.
- [134] Jolien D. E. Creighton and Robert B. Mann. Quasilocal thermodynamics of dilaton gravity coupled to gauge fields. *Phys. Rev.*, D52:4569–4587, 1995. doi: 10.1103/PhysRevD.52.4569.
- [135] Gungwon Kang. On black hole area in Brans-Dicke theory. *Phys. Rev.*, D54:7483–7489, 1996. doi: 10.1103/PhysRevD.54.7483.
- [136] Raphael Bousso and Netta Engelhardt. Generalized Second Law for Cosmology. *Phys. Rev.*, D93(2):024025, 2016. doi: 10.1103/PhysRevD.93.024025.
- [137] Raphael Bousso, Zachary Fisher, Stefan Leichenauer, and Aron C. Wall. Quantum focusing conjecture. *Phys. Rev.*, D93(6):064044, 2016. doi: 10.1103/PhysRevD.93.064044.

- [138] Jason Koeller and Stefan Leichenauer. Holographic Proof of the Quantum Null Energy Condition. 2015.
- [139] Raphael Bousso, Zachary Fisher, Jason Koeller, Stefan Leichenauer, and Aron C. Wall. Proof of the Quantum Null Energy Condition. *Phys. Rev.*, D93(2):024017, 2016. doi: 10.1103/PhysRevD.93.024017.
- [140] Zicao Fu and Donald Marolf. Does horizon entropy satisfy a Quantum Null Energy Conjecture? 2016.
- [141] Giampiero Esposito. An Introduction to quantum gravity. In *Section 6.7.17 of the EOLSS Encyclopedia by UNESCO*, 2011.
- [142] Subrahmanyan Chandrasekhar. The mathematical theory of black holes. In *Oxford, UK: Clarendon (1992) 646 p., OXFORD, UK: CLARENDON (1985) 646 P.*, 1985.
- [143] Xavier Calmet, editor. *Quantum aspects of black holes*, volume 178. Springer, 2015. ISBN 9783319108513, 9783319108520. doi: 10.1007/978-3-319-10852-0. URL <http://www.springer.com/978-3-319-10851-3>.
- [144] Ángel Rincón and Benjamin Koch. On the null energy condition in scale dependent frameworks with spherical symmetry. *J. Phys. Conf. Ser.*, 1043(1):012015, 2018. doi: 10.1088/1742-6596/1043/1/012015.
- [145] A. Hernández-Arboleda, Á. Rincón, B. Koch, E. Contreras, and P. Bargueño. Preliminary test of cosmological models in the scale-dependent scenario. 2018.
- [146] B. F. L. Ward. Planck Scale Remnants in Resummed Quantum Gravity. *Acta Phys. Polon.*, B37:1967–1974, 2006.
- [147] Alfio Bonanno, Benjamin Koch, and Alessia Platania. Cosmic Censorship in Quantum Einstein Gravity. *Class. Quant. Grav.*, 34(9):095012, 2017. doi: 10.1088/1361-6382/aa6788.
- [148] Roger Penrose. Gravitational collapse and space-time singularities. *Phys. Rev. Lett.*, 14:57–59, 1965. doi: 10.1103/PhysRevLett.14.57.
- [149] M. Born and L. Infeld. Foundations of the new field theory. *Proc. Roy. Soc. Lond.*, A144(852):425–451, 1934. doi: 10.1098/rspa.1934.0059.

- [150] Michael B. Green, J. H. Schwarz, and Edward Witten. *SUPERSTRING THEORY. VOL. 1: INTRODUCTION*. Cambridge Monographs on Mathematical Physics. 1988. ISBN 9780521357524. URL <http://www.cambridge.org/us/academic/subjects/physics/theoretical-physics-and-mathematical-physics/superstring-theory-volume-1>.
- [151] Michael B. Green, J. H. Schwarz, and Edward Witten. *SUPERSTRING THEORY. VOL. 2: LOOP AMPLITUDES, ANOMALIES AND PHENOMENOLOGY*. 1988. ISBN 9780521357531. URL <http://www.cambridge.org/us/academic/subjects/physics/theoretical-physics-and-mathematical-physics/superstring-theory-volume-2>.
- [152] Clifford V. Johnson. *D-branes*. Cambridge Monographs on Mathematical Physics. Cambridge University Press, 2005. ISBN 9780511057694, 9780521030052, 9780521809122, 9780511606540. doi: 10.1017/CBO9780511606540. URL <http://books.cambridge.org/0521809126.htm>.
- [153] Eloy Ayon-Beato and Alberto Garcia. Regular black hole in general relativity coupled to nonlinear electrodynamics. *Phys. Rev. Lett.*, 80:5056–5059, 1998. doi: 10.1103/PhysRevLett.80.5056.
- [154] Eloy Ayon-Beato and Alberto Garcia. New regular black hole solution from nonlinear electrodynamics. *Phys. Lett.*, B464:25, 1999. doi: 10.1016/S0370-2693(99)01038-2.
- [155] Nicolás Morales-Durán, Andrés F. Vargas, Paulina Hoyos-Restrepo, and Pedro Bargueño. Simple regular black hole with logarithmic entropy correction. *Eur. Phys. J.*, C76(10):559, 2016. doi: 10.1140/epjc/s10052-016-4417-x.
- [156] Ernesto Contreras, Fabi Villalba, and Pedro Bargueño. Effective geometries and generalized uncertainty principle corrections to the Bekenstein-Hawking entropy. *EPL*, 114(5):50009, 2016. doi: 10.1209/0295-5075/114/50009.
- [157] Pedro Bargueño and Elias C. Vagenas. Black holes with constant topological Euler density. *EPL*, 115(6):60002, 2016. doi: 10.1209/0295-5075/115/60002.
- [158] Mauricio Cataldo, Norman Cruz, Sergio del Campo, and Alberto Garcia. (2+1)-dimensional black hole with Coulomb - like field. *Phys. Lett.*, B484:154, 2000. doi: 10.1016/S0370-2693(00)00609-2.

- [159] Yan Liu and Ji-Liang Jing. Propagation and evolution of a scalar field in Einstein-Power-Maxwell spacetime. *Chin. Phys. Lett.*, 29:010402, 2012. doi: 10.1088/0256-307X/29/1/010402.
- [160] O. Gurtug, S. Habib Mazharimousavi, and M. Halilsoy. 2+1-dimensional electrically charged black holes in Einstein - power Maxwell Theory. *Phys. Rev.*, D85:104004, 2012. doi: 10.1103/PhysRevD.85.104004.
- [161] K. C. K. Chan and Robert B. Mann. Static charged black holes in (2+1)-dimensional dilaton gravity. *Phys. Rev.*, D50:6385, 1994. doi: 10.1103/PhysRevD.50.6385,10.1103/PhysRevD.52.2600. [Erratum: *Phys. Rev.*D52,2600(1995)].
- [162] Cristian Martinez, Claudio Teitelboim, and Jorge Zanelli. Charged rotating black hole in three space-time dimensions. *Phys. Rev.*, D61:104013, 2000. doi: 10.1103/PhysRevD.61.104013.
- [163] Mokhtar Hassaine and Cristian Martinez. Higher-dimensional black holes with a conformally invariant Maxwell source. *Phys. Rev.*, D75:027502, 2007. doi: 10.1103/PhysRevD.75.027502.
- [164] Mokhtar Hassaine and Cristian Martinez. Higher-dimensional charged black holes solutions with a nonlinear electrodynamics source. *Class. Quant. Grav.*, 25:195023, 2008. doi: 10.1088/0264-9381/25/19/195023.
- [165] Hernan A. Gonzalez, Mokhtar Hassaine, and Cristian Martinez. Thermodynamics of charged black holes with a nonlinear electrodynamics source. *Phys. Rev.*, D80:104008, 2009. doi: 10.1103/PhysRevD.80.104008.
- [166] S. H. Hendi and B. Eslam Panah. Thermodynamics of rotating black branes in Gauss-Bonnet-nonlinear Maxwell gravity. *Phys. Lett.*, B684:77–84, 2010. doi: 10.1016/j.physletb.2010.01.026.
- [167] M. Kord Zangeneh, A. Sheykhi, and M. H. Dehghani. Thermodynamics of higher dimensional topological dilation black holes with a power-law Maxwell field. *Phys. Rev.*, D91(4):044035, 2015. doi: 10.1103/PhysRevD.91.044035.
- [168] M. Kord Zangeneh, A. Sheykhi, and M. H. Dehghani. Thermodynamics of topological nonlinear charged Lifshitz black holes. *Phys. Rev.*, D92(2):024050, 2015. doi: 10.1103/PhysRevD.92.024050.

- [169] M. Kord Zangeneh, M. H. Dehghani, and A. Sheykhi. Thermodynamics of topological black holes in Brans-Dicke gravity with a power-law Maxwell field. *Phys. Rev.*, D92(10):104035, 2015. doi: 10.1103/PhysRevD.92.104035.
- [170] S. H. Hendi, B. Eslam Panah, and S. M. Mousavi. Some exact solutions of F(R) gravity with charged (a)dS black hole interpretation. *Gen. Rel. Grav.*, 44:835–853, 2012. doi: 10.1007/s10714-011-1307-2.
- [171] S. H. Hendi, B. Eslam Panah, S. Panahiyan, and M. Momennia. F(R) gravity’s rainbow and its Einstein counterpart. *Adv. High Energy Phys.*, 2016:9813582, 2016. doi: 10.1155/2016/9813582.
- [172] C. H. Brans. Mach’s Principle and a Relativistic Theory of Gravitation. II. *Phys. Rev.*, 125:2194–2201, 1962. doi: 10.1103/PhysRev.125.2194.
- [173] Jose P. Mimoso and David Wands. Anisotropic scalar - tensor cosmologies. *Phys. Rev.*, D52:5612–5627, 1995. doi: 10.1103/PhysRevD.52.5612.
- [174] John D. Barrow and J. P. Mimoso. Perfect fluid scalar - tensor cosmologies. *Phys. Rev.*, D50:3746–3754, 1994. doi: 10.1103/PhysRevD.50.3746.
- [175] Mark A. Scheel, Stuart L. Shapiro, and Saul A. Teukolsky. Collapse to black holes in Brans-Dicke theory. 2. Comparison with general relativity. *Phys. Rev.*, D51:4236–4249, 1995. doi: 10.1103/PhysRevD.51.4236.
- [176] M. Reuter and E. Tuiran. Quantum Gravity Effects in the Kerr Spacetime. *Phys. Rev.*, D83:044041, 2011. doi: 10.1103/PhysRevD.83.044041.
- [177] Roberto Percacci and Gian Paolo Vacca. The background scale Ward identity in quantum gravity. *Eur. Phys. J.*, C77(1):52, 2017. doi: 10.1140/epjc/s10052-017-4619-x.
- [178] M. Dehghani. Thermodynamics of (2+1)-dimensional charged black holes with power-law Maxwell field. *Phys. Rev.*, D94(10):104071, 2016. doi: 10.1103/PhysRevD.94.104071.
- [179] Barton Zwiebach. Curvature Squared Terms and String Theories. *Phys. Lett.*, 156B:315–317, 1985. doi: 10.1016/0370-2693(85)91616-8.
- [180] Steven Corley, David A. Lowe, and Sanjaye Ramgoolam. Einstein-Hilbert action on the brane for the bulk graviton. *JHEP*, 07:030, 2001. doi: 10.1088/1126-6708/2001/07/030.

- 
- [181] Yevgeny Kats, Lubos Motl, and Megha Padi. Higher-order corrections to mass-charge relation of extremal black holes. *JHEP*, 12:068, 2007. doi: 10.1088/1126-6708/2007/12/068.
- [182] Dionysios Anninos and Georgios Pastras. Thermodynamics of the Maxwell-Gauss-Bonnet anti-de Sitter Black Hole with Higher Derivative Gauge Corrections. *JHEP*, 07:030, 2009. doi: 10.1088/1126-6708/2009/07/030.
- [183] Rong-Gen Cai, Zhang-Yu Nie, and Ya-Wen Sun. Shear Viscosity from Effective Couplings of Gravitons. *Phys. Rev.*, D78:126007, 2008. doi: 10.1103/PhysRevD.78.126007.
- [184] S. H. Hendi and H. R. Rastegar-Sedehi. Ricci flat rotating black branes with a conformally invariant Maxwell source. *Gen. Rel. Grav.*, 41:1355–1366, 2009. doi: 10.1007/s10714-008-0711-8.
- [185] Hideki Maeda, Mokhtar Hassaine, and Cristian Martinez. Lovelock black holes with a nonlinear Maxwell field. *Phys. Rev.*, D79:044012, 2009. doi: 10.1103/PhysRevD.79.044012.
- [186] S. H. Hendi and S. Kordestani. The Effects of nonlinear Maxwell source on the magnetic solutions in Einstein-Gauss-Bonnet gravity. *Prog. Theor. Phys.*, 124:1067–1082, 2010. doi: 10.1143/PTP.124.1067.
- [187] Kyriakos Destounis, Grigoris Panotopoulos, and Ángel Rincón. Stability under scalar perturbations and quasinormal modes of 4D EinsteinBornInfeld dilaton spacetime: exact spectrum. *Eur. Phys. J.*, C78(2):139, 2018. doi: 10.1140/epjc/s10052-018-5576-8.
- [188] Erik Curiel. A Primer on Energy Conditions. *Einstein Stud.*, 13:43–104, 2017. doi: 10.1007/978-1-4939-3210-8\_3.
- [189] Wolfram Research, Inc. Wolfram—one, Version 11.3. Champaign, IL, 2018.
- [190] Leonardo Balart and Sharmanthie Fernando. A Smarr formula for charged black holes in nonlinear electrodynamics. *Mod. Phys. Lett.*, A32(39):1750219, 2017. doi: 10.1142/S0217732317502194.
- [191] Daisuke Ida. No black hole theorem in three-dimensional gravity. *Phys. Rev. Lett.*, 85:3758–3760, 2000. doi: 10.1103/PhysRevLett.85.3758.

- [192] A. Bonanno and M. Reuter. Cosmology of the Planck era from a renormalization group for quantum gravity. *Phys. Rev.*, D65:043508, 2002. doi: 10.1103/PhysRevD.65.043508.
- [193] R. Floreanini and R. Percacci. The Heat kernel and the average effective potential. *Phys. Lett.*, B356:205–210, 1995. doi: 10.1016/0370-2693(95)00799-Q.
- [194] R. Moti and A. Shojai. On the quantum improvement of black holes. 2018.
- [195] J. Polchinski. *String theory. Vol. 1: An introduction to the bosonic string*. Cambridge University Press, 2007.
- [196] J. Polchinski. *String theory. Vol. 2: Superstring theory and beyond*. Cambridge University Press, 2007.
- [197] M. Dehghani. Thermodynamics of (2+1)-dimensional black holes in Einstein-Maxwell-dilaton gravity. *Phys. Rev.*, D96(4):044014, 2017. doi: 10.1103/PhysRevD.96.044014.
- [198] Qing-Qing Zhao, Yue-Zhou Li, and H. Lu. Static Equilibria of Charged Particles Around Charged Black Holes: Chaos Bound and Its Violations. *Phys. Rev.*, D98(12):124001, 2018. doi: 10.1103/PhysRevD.98.124001.
- [199] W. B. Houthoff, A. Kurov, and F. Saueressig. Impact of topology in foliated Quantum Einstein Gravity. *Eur. Phys. J.*, C77:491, 2017. doi: 10.1140/epjc/s10052-017-5046-8.
- [200] C. Wetterich. Graviton fluctuations erase the cosmological constant. *Phys. Lett.*, B773:6–19, 2017. doi: 10.1016/j.physletb.2017.08.002.
- [201] Felipe Canales, Benjamin Koch, Cristobal Laporte, and Ángel Rincón. Vacuum energy density: deflation during inflation. 2018.
- [202] Marek Demianski. Static electromagnetic geon. *Foundations of Physics*, 16(2):187–190, 1986. ISSN 1572-9516. doi: 10.1007/BF01889380. URL <http://dx.doi.org/10.1007/BF01889380>.
- [203] O. Lauscher and M. Reuter. Flow equation of quantum Einstein gravity in a higher derivative truncation. *Phys. Rev.*, D66:025026, 2002. doi: 10.1103/PhysRevD.66.025026.